AN EXAMINATION OF THE SYNTHESIS AND COMPLEXATION PROPERTIES OF SELECTED MACROCYCLIC COMPOUNDS

SABRINA DAWN GIDDINGS

NOTE TO USERS

Page(s) not included in the original manuscript and are unavailable from the author or university. The manuscript was scanned as received.

xii & 64

This reproduction is the best copy available.

UMI®

AN EXAMINATION OF THE SYNTHESIS AND COMPLEXATION PROPERTIES OF SELECTED MACROCYCLIC COMPOUNDS

by

Sabrina Dawn Giddings

(B. Sc., University of New Brunswick, 2000)

A thesis submitted to the school of Graduate Studies in partial fulfillment of the requirements of the degree of Master of Science

Department of Chemistry

Memorial University of Newfoundland

December 2003

St. John's Newfoundland

Your file Votre référence
ISBN: 0-612-99076-1
Our file Notre référence
ISBN: 0-612-99076-1

Abstract

Calix[4]naphthalenes are "basket shaped" molecules capable of supramolecular complexation with neutral species such as C_{60}. They were first synthesized by Li and Georghiou in 1993. Over the past decade much progress has been made towards developing practical synthetic routes to other regioisomeric calixnaphthalenes. To date, the best synthetic route involves a "one-pot" $TiCl_4$-mediated cyclocondensation of 3-(hydroxymethyl)-2-naphthol, but affords low yields. Since the chemical properties of calix[4]naphthalenes need to be fully explored, there is a need for more efficient methods of synthesizing these types of compounds.

Ionic liquids, have shown great potential for use in organic synthesis. Several reports have been published which describe the efficient synthesis of cyclotriveratrylene, another basket shaped compound of interest, in ionic liquids.[29,30] In principle, the methodology employed could be applicable to the synthesis of calix[4]naphthalenes. We therefore explored the use of ionic liquids for their synthesis of calix[4]naphthalenes.

Recently, an unusual method for synthesizing the related calix[4]azulene was reported. This synthesis involved a Florisil^R-mediated reaction between azulene and paraformaldehyde. We investigated the generality of this process for the synthesis of calix[4]naphthalenes. The synthesis of calix[4]azulene was reproducible and provided us with a unique chance to look at an unfunctionalized "basket-like" molecule and its supramolecular complexation with C_{60}. The low solubility of calix[4]azulene also allowed us to use a unique method for the ^{1}H NMR and uv-vis spectroscopy studies. We report our methods and results in this thesis. These methods were then used to examine the stoichiometry of complexes formed between two different calix[*n*]arene with C_{60}.

Acknowledgements

I would like to thank Dr. Paris Georghiou and the Georghiou Research Group both past and present, for their guidance and friendship throughout this endeavor. I would also like to express my appreciation to Dr. Dave Thompson and the Thompson Research Group especially Adam Bishop and Skylar Stroud for assistance in the development of the complexation project. Thanks to Mr. David Miller, and Ms. Rosemarie Harvey for NMR and X-ray crystallography, as well as Ms. Marion Braggs and Dr. Brian Gregory for mass spectra, and Ms. Linda Windsor for LCMS and MALDI.

I would like to thank my supervisory committee, Dr. Peter Pickup and Dr. Hugh Anderson, for their patience while reading my thesis.

I would also like to express my appreciation to Dr. Rob Singer of St. Mary's University, NS for answering some of our questions on ionic liquids.

I cannot thank my friends and family enough for sticking with me through this. Thanks Mom and Dad for that extra push when I did not have the energy to do it myself. Thanks to my sister and brother-in-law, Kim and Jamie, for all those late night telephone calls. Thanks to Karen and Erin for our many conversations and for providing an ear when I needed one.

Thanks to the many others helped me along the way. I have not forgotten you. There are too many for me to name, but know that your contribution did not go unnoticed.

I would like to acknowledge the School of Graduate Studies and NSERC for funding.

Table of Contents

Abstract ii

Acknowledgments iii

Table of Contents iv

List of Figures viii

List of Schemes xi

List of Tables xii

List of Symbols and Abbreviations xiv

Chapter 1 Introduction 1

1.1. Introduction 1

1.2. Calixarenes: Derivatives and Analogues 2

1.3. Conformations of Calix[4]arenes and Calix[4]naphthalenes 7

1.3.1. The Conformations of Calix[6]arenes and Calix[8]arenes 10

1.4. Synthesis of Calixarenes and Calixnapthalenes 12

1.4.1. One-Pot Procedure for the Synthesis of Calixarenes 12

1.4.2. Stepwise Synthesis of Calixarenes 15

1.4.3. Synthesis of Calix[4]naphthalenes 18

1.5. Supramolecular Complexation Properties of Calixarenes and Calixnaphthalenes 19

1.5.1. Supramolecular Complexation Properties of Calix[*n*]arenes 23

1.5.2. Supramolecular Complexation Properties of Calix[4]naphthalene 26

1.6. The Problem 27

1.7. Description of Thesis Content 28

Chapter 2 **Progress Towards the Synthesis of Calix[4]naphthalene in Ionic Liquids** **30**

2.1. Introduction 30

2.1.1. Ionic liquids: Definition and Properties 31

2.1.2. Ionic Liquids – A New Medium for Organic Synthesis 35

2.2. Synthesis of Ionic Liquids 36

2.2.1. The Formation of Butylmethylimidizolium Hexafluorophosphate ([bmim]PF_6) 36

2.2.2. Synthesis of tri-*n*-butylhexylammonium ion with bis(trifluoromethanesulfonyl)-amide (N_{6444} Imide) 37

2.3. Synthesis of CTV (**31**) in Ionic Liquids 37

2.3.1. Previous Work 37

2.3.2. The Synthesis of CTV with a Range of Lewis Acids 38

2.4. Attempted Synthesis of Calix[4]naphthalene in Ionic Liquids 41

2.5 Conclusions 46

2.6. Experimental 47

Chapter 3 **The Attempted Synthesis of Calix[4]naphthalene using a Florisil^R-Mediated Cyclocondensation** **58**

3.1. Introduction 58

3.2. Attempted Synthesis of CTV and Calix[4]naphthalene Using a Florisil^R-Mediated Cyclocondensation 60

3.3. Conclusions 65

3.4 Experimental 66

Chapter 4 **A Study of Supramolecular Complexation between Calix[4]azulene and C_{60}** **71**

4.1. Introduction 71

	4.1.1. C_{60}	75
	4.1.2. Determining the Stoichiometry and K_{assoc} of a Supramolecular Complex	76
4.2.	Synthesis and Characterization of calix[4]azulene (**11**)	81
	4.2.1 Determining the Absorption Structure of **11**	82
4.3.	Supramolecular Binding by UV-Visible Spectroscopy and ^{1}H NMR Spectroscopy	84
	4.3.1. UV-Visible Studies-General Observations	84
	4.3.2. NMR Studies-General Observations	87
4.4.	Evidence for Supramolecular Complexation between C_{60} and **11**	92
	4.4.1. Equilibrium Constants by UV-Visible Spectroscopy	92
4.5.	Determining K_{assoc} of C_{60} with Calix[4]azulene (**11**)	94
4.6	Conclusions	96
4.7.	Experimental	102
Chapter 5	**An Examination of the Supramolcular Complexation Stoichiometry of *tert*-butylmethoxycalix[*n*]arenes and C_{60}**	**105**
5.1.	Introduction	105
5.2.	Characterization of *tert*-butylmethoxycalix[6]arene (**44**) and *tert*-butylmethoxycalix[8]arene (**45**)	106
5.3.	Supramolecular Binding by UV-Visible and ^{1}H NMR Spectroscopy	106
	5.3.1. UV-Visible Spectroscopic Studies-General Observations	106
	5.3.2. NMR Studies-General Observations	110
	5.3.3. Determining the Stoichiometry of the **44**:C_{60} Complex and the **45**:C_{60} Complex by UV-visible Spectroscopy	112
5.4	Conclusions	112

5.5. Experimental 114

References **117**

Appendix A **^{1}H NMR of Selected Compounds from Chapter 2** **124**

Appendix B **^{1}H NMR of Selected Compounds from Chapter 3** **130**

Appendix C **Benzene-d_6 Experiment and Experimental and Calculated Data for Chapter 4** **134**

Appendix D **^{1}H NMR of Compounds 44 and 45 and Experimental and Calculated data from Chapter 5** **144**

List of Figures

page

Figure 1.1. General structure of calix[*n*]arenes.....2

Figure 1.2. Some calix[*n*]arene derivatives 3

Figure 1.3. Some calix[4]naphthalenes.....4

Figure 1.4. Depth and width of a calix[4]arene compared with a calix[4]naphthalene.....5

Figure 1.5. The electrostatic potential maps on the concave surfaces (the "cavities") of (a) calix[4]naphthalene (**8**) and (b) calix[4]arene (**1**) as determined by molecular modeling Spartan Pro. V.5.0. 6

Figure 1.6. Numbering system employed for the carbon positions of calix[4]naphthalenes.....7

Figure 1.7. Structure of calix[4]azulenes.....8

Figure 1.8. Conformational isomers of calix[4]arene.....9

Figure 1.9. Conformational isomers of calix[4]naphthalene.....10

Figure 1.10. Interconversion between enantiomeric *cone*-conformers of **8**.....11

Figure 1.11. Conformational isomers of calix[6]arene.....12

Figure 1.12. The "*pleated loop*" conformation of calix[8]arene.....13

Figure 1.13. The four regioisosmers of *exo*-calix[4]naphthalene.....20

Figure 1.14. *Double cone*-conformation of a calix[6]arene.....25

Figure 2.1. The effect of the cation on the melting points of salts.....32

Figure 2.2. The effect of the anion on the melting points of salts.....32

Figure 2.3. Proposed mechanism for the cyclocondensation of **20** to form **8**.....43

Figure 4.1. The hydrogen bonding in DNA base-paring.....72

Figure 4.2. Electrostatic interactions.....72

Figure 4.3. The $\pi - \pi^*$ interactions.....74

Figure 4.4. A σ – π interaction.....74

Figure 4.5. The solvophobic effect.....75

Figure 4.6. NMR spectrum of calix[4]azulene at 1.03 mM in CS_2.....81

Figure 4.7. The UV-visible spectrum of calix[4]azulene (1.03 mM) and C_{60} (0.938 mM) in CS_2, at 298K.....83

Figure 4.8. Absorbance spectrum of calix[4]azulene(1.03 mM) vs the absorbance spectrum of azulene (1.49 mM).....84

Figure 4.9a. Absorbance spectra of continuous variations experiments in CS_2 where the mole ratio of calix[4]azulene to C_{60} are 1:1 to 9:1 85

Figure 4.10. Absorbance spectra of continuous variations experiments in CS_2 where the mole ratio of calix[4]azulene to C_{60} are1:9 to 4:6 86

Figure 4.11. Job plot of the chemical shift changes of the methylene signal of calix[4]azlulene in CS_2 as the mole fraction of C_{60} increase 90

Figure 4.12. *Pinched cone* conformer of calix[4]azulene 91

Figure 4.13. The 1:1 C_{60}: calix[4]azulene complex as generated using the PC Spartan Pro. V.5.0 molecular modeling program.....91

Figure 4.14. The 2:1 calix[4]azulene: C_{60} complex as generated using the PC Spartan Pro. V.5.0 molecular modeling program.....92

Figure 4.15. Job plot of calix[4]azulene vs C_{60} at wavelength 520 nm in CS_2.....94

Figure 4.16. The absorbance spectra from the titration of calix[4]azulene into a solution of C_{60}.....97

Figure 4.17. The Benesi-Hildebrand plot at 650 nm of the titration of calix[4]azulene into a solution of C_{60} and CS_2, obtained from the absorbance spectra shown in Figure 4.16.....98

Figure 4.18. The absorbance spectra from the titration of C_{60} into a solution of calix[4]azulene.....99

Figure 4.19. The Benesi-Hildebrand plot at 650 nm of the titration of C_{60} into a solution of calix[4]azulene and CS_2, obtained from the absorbance spectra shown in Figure 4.18.....100

Figure 4.20. Plot of ΔA vs [**11**].....101

Figure 5.1. *Tert*-butylmethoxycalix[6]arene and *tert*-butylmethoxycalix[8]arene....105

Figure 5.2. Absorbance spectra from continuous variation experiment for **44** and C_{60}.....107

Figure 5.3. Absorbance spectra from continuous variation experiment for **45** and C_{60}.....108

Figure 5.4. Mathematically transformed absorbance of **44** in CS_2.....109

Figure 5.5. Mathematically transformed absorbance of **45** in CS_2.....110

Figure 5.6. Job plot of **44** with C_{60} in CS_2 at 520 nm.....113

Figure 5.7. Job plot of **45** with C_{60} in CS_2 at 520 nm.....113

Figure C.1. Absorbance spectra from the continuous variation experiment in benzene-d_6 for the mole ratios of 4:6 to 9:1 of calix[4]azulene to C_{60}...135

Figure C.2. The absorbance spectra from the continuous variation experiment in benzene-d_6 for the mole ratios of 1:9 to 3:7 of calix[4]azulene to C_{60}...136

Figure C.3. Job plot of the chemical shift change for the methylene signal of calix[4]azulene in benzene-d_6, as the mole fraction of C_{60} increases.....137

Figure C.4. Job plot of calix[4]azulene vs C_{60} at wavelength 530 nm in benzene-d_6.....137

List of Schemes

Page

Scheme 1.1. Optimized conditions for the base-catalyzed synthesis of calix[*n*]arene ($n = 4, 6, 8$).....14

Scheme 1.2. Acid-catalyzed synthesis of calixarenes.....15

Scheme 1.3. Nonconvergent synthesis of *p*-tetraalkylcalix[4]arenes.....17

Scheme 1.4. A [2 + 2] fragmentation condensation.....18

Scheme 1.5. Synthesis of calix[4]naphthalene **8**.....21

Scheme 1.6. Synthesis of *tert*-butylcalix[4]naphthalene **9**.....22

Scheme 1.7. Purification of fullerene mixture containing C_{60} and C_{70} using octa-*tert*-butylcalix[8]arene.....26

Scheme 2.1. The synthesis of 1-butyl-3-methylimidazolium chloride (**23**).....36

Scheme 2.2. The synthesis of 1-butyl-3-methylimidazolium hexafluorophosphate (**24**).....37

Scheme 2.3. The synthesis of N_{6444}Imide (**28**).....39

Scheme 2.4. The synthesis of CTV using Moens' conditions.....40

Scheme 2.5. The synthesis of CTV using Scott's conditions.....40

Scheme 2.6. The synthesis of methoxycalix[4]naphthalene (**34**).....45

Scheme 3.1. The synthesis of [1.1.1.1] (1, 3)-methoxyazulenophane (**10**).....59

Scheme 3.2. The synthesis of calix[4]azulene (**11**).....61

Scheme 3.3. The synthesis of a naphthol dimer **41**.....62

Scheme 3.4. The synthesis of the 2-hydroxy-3-naphthaldehyde(**42**).....63

Scheme 3.5. The synthesis of the diol **43**.....64

Table C.8 Concentration of samples used for the titration of C_{60} into a solution of **11**.....141

Table C.9. Calculated values used for the Benesi-Hildebrand plot for the titration of C_{60} into a solution of **11**.....142

Table C.10. Calculated values used for the Benesi-Hildebrand plot for the titration of **11** into a solution of C_{60} in CS_2.....142

Table C.11. Calculated and experimental absorbances for the titration of **11** into a solution of C_{60} in CS_2.....143

Table D.1. Concentrations in CS_2 of C_{60} and **44** used for the Job plot.....147

Table D.2. Concentrations in CS_2 of C_{60} and **45** used for the Job plot.....147

Table D.3 Calculated values used for the uv-vis Job plot for **44** in CS_2.....148

Table D.4. Calculated values used for the uv-vis Job plot for **45** inCS_2.....148

List of Symbols and Abbreviations

APCI	atmospheric pressure chemical ionization
b.p.	boiling point
[bmim]Cl	1-butyl-3-methylimidazolium chloride
[bmim]PF_6	1-butyl-3-methylimidazolium hexafluorophosphate
C_{60}	buckminsterfullerene-60
C_{70}	buckminsterfullerene-70
cm	centimetre (s)
^{13}C NMR	carbon 13 nuclear magnetic resonance (spectroscopy)
CS_2	carbon disulfide
CTV	cyclotriveratrylene
δ	chemical shift
$\Delta\delta$	change in chemical shift
d	doublet (NMR), downward (conformations), day(s)
dd	doublet of doublets (NMR)
DMF	*N,N*-dimethylformamide
f.p.	freezing point
g	gram(s)
h	hour(s)
^1H NMR	proton nuclear magnetic resonance (spectroscopy)
Hz	Hertz
IR	infrared spectroscopy
J	coupling constant (NMR)

K_{assoc}	association constant
λ_{max}	maximum wavelength
l	litre(s)
LAH	lithium aluminum hydride
LCMS	liquid chromatography mass spectrum
lit	literature
m	multiplet (NMR)
mg	milligram(s)
MHz	megahertz
µl	microlitre(s)
min	minute(s)
ml	millilitre(s)
mm	millimetre(s)
mM	millimolar
mol	mole(s)
mmol	millimole(s)
m.p.	melting point
mV	millivolt(s)
nm	nanometre(s)
NaCl	sodium chloride
NMR	nuclear magnetic resonance (spectroscopy)
o	*ortho*
p	*para*

ppm	parts per million
Δppm	change in parts per million
rt	room temperature
s	singlet (NMR)
S_0	ground state
S_1	singlet excited state
t	triplet (NMR)
t	tertiary
THF	tetrahydrofuran
TLC	thin layer chromatography
TMS	trimethylsilyl
uv-vis	ultraviolet to visible spectrum

Chapter 1

Introduction

1.1. Introduction

There is a wide range of classes of organic molecules which show potential for biological activity. The compounds collectively known as calixarenes are one such class.[1] Calixarenes encompass a large group of compounds, their derivatives and analogues. In certain conformations, many calixarenes can be considered to be "basket-shaped" molecules, and the cavities of these molecules can bind guest-like molecules.[2] Calixarenes are made up of individual substituted phenyl subunits linked by methylene groups (Figure 1.1). The cavities generated in these compounds are π electron-rich. As the number of subunits increases, so does the size and the flexibility of the "basket". The most common calixarenes have between 4-12 subunits; however, most studies have been conducted on the smaller, 4-8 subunit-containing calixarenes. Their different conformational properties have been extensively studied and their electron-rich cavities formed by the phenyl sub-units make them good candidates for supramolecular charge-transfer complexation studies.

There have been many studies reported on the complexation properties of calixarenes and their analogues with ions and other guest molecules, in particular C_{60}.[3,4] Calixarenes have also shown potential to act as selective ionophores and it is note worthy that some enzymes act as ionophores[5] that help in a cell's absorption and removal of ions.

The "baskets" formed by calixarenes have two rims, an "upper" and a "lower" one, onto which functional groups can be added in order to change some of their chemical characteristics. Changing the functional groups on calixarenes means they can be designed to hold their "basket-like" conformations, as well as decrease or increase the depths and

widths of their cavities. The large variety of calixarenes which can be synthesized also make them challenging targets in their own right for organic synthesis. Various analogues of calixarenes have been successfully synthesized. Two such analogues are the naphthol-based calixnaphthalenes[6] and the azulene-based calixazulene.[7, 8]

1.2. Calixarenes: Derivatives and Analogues

Calixarenes are composed of *n* repeating phenol subunits with a methylene bridge between each subunit, forming a cyclic compound (e.g.**1-4**, where $n = 4–12$). They can

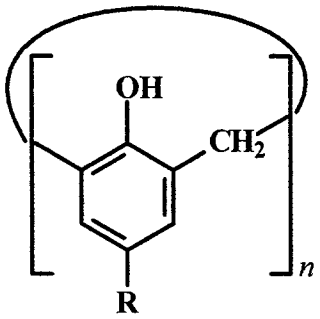

1. ***n* = 4: calix[4]arene; R = H or alkyl groups**
2. ***n* = 5: calix[5]arene; R = H or alkyl groups**
3. ***n* = 6: calix[6]arene; R = H or alkyl groups**
4. ***n* = 8: calix[8]arene; R = H or alkyl groups**

Figure 1.1. General structure of calix[*n*]arenes.

also carry various functional groups on their subunits, on either the upper rim or the lower rim.[1] The "lower rim" is where the hydroxy groups are located; the "upper rim" substituents are therefore in the positions *para* to the hydroxy groups.

Changing the functional groups of a calixarene can change its chemical characteristics and help stabilize its conformation. For example, converting the hydroxy groups to the corresponding ethers increases the solubility of the calixarene (e.g. **5**; Figure 1.2) in organic solvents. Addition of a sulfonato group to the upper rim, on the other hand,

creates a calixarene e.g. **6** which is hydrophilic.[9] The most common calixarenes have *tert*-butyl moieties on the upper rim, e.g. **7**.

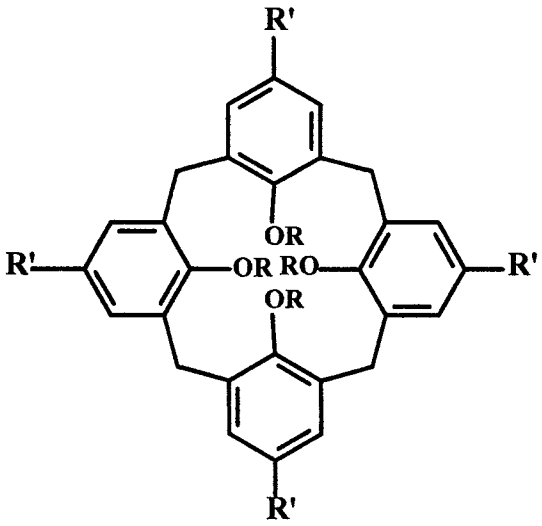

1. **R = R' = H**
5. **R = CH_3; R' = H**
6. **R = H; R' = SO_3H**
7. **R = H; R' = *tert*-butyl**

Figure 1.2. Some calix[*n*]arene derivatives.

Another way to change the chemical character of a calixarene is to change the subunits, for example, by replacing the phenol subunits of a calixarene by a different aromatic subunit. An example is to replace the phenols with naphthols to form calixnaphthalenes such as **8** (Figure 1.3). The second fused aromatic ring of the naphthalene unit in compounds such as **8** creates a deeper and wider basket. The depth of a typical calix[4]arene in its "*cone*" conformation is 5.2 Å and its width is 8.5 Å, whereas for a similar "*cone*" conformation of calix[4]naphthalene, the corresponding depth is 7.7 Å and its comparable width is 11.6 Å (Figure 1.4.).[10] The electrostatic potential maps of

calix[4]arene and calix[4]naphthalene (Figure 1.5) clearly show that the calixnaphthalene has a deeper, more π electron-rich concave surface.

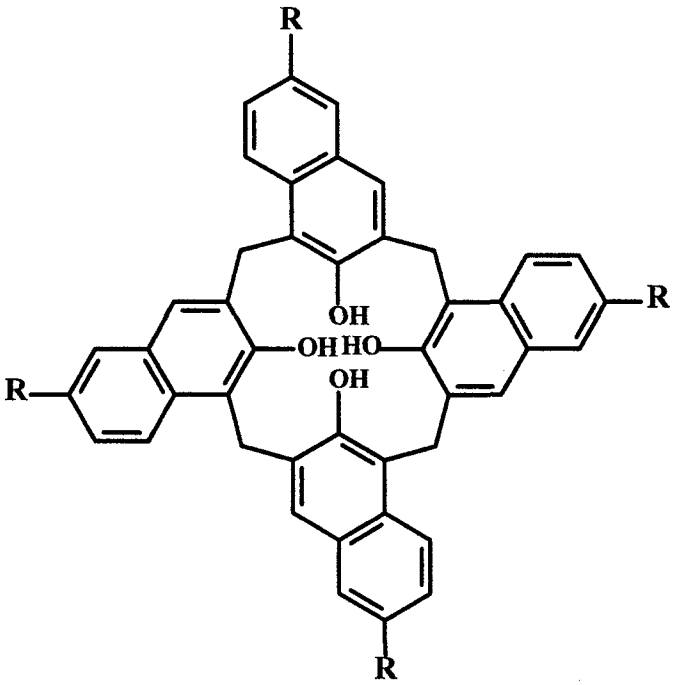

8. R = H
9. R = *tert*-butyl

Figure 1.3. Some calix[4]naphthalenes.

While calixnaphthalenes have been much less studied than calixarenes, they have been extensively studied by the Georghiou Research Group since they were first reported by Li and Georghiou in 1993.[11] Calixnaphthalenes show similar potential to calixarenes for being functionalized on their upper and lower rims. The "lower" rim of calix[4]naphthalene is the one defining the intra-annular 16-membered ring; the "upper" rim is defined by the positions labeled 7, 17, 27, and 37 (Figure1.6). Common upper rim substituents are *tert*-butyl groups, and a common lower rim functionalization is the alkylation of the hydroxy groups.

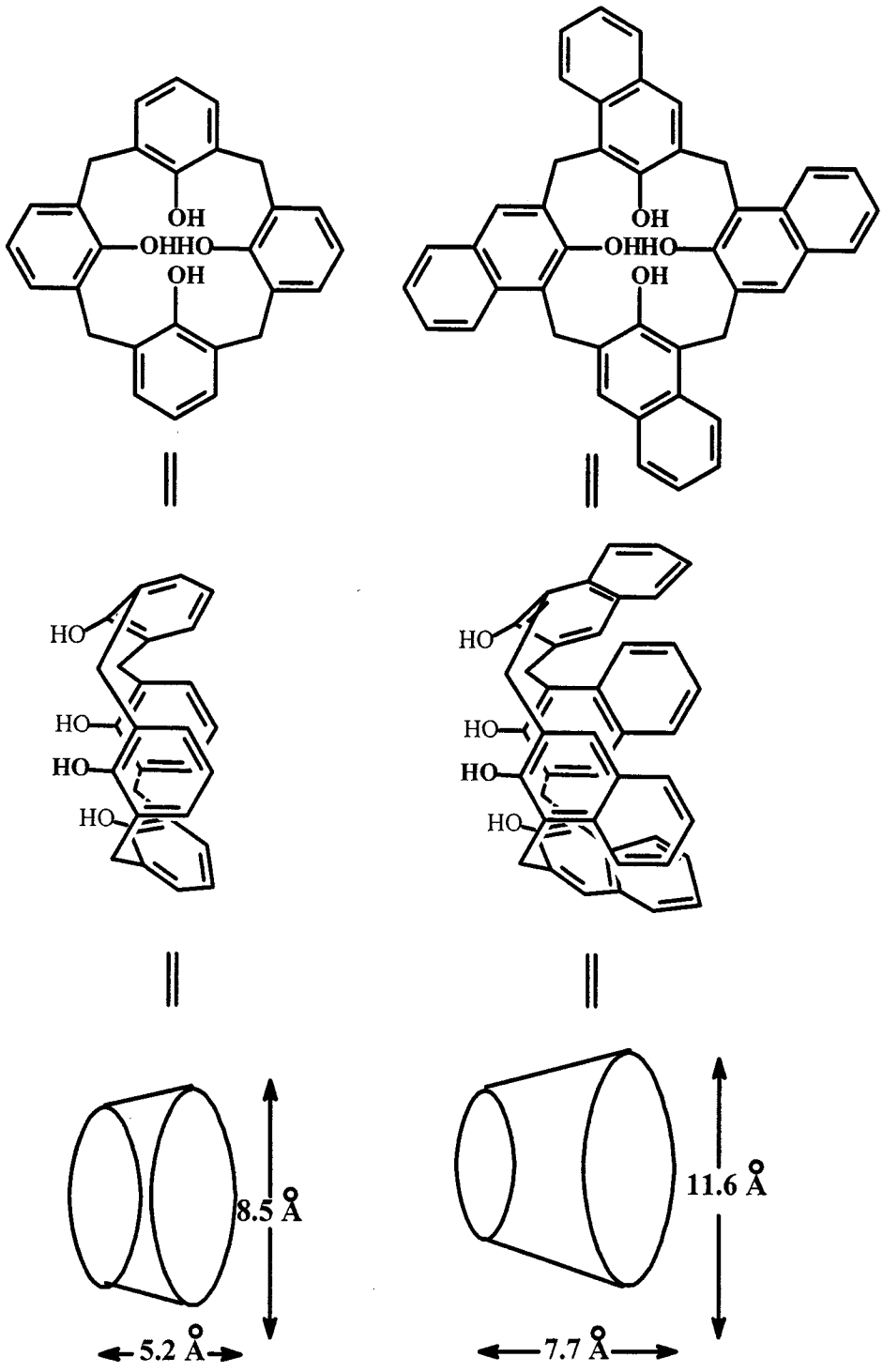

Figure 1.4. Depth and width of a calix[4]arene compared with calix[4]naphthalene.

(a)

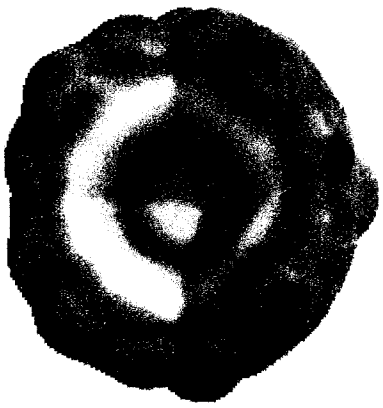

(b)

Figure 1.5. The electrostatic potential maps on the concave surfaces (the "cavities") of : *a)* calix[4]naphthalene (8) and *b)* calix[4]arene (1) as determined by molecular modeling using Spartan Pro. V. 4.0.[4]

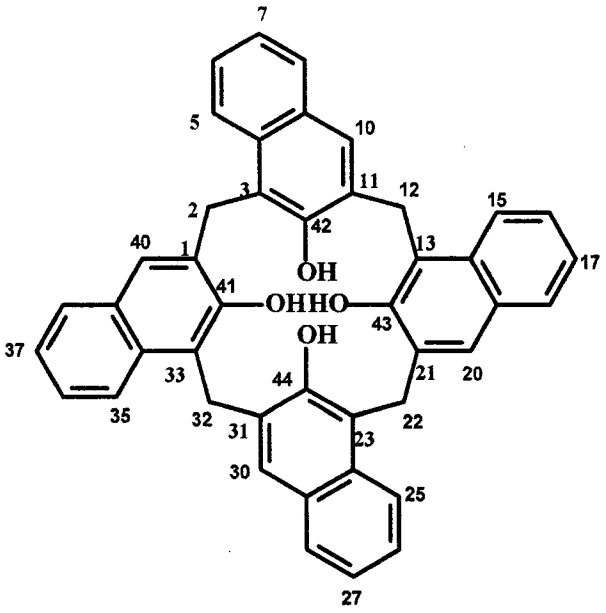

Figure 1.6. Numbering system employed for the carbon positions of calix[4]naphthalenes.

Other less-known analogues of calixarenes are the calixazulenes, e.g. **10**[7] and **11**.[8] Calix[4]azulene **10** has an azulene subunit with a methoxy group attached at the lower rims, whereas **11** is the parent hydrocarbon, with the intrannular 16-membered ring still being referred to as the lower rim. There is scant literature available on these two molecules other than their synthesis; however, they both show potential for supramolecular studies. Chapter 4 of this thesis reports the supramolecular binding properties of the unfunctionalized calix[4]azulene, **11**.

1.3. Conformations of Calix[4]arenes and Calix[4]naphthalenes

The conformations of calixarenes have been extensively studied. The common reference to calixarenes as being basket-shaped molecules derives from both their NMR spectra and single crystal structures.[12] The conformation of a calixarene in which all of its

hydroxyls point in the same direction, is called a *cone* (or "*crown*") conformation. *Cone* conformations are stabilized by the formation of hydrogen bonds between the lower rim hydroxy groups.

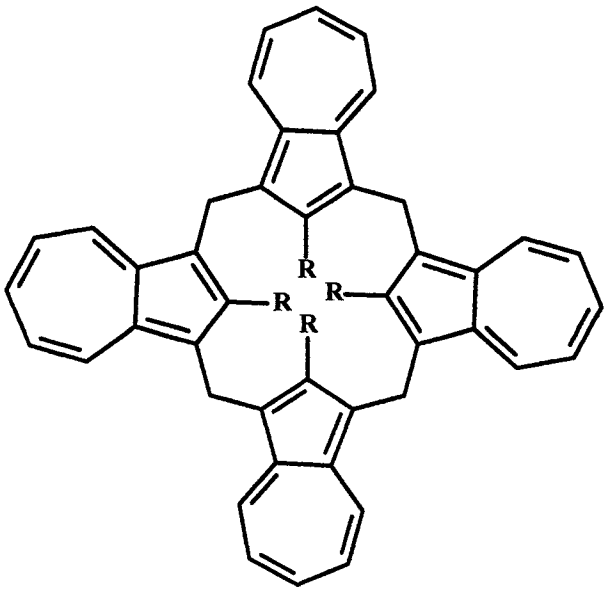

10. R = OCH_3
11. R = H

Figure 1.7. Structure of calix[4]azulenes.

The conformations of calix[4]arene can be defined by the direction of the aryl groups. In calix[4]arenes the methylene bridges define the average plane of the molecule. The aryl groups are perpendicular to this average plane and can be pointed upward (u) or downward (d) relative to the methylene bridges.

In solution, calixarenes are much more flexible than in the solid state. The σ-bonds of the methylene bridge allow for free rotation of the subunits, and allow these molecules to form different conformations. Gutsche[13] has classified four major conformers of calix[4]arene as follows (Figure 1.8):

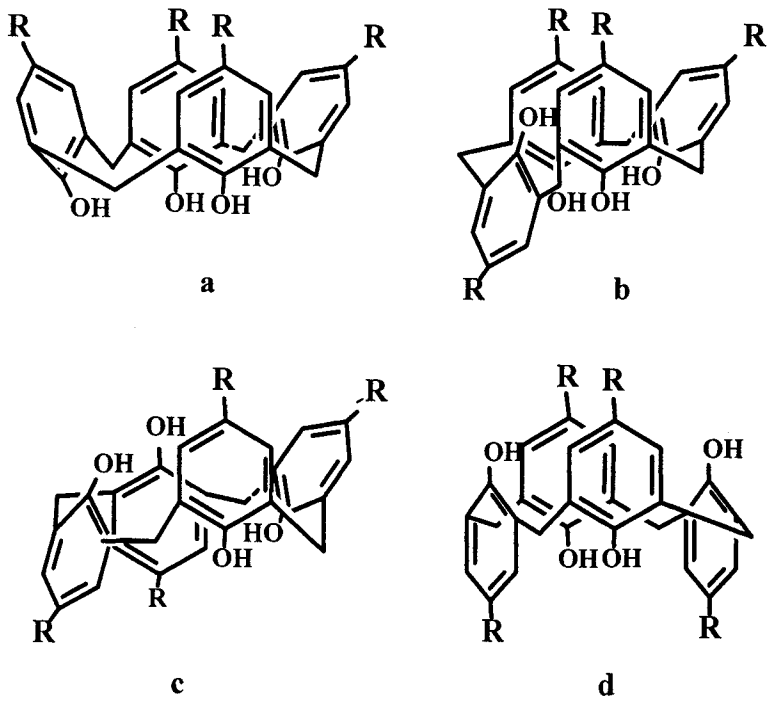

Figure 1.8. Conformational isomers of calix[4]arene.[4]

a. The "*cone*" or the "*crown*" conformation, in which all four hydroxyl groups are *syn* to one another (u,u,u,u);

b. The "*partial cone*" or "*partial crown*" conformation, where three hydroxy groups are *syn* to each other and the fourth one is *anti* to the others (u,u,u,d);

c. The "*1,2-alternate*", where two adjacent hydroxy groups are *syn* to each other and *anti* to the other two hydroxy groups (u,d,u,d); and

d. The "*1,3-alternate*", where alternating hydroxy groups are *syn* to each other and are *anti* to adjacent hydroxy groups (u,u,d,d).

Calix[4]naphthalenes show the same four major conformations as calixarenes (Figure1.9), but they also show additional characteristics which are not associated with calixarenes. When calix[4]naphthalene inverts through its annulus it forms its own enantiomer. Therefore calix[4]naphthalenes are inherently chiral (Figure1.10). When the

calix[4]naphthalene inverts through its annulus, the direction in which the naphthalene rings point becomes inverted.

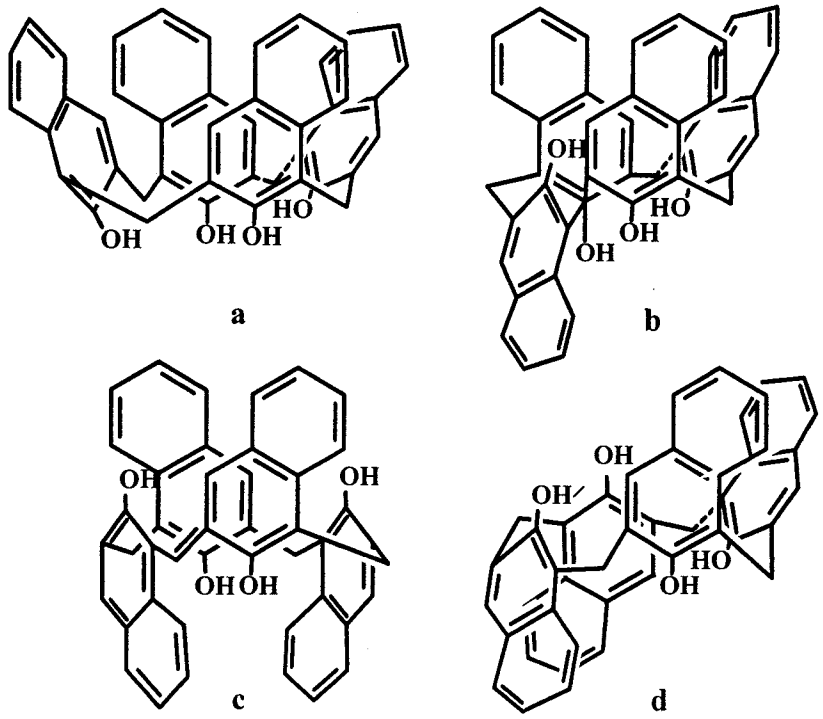

Figure 1.9. Conformational isomers of calix[4]naphthalene.[4]

1.3.1. The Conformations of Calix[6]arenes and Calix[8]arenes

While calix[4]arenes show a true up/down direction, calix[6]arenes and calix[8]arenes are larger and more flexible.[14] The aryl groups are no longer perpendicular but point at angles of 45° or more either toward the center, interior or to the exterior of the intrannular ring.

In the solid state, calix[6]arene adopts one of two conformations, the *"pinched cone"*[15] or the *"1,2,3-alternate"*[15] conformations. In solution, calix[6]arene can adopt a

third conformation, the *"winged cone"*[15] conformation. These conformations are defined as shown in Figure 1.11.:

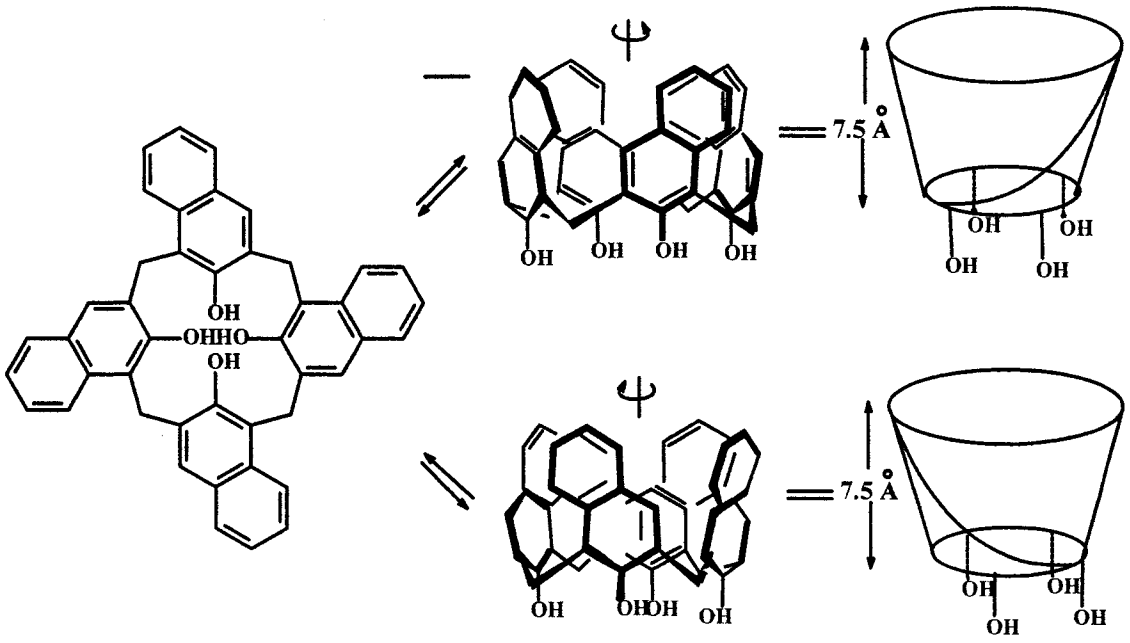

Figure 1.10. Interconversion between enantiomeric *cone*-conformers of 8.

a. The "p*inched cone"* or *"winged"* conformation, in which all oxygens lie on the same side of the molecule and two opposite methylene groups point toward the center of the cavity;

b. The *"1,2,3-alternate"* or *"double partial cone"* conformations, in which three adjacent oxygens are found on one side and the other three oxygens are found on the opposite side of the molecule; and

c. The *"winged cone"* conformation which shows an outward orientation of all methylene groups where two opposite phenols are bent outward and the four other aryl groups are aligned in an upward orientation.

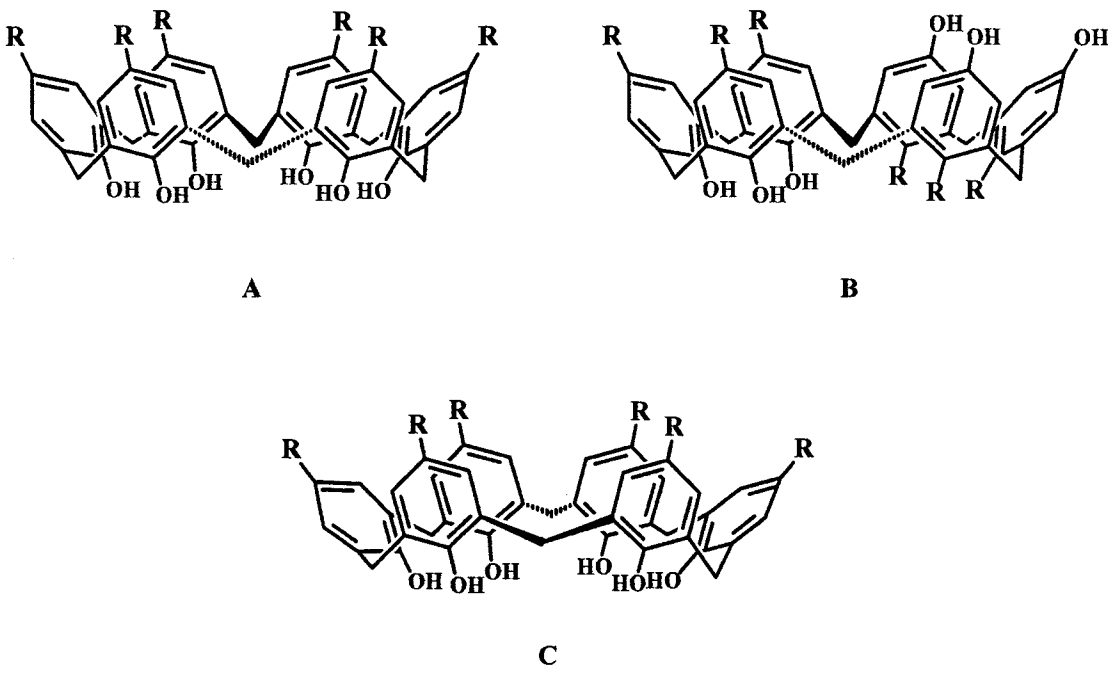

Figure 1.11. Conformational isomers of calix[6]arene.

Calix[8]arene is a larger calixarene which would indicate that it has greater flexibility; however, calix[8]arene shows an affinity for the *"pleated loop"* conformation (Figure 1.12).[16,17]

1.4. Synthesis of Calixarenes and Calixnaphthalenes

1.4.1. One-Pot Procedure for the Synthesis of Calixarenes

1.4.1.a. Base-Catalyzed Synthesis of Calixarenes

Over fifty years ago Zink and Ziegler reported the first synthesis of a cyclic tetrameric structure,[18] now known as a calix[4]arene, from the base-catalyzed reaction of *p*-alkylphenols with formaldehyde at high temperature. However, this simple synthesis was unreliable and difficult to reproduce.

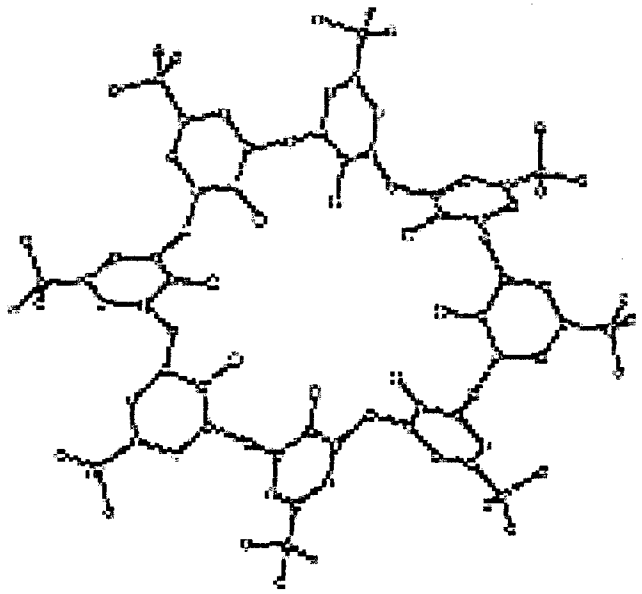

Figure 1.12. The "*pleated loop*" conformation of calix[8]arene.[16]

During the 1970's Gutsche and co-workers developed more reliable syntheses of calix[4]arene, calix[6]arene and calix[8]arene.[19] These base-catalyzed reactions employed different amounts of either NaOH or KOH and diphenylether or xylene as solvents with *p*-tert-butylphenol and formalin. Some optimized reactions are shown in Scheme 1.1.

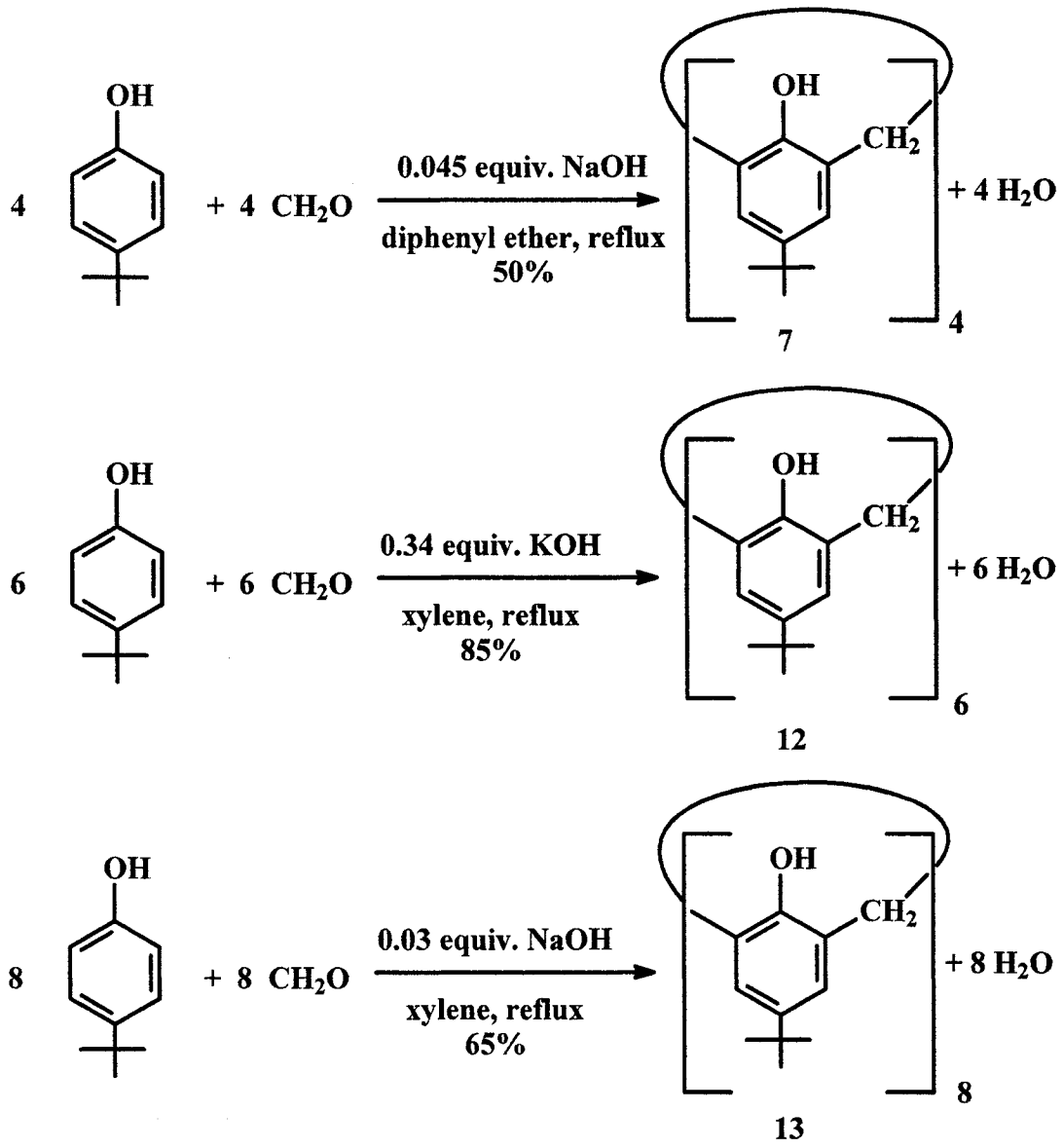

Scheme 1.1. Optimized conditions for the base-catalyzed synthesis of calix[*n*]arene (*n*= 4, 6, 8).[6]

1.4.1.b. Acid-Catalyzed Synthesis of Calixarenes

Previously, it was thought that the condensation of *p*-alkylphenols with paraformaldehyde in acidic conditions only gave long-chain polymers; however, more in-depth studies of such condensations have been shown to yield large calix[*n*]arenes, where *n*

≥ 20. The yields of the large calixarenes were found to be almost quantitative.[1,20] Though largely base-induced, the synthesis of other calixarenes can also be achieved using acid-catalyzed reactions. A wide range of acid conditions have been used e.g. the reaction of the hydroxymethyl compound **14** with a Lewis acid such as $TiCl_4$ in refluxing dioxane for 110 hours afforded the calix[4]arene **15** (Scheme 1.2)with 5-29% yeild.[21,22]

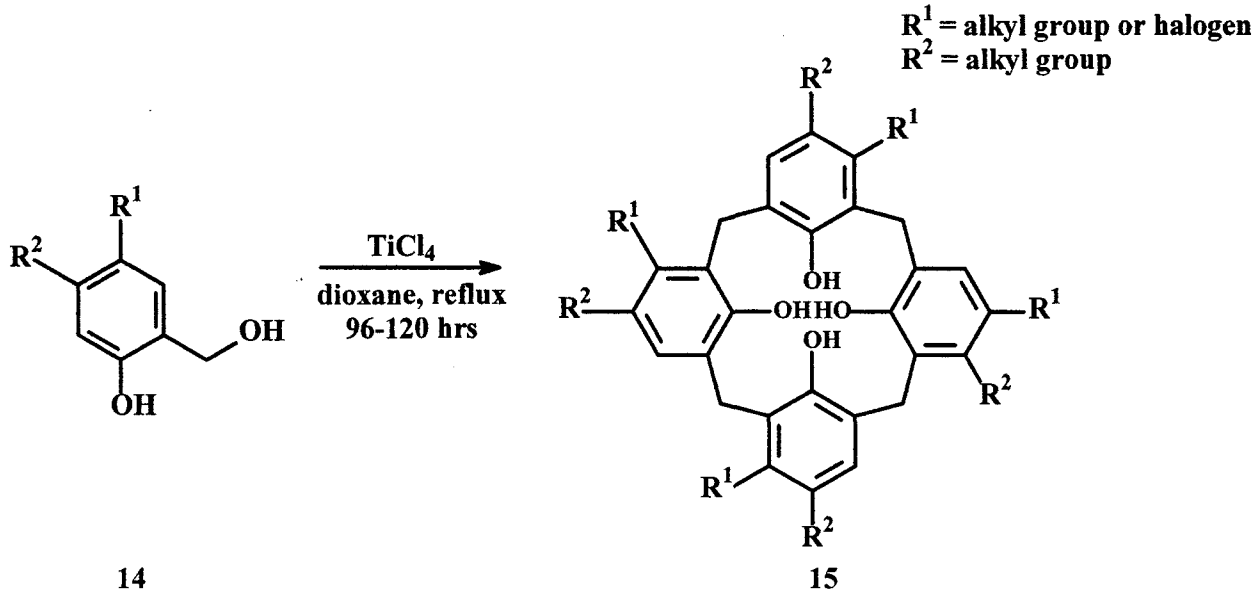

Scheme 1.2. Acid-catalyzed synthesis of calixarenes.[6]

1.4.2. Stepwise Synthesis of Calixarenes

The synthesis of calixarenes having different *para*-substituents on their individual subunits can be achieved using a stepwise procedure. Two examples of stepwise procedures are (a) non-convergent syntheses, and (b) fragmentation syntheses. Stepwise procedures in general, have a disadvantage of being lengthy and giving low overall yields.

1.4.2.a. Non-Convergent Syntheses[23]

In non-convergent syntheses of calixarenes, the *para*-alkylated phenols are incorporated one at a time (Scheme 1.3). A common procedure is to start with *o*-bromo-*p*-

alkylphenol and use alternating hydroxymethylations. The eventual oligomer formed needs to have a hydroxymethyl group at one end to perform the final condensation step which will form the final methylene bridge. The opposite end would then have a bromine atom (as a blocking group) in the *ortho*-position which would have to be removed. The subsequent condensation step would have to be carried out in high dilution so that the oligomers do not react with one other to form undesired long-chained polymers. The synthesis of calix[*n*]arenes in this manner involves several reactions, which increase in number as *n* becomes larger. Each step required to synthesize the desired calix[*n*]arene results in a decrease in the overall yield.

1.4.2.b. Fragmentation Condensations

Böhmer *et al.*[24] used a typical fragmentation-type synthesis of calixarene. In a non-convergent synthesis of calixarenes the final step involves an intramolecular cyclocondensation. By contrast, the fragmentation synthesis joins two or more fragments for the intermolecular condensation step. The methods employed to develop a wide range of calix[4]arenes with varying substituents at the *para*-positions are the [3+1],[25, 26] the [2+2][27] (Scheme1.4), and the [2x1+2x1][24] cyclization reactions.

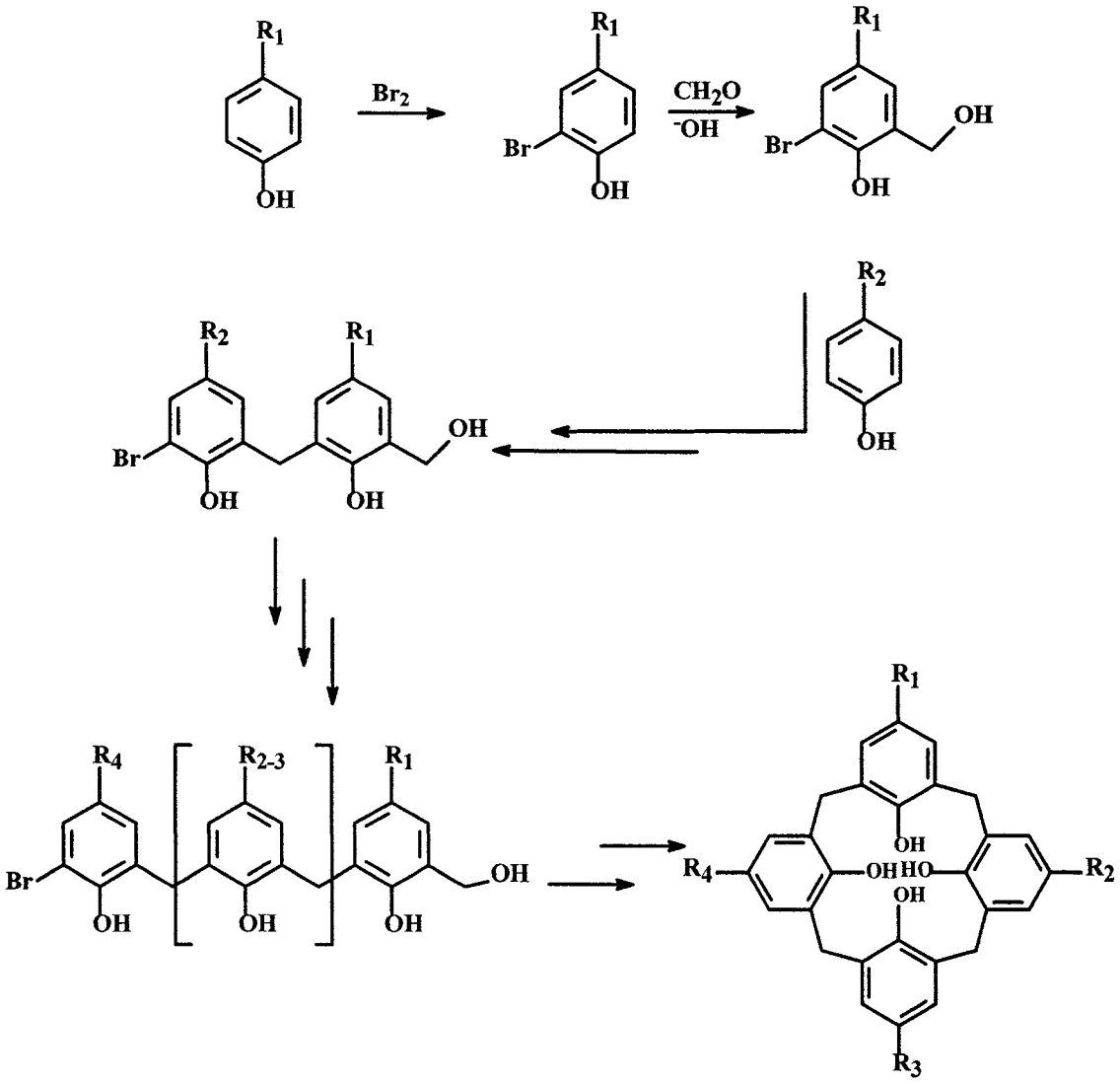

Scheme 1.3. Nonconvergent synthesis of *p*-tetraalkylcalix[4]arenes.[6]

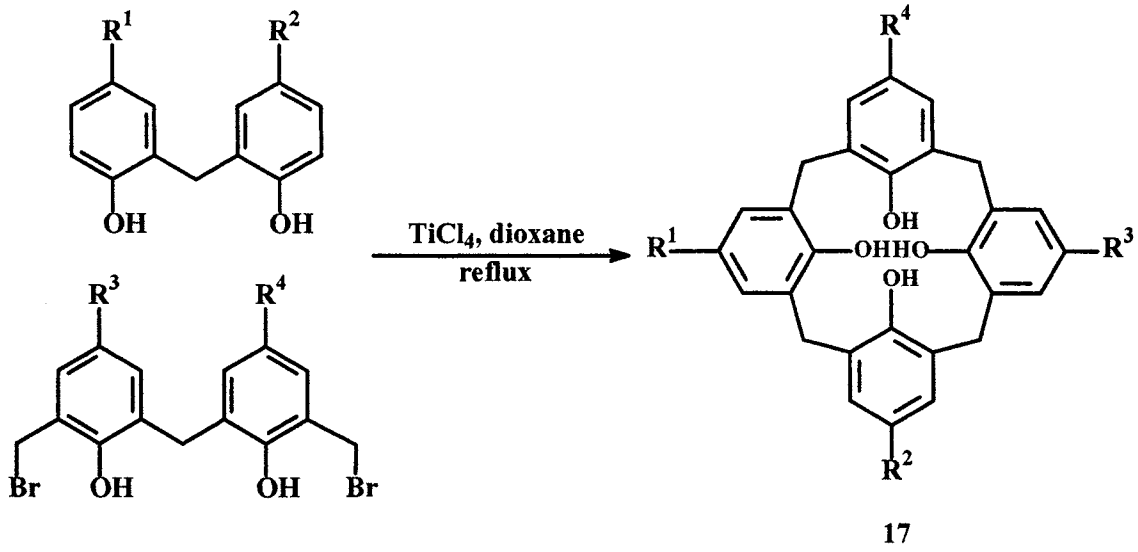

17

Scheme 1.4. A typical [2 + 2] fragmentation condensation.[6]

1.4.3. Synthesis of Calix[4]naphthalenes

Li and Georghiou reported the first synthesis of an *exo*-calix[4]naphthalene[11] by the cyclocondensation of 1-naphthol and paraformaldehyde, in DMF with K_2CO_3. Of the four potential regioisomers designated "C-11", "C-12", "C-23" and "C-44" on the basis of their expected ^{13}C NMR spectra (Figure 1.11), only "C-12" was not found. However, the yields of all three regioisomers were low and they were difficult to separate.

Böhmer *et al.* were the first to synthesize the *endo*-calix[4]naphthalene **8** in a 5% yield,[28] by a $TiCl_4$-mediated cyclocondensation of 3-(hydroxymethyl)-2-naphthol in dioxane. However, they did not fully characterize the molecule. Ashram and Georghiou[6] re-investigated the Böhmer's conditions and found the conditions to be unreliable. However, they did improve on the conditions to get a reproducible 13% yield of **8** and a 31% yield for the *tert*-butyl derivative, **9**. The synthesis (Scheme 1.5) of **8** starts with the methylation of 3-hydroxy-2 naphthoic acid (**18**) to give methyl-3-hydroxy-2-napthoate (**19**)

in 97% yield, which is then reduced by $LiAlH_4$ to give 3-(hydroxymethyl)-2-naphthol (**20**) in 94% yield. The final step is the cyclocondensation of **20** to yield calix[4]naphthalene (**8**).

The synthesis of the *tert*-butyl derivative (Scheme 1.6) involves alkylation of **18** via the ester using Friedel-Crafts conditions to give methyl-7-*tert*-butyl-3-hydroxy-2-naphthoate (**21**) in 73% overall yield. This is then followed by the reduction and cyclocondensation steps to give respectively, a 90% yield of 6-*tert*-butyl-3-hydroxymethyl-2-naphthol (**22**) and a 31% yield of *tert*-butylcalix[4]naphthalene (**9**).

As indicated previously, the synthesis of calix[4]naphthalenes still needs to be optimized in order to have large enough quantities to further investigate their properties. Two relatively new methods for synthesizing similar macrocyclic compounds have recently been published.[29, 30] Ionic liquids have shown promise in the synthesis of compounds such as cyclotriveratrylene (CTV),[29,30] and another recent publication has described the synthesis of a calix[4]azulene **11** using a Florisil-mediated cyclocondensation.[8] Chapter 2 will discuss attempts to synthesize *endo*-calix[4]naphthalene **8** in ionic liquids; Chapter 3 will discuss attempts to synthesize **8** using Florisil.

1.5. Supramolecular Complexation Properties of Calixarenes and Calixnaphthalenes

The *"cone"* conformers of calix[4]arenes and calix[4]naphthalenes suggest that they may be able to sequester other species, such as metal ions, or even organic molecules into their cavities using intramolecular forces to form complexes. These multi-species complexes are known as supramolecular complexes.

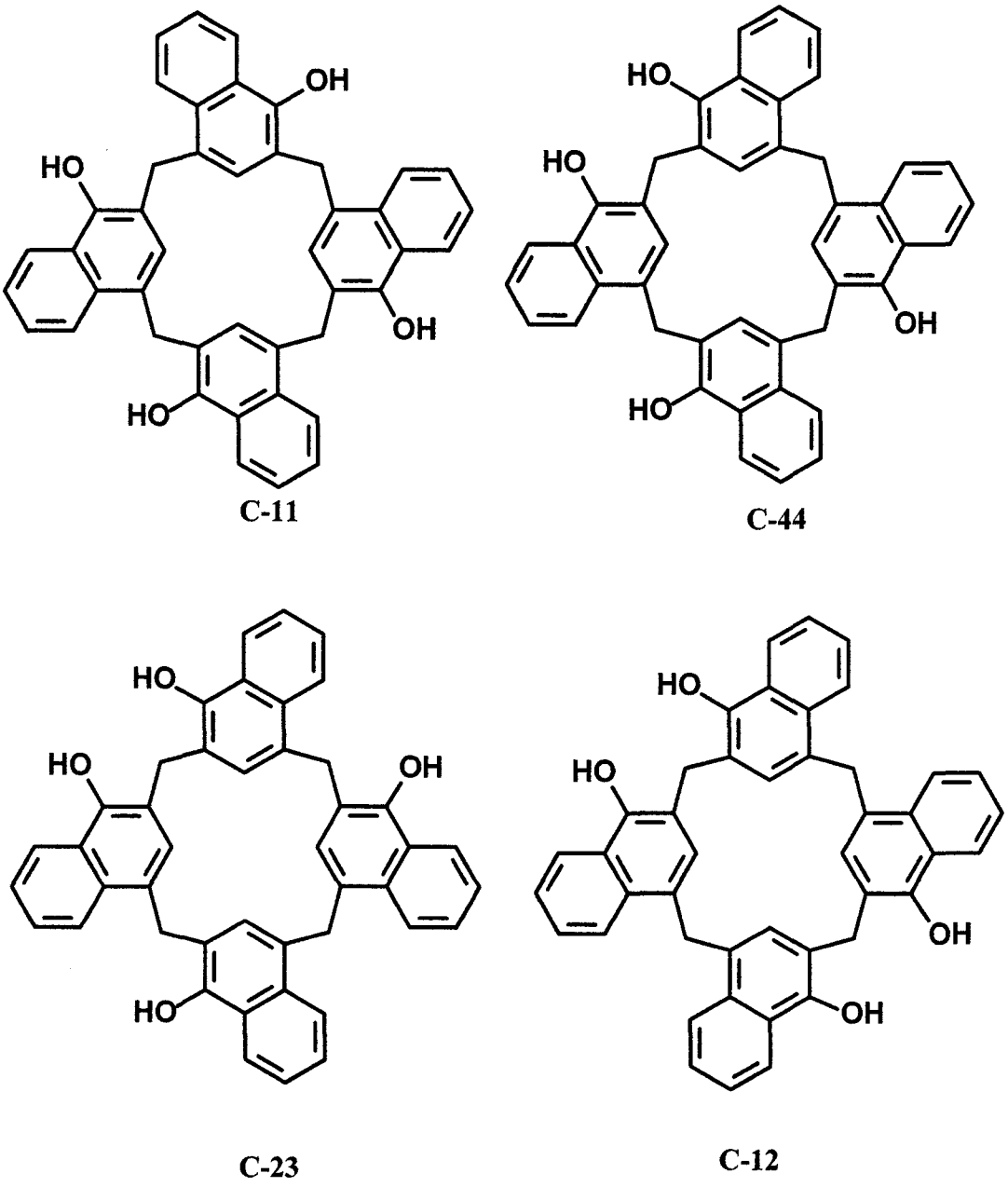

Figure 1.13. The four regioisomers of *exo*-calix[4]naphthalene.

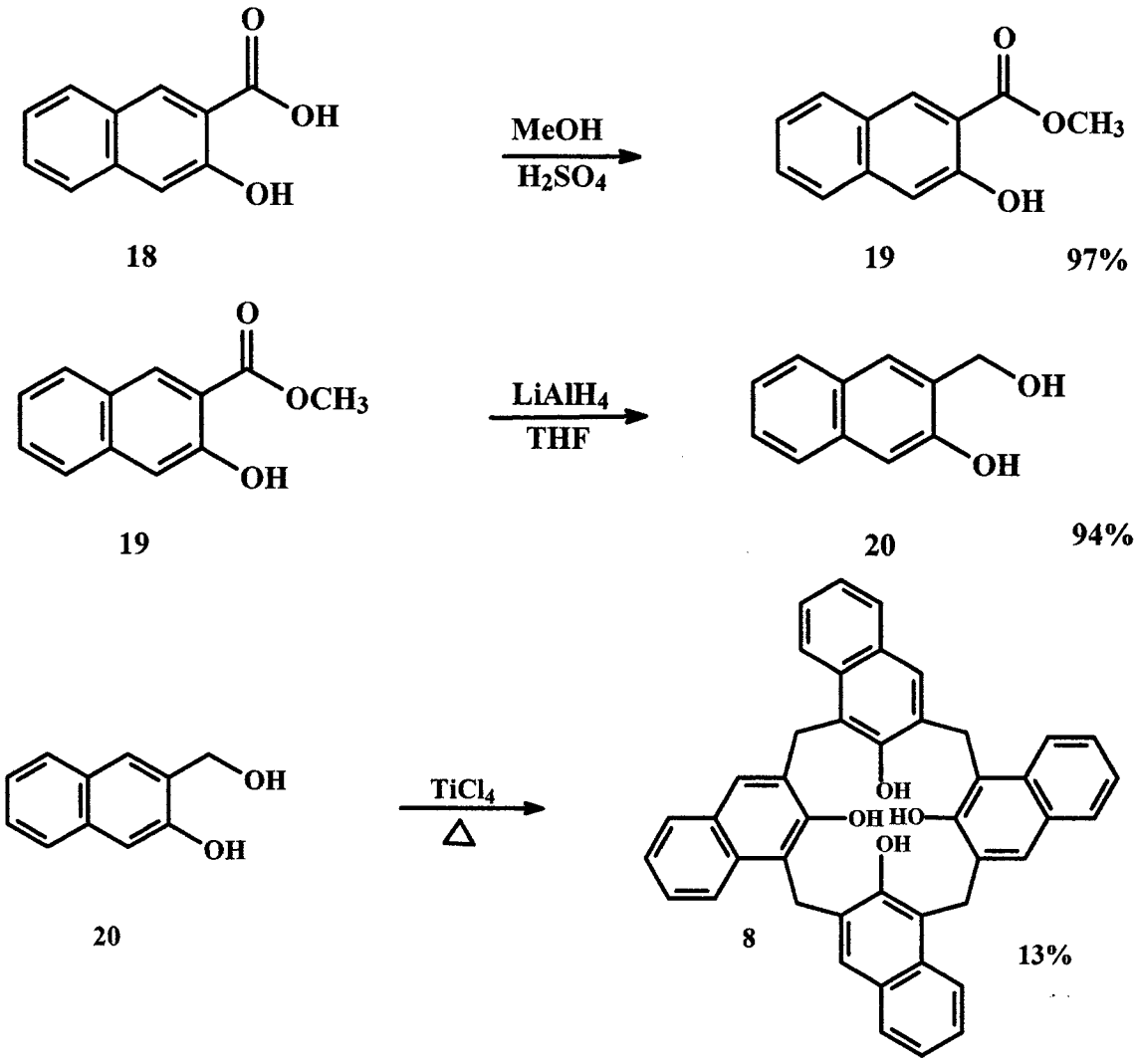

Scheme 1.5. Synthesis of calix[4]naphthalene 8.

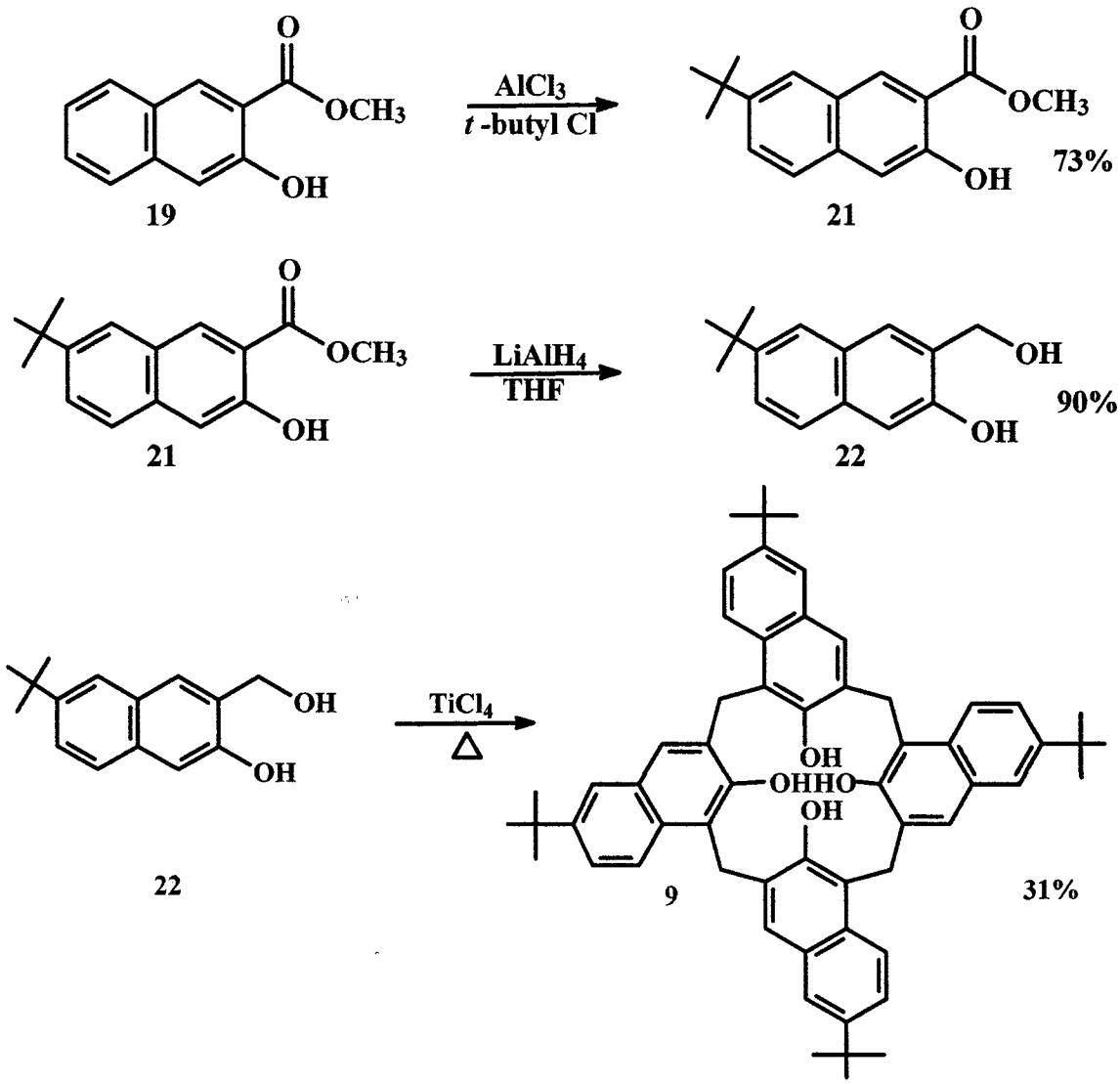

Scheme 1.6. Synthesis of *tert*-butylcalix[4]naphthalene 9.

It has been shown by several groups that calixarenes can form supramolecular complexes with C_{60}.[31-35] The structures of several such complexes have been determined by X-ray crystallography. Complexations studies in solution in various solvents have been used to determine the association equilibrium constants, K_{assoc} (Equation 1.1) for such complexes, where [H] is defined as the concentration of the host molecule, [G] is defined

as the concentration of the guest molecule and [H:G] is defined as the concentration of the complex.

$$K_{assoc} = \frac{[H:G]}{[H]\bullet[G]} \qquad (1.1)$$

1.5.1. Supramolecular Complexation Properties of Calix[*n*]arenes

The study of supramolecular complexes is typically conducted using ultraviolet-visible (uv-vis) spectroscopy. Uv-vis spectroscopy can be used to measure the changes in the absorbance spectrum of a pure compound when a second compound is added to the solution. A significant change in the absorbance spectrum can be related to the formation of a new product, such as a complex. The absorbance data can be analyzed using several different methods to determine the association constant, K_{assoc}, as long as the changes in absorbance are related to the formation of a complex or a new reaction product, and are not a result of simple addition.

Tert-butylcalix[4]arene shows little absorbance change when added to a solution of C_{60}.[36] This indicates that calix[4]arene does not easily form a complex with C_{60}. This may be due to the fact that the diameter of C_{60} is 10.2 Å, whereas the maximum width of the *tert*-butylcalix[4]arene basket is only 8.4 Å, and thus C_{60} would not be expected to fit into the "basket". However, it has been proposed that a short lived monomeric 1:1 intermediate between *tert*-butylcalix[4]arene and C_{60}, does form.[31] This intermediate distorts the electron cloud of C_{60}, favoring a micelle-like formation featuring fullerene-fullerene interactions in the interior core. In this intermediate the C_{60} is completely encapsulated by *tert*-butylcalix[4]arene molecules.

Tert-butylcalix[6]arene is a larger and more flexible calixarene and with a correspondingly larger "basket". The increased size of the concave surface of *tert*-butylcalix[6]arene allows for a longer-lived complex with C_{60} than for *tert*-butylcalix[4]arene. As mentioned previously, *tert*-butylcalix[6]arene also differs from *tert*-butylcalix[4]arene in its conformations. In complex formation with C_{60} the latter is in a "*cone*" conformation whereas the former adopts a "*double-cone*" conformation (Figure 1.14). The addition of *tert*-butylcalix[6]arene has been shown to induce a significant change in the uv-vis spectrum of C_{60}. This has been associated with the inclusion of two C_{60} molecules into the "*double cone*" cavities of the *tert*-butylcalix[6]arene.[32] *Tert*-butylcalix[6]arene was shown to form a complex with C_{60} and C_{70} in a 2:1 ratio of fullerene to calix[6]arene in both cases. This was seen in both the solid state and in solution. The stabilization of the "*double cone*" conformation was not lost when the two fullerene molecules were encapsulated into the calixarene. The resulting K_{assoc} was found to be 230 ± 4 M^{-1} in toluene.

In 1992 Verhoeven[33] reported on the absorbance spectra of C_{60} in toluene and the change in absorbance when *tert*-butylcalix[8]arene is added. He observed a change in absorbance which he interpreted to result from charge-transfer interactions, where the electron-rich calixarene donates an electron to the electron-poor C_{60}. Atwood[34] and later Shinkai,[35] both found that C_{60} and *tert*-butylcalix[8]arene in toluene formed a precipitate which was later identified to be a 1:1 complex. Further investigation revealed that calix[8]arene did not maintain its conformation in the same way that calix[6]arene does.

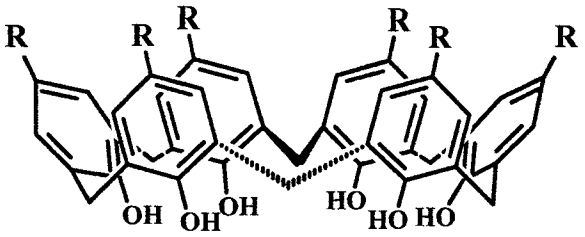

Figure 1.14. ***Double cone*-conformation of a calix[6]arene.**

A change in infrared (IR) absorbance due to the $\nu_{O\text{-}H}$ stretch was observed. This change indicated that the calix[8]arene switches from a *"pleated-loop"* conformation to a *"two-winged"* conformation. The value of K_{assoc} was determined to be 381 ± 4 M^{-1} in toluene. However, this complex dissociates in chloroform and in dichloromethane.[34] These solvents compete with C_{60}, interacting with the aromatic rings of the calixarene, and when this occurs there is no longer room for the C_{60} to be encapsulated within the cavity of the calixarene. As a result, the complex is broken.

The unique properties of the calix[8]arene: C_{60} complex reveals a simple application of this kind of chemistry. When added to a solution of fullerenes such as is found in "fullerite", calix[8]arene will only bind with C_{60} and not with other fullerenes such as C_{70}. As a result, calix[8]arene can be used to purify C_{60}, since it forms an insoluble complex in toluene, and precipitates. The collected precipitate is dissolved in chloroform causing the complex to dissociate: calix[8]arene is soluble in chloroform and remains in solution whereas C_{60} is insoluble in chloroform and precipitates out of solution (Scheme 1.7). This procedure allowed for an effective separation/purification of C_{60} and C_{70}.

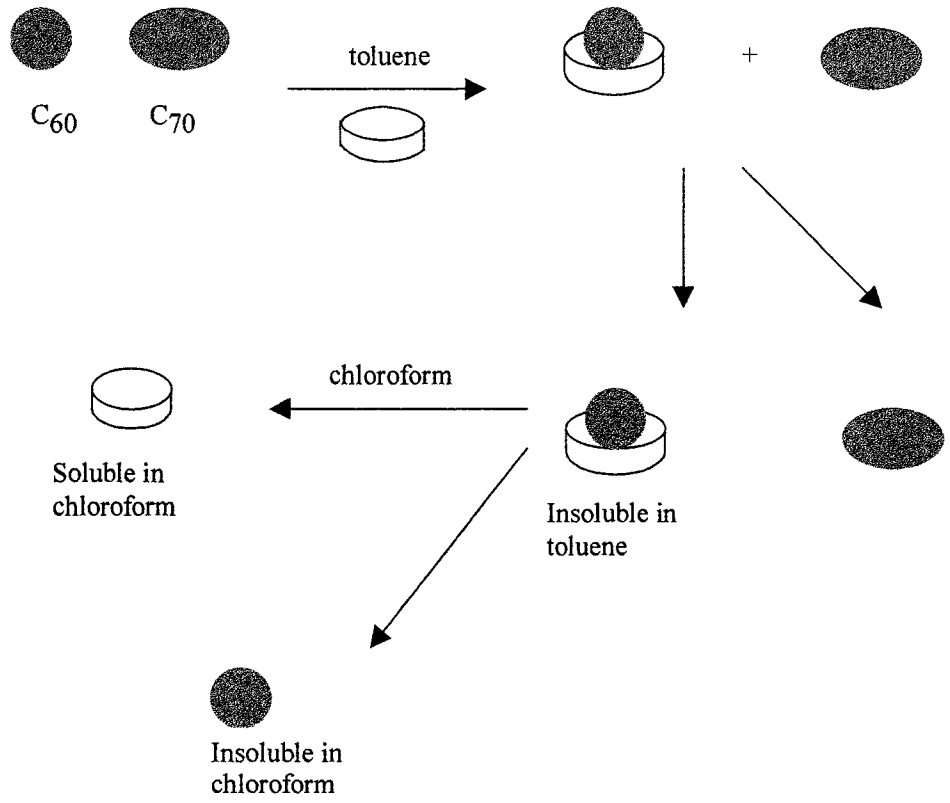

Scheme 1.7. Purification of fullerene mixture containing a mixture of C_{60} and C_{70} using octa-*tert*-butylcalix[8]arene.

1.5.2 Supramolecular Complexation Properties of Calix[4]naphthalene

As can be seen from Figures 1.4 and 1.5, calix[4]naphthalenes have larger, more π-electron-rich cavities than calix[4]arenes. The increased size of the "basket" gives a greater potential for the inclusion of neutral, electron-deficient or electron-poor guest molecules such as C_{60}. The second aromatic ring on each subunit of a calix[4]naphthalene allows for increased π-π interaction between guest and host compared to calix[4]arenes.

The color of C_{60} in benzene, toluene and carbon disulfide (CS_2) is purple, or magenta. Addition of calix[4]naphthalene to a solution of C_{60} causes a change from magenta to brown.[4] Such color changes in solutions are often an indication that a complex

has been formed. The same color change is observed when *tert*-butylcalix[4]naphthalene is added to a solution of C_{60}, again indicating the formation of a complex.

Previous work in our group studied the uv-vis spectra of C_{60} after the addition of both calix[4]naphthalene **8** and its *tert*-butyl derivative **9**. Similar bands to those reported by Verhoeven[33] with calixarenes, and by Atwood[34] with CTV were found. It was determined that the spectral changes caused by the addition of calix[4]naphthalene to C_{60} are a result of a complex (or complexes) being formed. A continuous variation method (see Chapter 4, section 4.1.2) was used to determine the stoichiometry of the complex being formed in each case, and revealed 1:1 complexes were formed, as follows:

$$\mathbf{8} + C_{60} \rightleftharpoons \mathbf{8}{:}C_{60} \qquad \textbf{(1.2.)}$$

$$\mathbf{9} + C_{60} \rightleftharpoons \mathbf{9}{:}C_{60} \qquad \textbf{(1.3.)}$$

The K_{assoc} equation can therefore be defined as:

$$K\text{assoc} = \frac{[8{:}C60]}{[8]\bullet[C60]} \qquad \textbf{(1.4.)}$$

$$K\text{assoc} = \frac{[9{:}C60]}{[9]\bullet[C60]} \qquad \textbf{(1.5.)}$$

1.6. The Problem

Calix[4]naphthalenes **8** and **9** have proven to be challenging synthetic targets. The on-going investigation into their supramolecular properties provided incentive to optimize their syntheses. This prompted the exploration of the use of ionic liquids, a new medium for organic synthesis, to help increase the yields of **8** or **9**. Ionic liquids have shown promise for this type of chemistry, as a result of the successful synthesis of

cyclotriveratrylene ("CTV" See scheme 2.4) in ≥ 85% yield directly from its precursor veratryl alcohol, by Moens' group.[29]

A different attempt to optimize the synthesis of **8** was investigated by the use of Florisil^R (instead of $TiCl_4$) to mediate the cyclocondensation of **20** to form **8**. Florisil^R had previously been shown by Colby and Lash[8] to facilitate the synthesis of calix[4]azulene (**11**) in relatively high yields.

The availability of **11** in relatively high quantities prompted an investigation into its supramolecular properties in conjunction with the previously mentioned on-going supramolecular studies in our lab, since it represented a novel hydrocarbon analogue of the calix[4]naphthalenes.

1.7. Description of Thesis Content

In this thesis, attempts to improve the cyclocondensation of **8** using two new methods are described. As well, the complexation properties of **11** with C_{60} were studied, using both ^1H NMR spectroscopy and uv-vis spectrophotometry.

Chapter Two of this thesis discusses the results which were obtained from the synthesis of CTV using ionic liquids as the solvent system, and catalysis using several different Lewis acids. The results obtained from the attempted cyclocondensation of **20** to form **8,** using similar methods as were used for the synthesis of CTV are discussed.

Chapter Three discusses the attempted synthesis of **8** using Colby and Lash's Florisil-mediated conditions[8] for the cyclocondensation of **20**. This cyclocondensation was also attempted using the Florisil-mediated system in conjunction with several different Lewis acids.

Chapter Four describes the results of the complexation of **11** with C_{60} in different solvents as determined by uv-vis spectrophotometry and NMR spectroscopy.

Chapter 5 discusses the results obtain from an analysis of a complexation study of hexa-*tert*-butylhexamethoxycalix[6]arene **44** and octa-*tert*-butlyoctamethoxy-calix[8]arene **45** with C_{60} using CS_2 as the solvent.

Chapter 2

Progress Toward the Synthesis of Calix[4]naphthalene in Ionic Liquids

2.1. Introduction

Traditionally, synthetic organic chemistry is usually carried out in organic solvents. Organic solvents have a variety of properties, such as low viscosity and a wide range of melting points (m.p.) and boiling points (b.p.), which make them useful for organic synthesis. For instance, a reaction which requires low temperatures would be conducted in a solvent which has a freezing point (f.p.) below the temperature required. A reaction which requires high temperatures would be conducted in an organic solvent which has a high boiling point and high thermal stability. Organic solvents range from nonpolar solvents, characterized by a low dielectric constant, such as hexanes or benzene, to polar solvents, such as ether or ethyl acetate which have dielectric constants that are somewhat higher. The organic solvent which is chosen to conduct the desired chemical reaction is related to the polarity of the starting material.

Organic solvents also have some less desirable properties. Many organic solvents, such as chloroform, are volatile and relatively toxic. As well, a large number of organic solvents such as diethyl ether, are highly flammable.[37] Hazards such as these, including environmental effects, mean that chemists have to take appropriate precautions when using organic solvents. Though the usefulness of organic solvents is indisputable, efforts have been made to discover new, safer media for synthetic reactions.

A new class of solvents, collectively called "ionic liquids", has recently been reported in the literature as useful solvent systems for diverse organic reactions. The first ionic liquid discovered, in 1914, was ethylammonium nitrate.[38] A diverse range of ionic

liquids have since been developed and they have been used for many different purposes in many fields of chemistry.

2.1.1. Ionic liquids: Definition and Properties

2.1.1.a. Definition

The simplest definition of an ionic liquid is that it is a type of molten salt.[39, 40] Molten salts include a large number of liquid state ionic compounds, such as sodium chloride (NaCl), which melts at 801 °C.[37] Liquid NaCl is a highly viscous and corrosive substance, and as such is not practical for most chemical requirements or study. The definition of ionic liquids has been further refined to salts which are liquids at relatively low temperatures (below 100 °C).[39] These lower temperature ionic liquids are much more convenient and easier to employ.[41] The salts which are liquids at these lower temperatures have lower viscosity and are less corrosive,[39] and so they are easier and safer to handle.

2.1.1.b. Melting Points

Ionic liquids have relatively low melting points which are related to their compositions. Alkali metal salts such as NaCl or potassium iodide (KI) have strong attractions between their ions in each case, creating a tight lattice and resulting in high melting points. NaCl and KI have melting points of 801 °C and 770 °C, respectively. If the alkali metal is replaced by an organic cation, such as dialkylimidazolium, alkylpyridinium or tetraalkylammonium, the melting point of the resulting salt drops below 150 °C (Figure 2.1).[39, 42]

The decrease in melting point is related to many of the characteristics of the cation/anion pair, such as low symmetry,[43] widely dispersed charge[44] and a decrease in

intermolecular interactions.[45] The three examples of organic cations shown below, all low symmetry, which inhibits and interferes with the formation of single crystals. If the ionic liquid possesses a large cationic moiety,[39] it would be expected that the distance between the opposing charges will increase therefore causing the melting point to decrease.

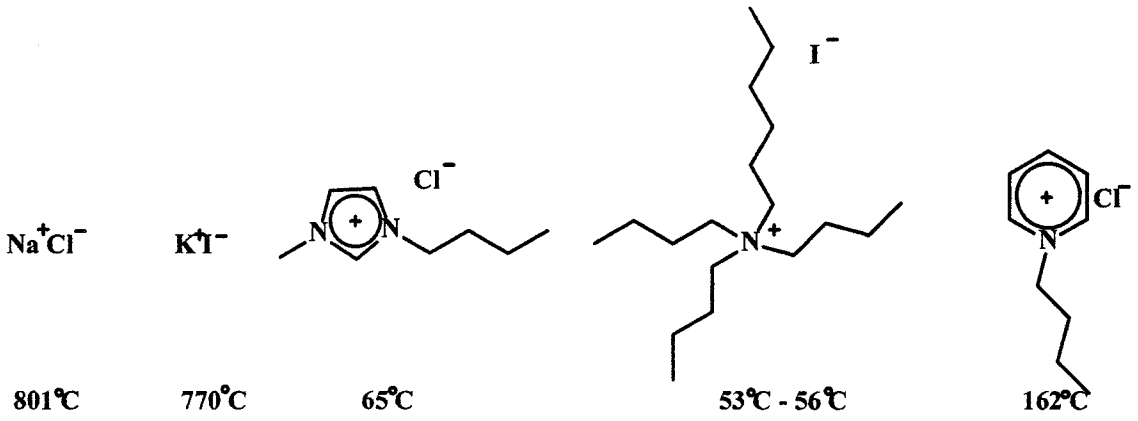

Figure 2.1. The effect of the cation on the melting points of salts.

The melting points of ionic liquids are also dependent on the nature of the anion.[39] In general, the larger the anion, the lower the melting point (Figure 2.2). The PF_6^- anion has an anionic radius which is much lager than that of the chloride ion, and this results in a depression of the melting point.

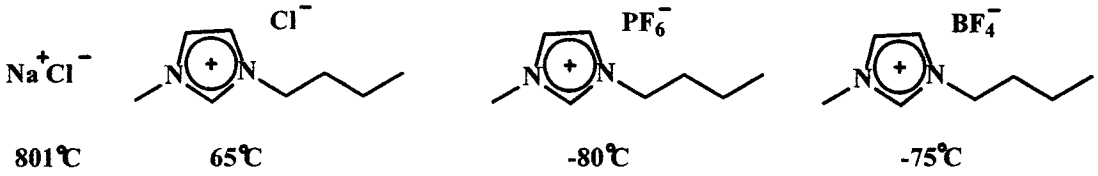

Figure 2.2. The effect of the anion on the melting points of salts.

2.1.1.c. Viscosity

The viscosities of ionic liquids are much lower than those of other molten salts. The lower viscosity makes ionic liquids easier to handle; they can be easily transferred from one flask to the next and they can be weighed accurately, since no loss due to volatility occurs. The viscosity of a liquid is related to the degree of intermolecular interactions such as, hydrogen bonds, van der Waals interactions, London forces and dipole-dipole interactions. As a result, the viscosity of an ionic liquid is strongly related to its composition.[40] An example of the effect of composition on the viscosity is the apparent dipole-dipole interactions which exist between ions of an ionic liquid. The strength of a dipole-dipole interaction is proportional to $1/r^7$, where r is the distance between charges. It becomes obvious how the short distance which exists between small ions creates a highly viscous liquid, such as liquid NaCl, and how a small increase in the distance between ions will decrease the viscosity significantly. For example, 1-butyl-3-methylimidazolium chloride ([bmim]Cl), has greater distance between its ions, than NaCl and therefore has a greatly decreased viscosity.

An example[46] of composition affecting the viscosity can be seen by changing the concentration of aluminum chloride ($AlCl_3$) in an ionic liquid. When the ratio of $AlCl_4^-$ to [bmim] is 0.35:1 in [bmim]$AlCl_4$, this gives rise to an ionic liquid with a higher viscosity than when the ratio is increased to 0.5. The origin of this effect can be rationalized by the equilibrium between $2AlCl_3 + Cl^-$ and $Al_2Cl_7^-$. The larger $Al_2Cl_7^-$ increases electron distribution and reduces the charge density.

2.1.1.d. Solvation Strength and Solubility Characteristics

Ionic liquids as solvents, have a wide range of solvation and solubility properties which are related to the combination of anions and cations chosen. Ionic liquids are capable of solvating a wide range of organic and inorganic compounds.[39] Small changes in the composition can change the polarity of the ionic liquid. For example, the butyl chain on [bmim]PF_6, can be exchanged for an ethyl group to create a more polar ionic liquid. To create a less polar ionic liquid, the butyl chain can be exchanged for a six-carbon or larger chain.[47]

Exchanging the anion[45] will also affect the solubility of an ionic liquid. For example, the 1-butyl-3-methylimidizolium cation forms hydrophobic ionic liquids with the anions PF_6^- or $(CF_3SO_2)_2N^-$, whereas exchanging the anions for BF_4^-, Br^-, CF_3COO^- or $CF_3SO_3^-$ creates hydrophilic ionic liquids.

2.1.1.e. Thermal Stability and Vapor Pressure

Many ionic liquids are stable over a wide range of temperatures. For example,[45] 1-ethyl-3-methylimidazolium and bis(trifluoromethanesulfonyl)amide ion, which has a m.p. of -3°C and remains stable with temperatures exceeding 400 °C. However, the stability of an ionic liquid is limited by the strength of its heteroatom-carbon and heteroatom-hydrogen bonds.[39]

An important property of ionic liquids is the lack of any measurable vapor pressure.[29, 39] This means they do not evaporate and, unlike organic solvents, they are not lost to the atmosphere and the chance of fire and explosion is decreased. As well, this decreases the amount of breathable, harmful fumes. The lack of vapor pressure allows

liquid products to be distilled out of an ionic liquid without azeotrope formation. Ionic liquids can be used under vacuum without loss of the reaction medium.

2.1.1.f. Environmental Friendliness

Non-volatile ionic liquids decrease the toxic fumes being released into the environment, making them more environmentally-friendly than volatile organic solvents. Once an ionic liquid has been used to perform a chemical reaction, it can be easily cleaned, recovered and reused repeatedly. Caution however, must be taken when handling and disposing of ionic liquids. Their toxicity to humans and the environment remains largely unknown. It is recommended that ionic liquids should be handled according to how their components are handled. For instance,[39,48] an ionic liquid containing $AlCl_3$ should be handled as if it were the water-sensitive reagent, and should be kept in an anhydrous environment.

2.1.2. Ionic Liquids - A New Medium for Organic Synthesis

To date, many different kinds of organic reactions have been attempted in ionic liquids. There have been numerous methods described and used to perform organic reactions[40] in ionic liquids. The most obvious method is to place all the components of an organic reaction in a specifically chosen ionic liquid solvent. A second way to use ionic liquids is to add an ionic liquid to an organic solvent. Some experiments have shown that the presence of an ionic liquid reduces the number of side reactions in the organic reaction. A third method is to use the properties of solubility and miscibility and create a two- or three-phase system. In such a system, an ionic liquid is chosen which will dissolve the catalyst, then water or an organic solvent which is immiscible with the ionic liquid is

chosen to dissolve the starting materials. The layers are then vigorously stirred to allow contact between reactants and catalyst. If the ionic liquid and organic solvents are chosen properly, the product will remain in the organic solvent and the catalyst will remain in the ionic liquids, reducing the amount of subsequent purification required.

The number of reactions that have been conducted in ionic liquids has been growing rapidly in recent years, and these include Diels-Alder,[50] hydroformylation,[51-53] hydrogenation,[54,55] Heck reaction,[56] olefine dimerization[57,58] and many others. Two recent[29,30] reports on the cyclocondensation of veratryl alcohol (**29**) to form CTV in ionic liquids have appeared. These two reports were the inspiration for the attempts to synthesize calix[4]naphthalenes in ionic liquids, which is described in this thesis.

2.2. Synthesis of Ionic Liquids[59]

2.2.1. The Formation of Butylmethylimidazolium Hexafluorophosphate ([bmim]PF_6) (24)[60]

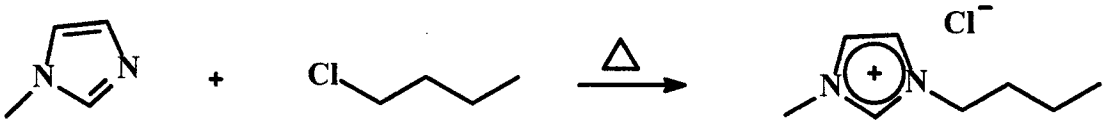

23

Scheme 2.1. The synthesis of 1-butyl-3-methylimidazolium chloride (23).

The formation of the *n*-butyl-methylimidazolium ion is accomplished by the *N*-alkylation of 1-methylimidazole with 1-chlorobutane (Scheme 2.1). The two reactants are mixed in the absence of any solvent. Two layers are formed over a 24 h period; the bottom layer is the ionic liquid, the top layer is the unreacted 1-methyl-imidazole and 1-chlorobutane. When the two layers form one unified layer, the reaction is complete. The

resulting salt is a clear, colorless crystal which is hygroscopic, and is stable under anhydrous conditions for several weeks. The chloride ion is then exchanged by the addition of hexafluorophosphoric acid under aqueous conditions (Scheme 2.2).

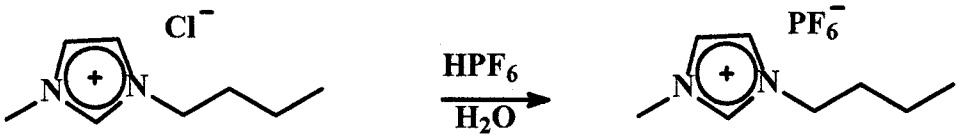

23 24

Scheme 2.2.The synthesis of 1-butyl-3-methylimidazolium hexafluorophosphate (24).

2.2.2. Synthesis of tri-*n*-butylhexylammonium ion with bis(trifluoromethanesulfonyl)-amide (N_{6444} Imide) (28)[61]

N_{6444} Imide (**28**) requires a convergent-type of synthesis, in that both the cation and anion must be synthesized separately, then put together (Scheme 2.3). We first attempted to form the cation by the alkylation of a tributylamine with 1-chlorohexane; however the chlorohexane was not active enough to alkylate the amine. The more reactive 1-iodohexane was then successfully used to synthesize the cation. The formation of the anion was accomplished by the deprotonation of $(CF_3SO_2)_2NH$ with *n*-butyllithium at -78 °C. The two ions were then combined under aqueous conditions to form the N_{6444} Imide.

2.3. Synthesis of CTV (31) in Ionic Liquids

2.3.1. Previous Work

In 2000, two groups reported the synthesis of CTV in ionic liquids. The first group was that of Moens *et al.*[29] who reported the synthesis of CTV in [bmim]PF_6 using vanadium acetate as the Lewis acid (Scheme 2.4). Their yields were not reported; however, in attempts to repeat the work, a 85 % yield of highly pure colorless crystals of CTV (**31**),

was achieved. The second group to report the synthesis of CTV was that of Scott *et al.*[30] who reported the use of N_{6444} Imide with H_3PO_4 as the acid catalyst (Scheme 2.5). They reported a yield of 89 % of **31**, which did not require purification. This result was easily reproduced in our lab, as could be ascertained by the NMR and mass spectra of the CTV produced (Section 2.6, Appendix A).

2.3.2. The Synthesis of CTV with a Range of Lewis Acids

CTV was easily prepared using Moen's conditions; however, it was unclear whether the cyclocondensation of veratyrol was dependent on the Lewis acids used in this reaction. We then explored the effect of changing the Lewis acid on the synthesis of CTV in ionic liquids. The reaction conditions developed in these experiments were then used to attempt to synthesize calix[4]naphthalene **8** and **9**.

Table 2.1. Yields using ionic liquids and a variety of Lewis acids in the synthesis of CTV.

Acid	Ionic liquid	% Yields
$TiCl_4$	**[bmim]PF_6**	**42 %**
$SnCl_4$	**[bmim]PF_6**	**68 %**
$Sc(OTf)_3$	**[bmim]PF_6**	**40 %**

Table 2.1 lists three Lewis acids which were used in the syntheses of CTV in [bmim]PF_6. Titanium (IV) chloride ($TiCl_4$) was chosen because it is the Lewis acid which has been used previously for the syntheses of calyx[4]naphthalenes **8** and **9**.

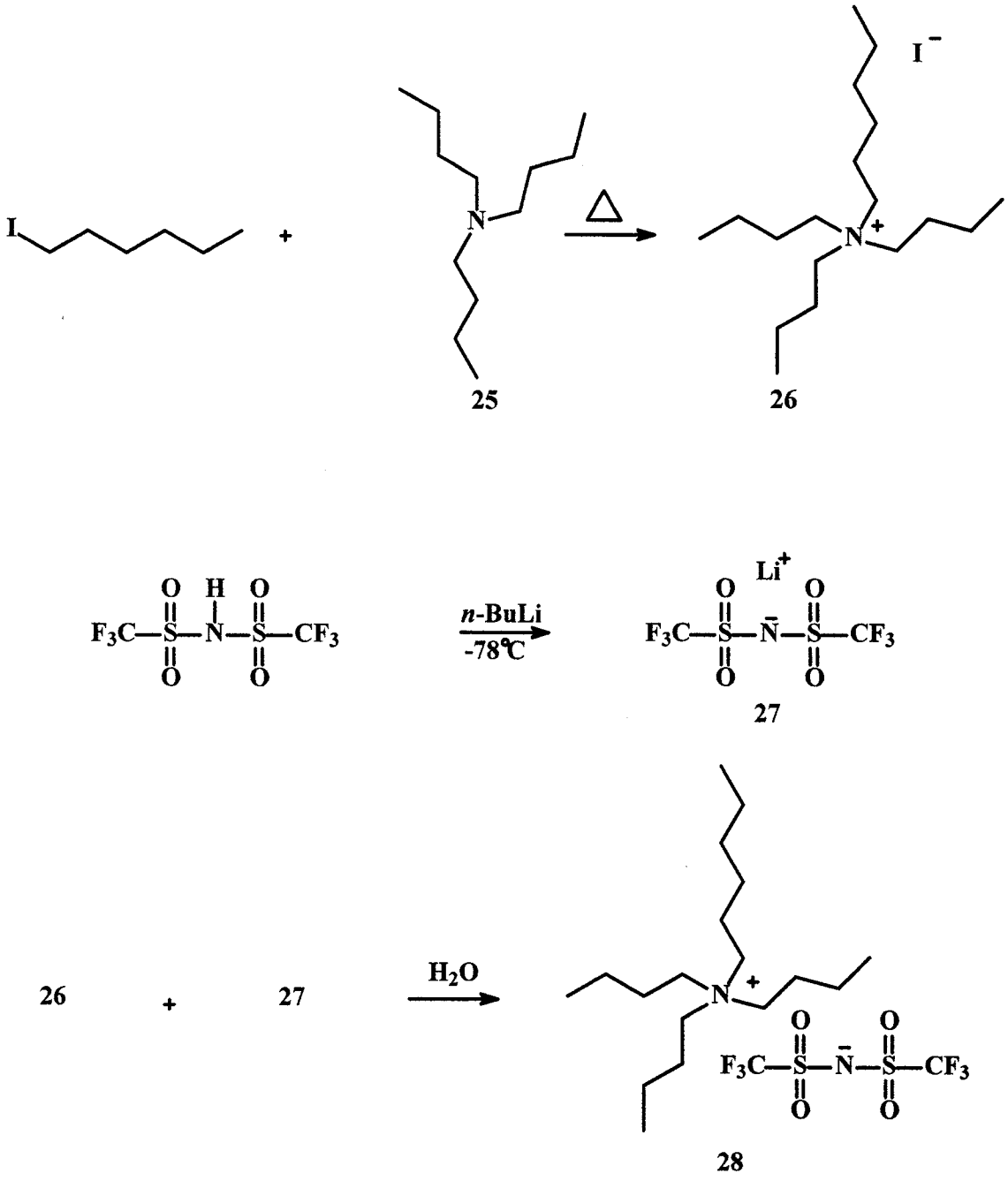

Scheme 2.3. The synthesis of N_{6444} Imide (28).

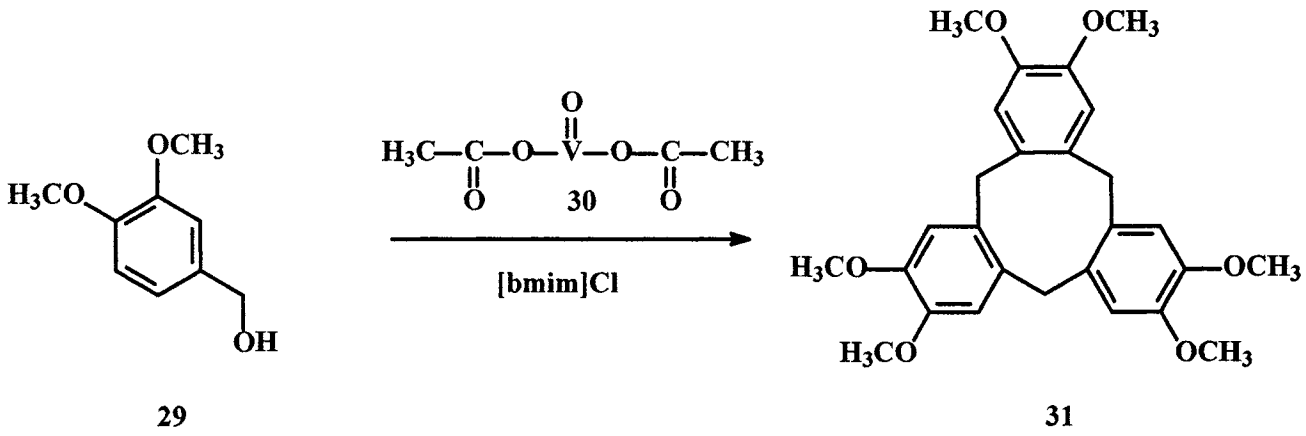

29 31

Scheme 2.4. The synthesis of CTV using Moens' conditions.[29]

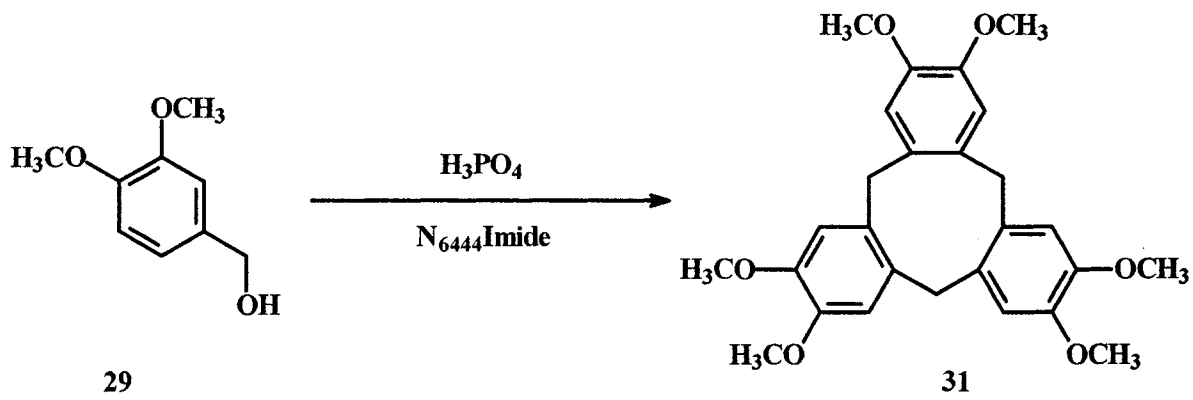

29 31

Scheme 2.5. The synthesis of CTV using Scott's conditions.[30]

When $TiCl_4$ was added to the reaction, the colorless ionic liquid turned to dark purple, and within several minutes formed a thick slurry. The precipitate was CTV, which is insoluble in the ionic liquid. This reaction yielded 42 % of high purity CTV.

The second Lewis acid used was tin (IV) chloride ($SnCl_4$) because of its similarities to $TiCl_4$. When the $SnCl_4$ was added to the ionic liquid, a dark purple color evolved. However, the development of the slurry was much slower and took between 6 and 7 h. The average yield obtained using $SnCl_4$ (68 %) was found to be much higher than the average yield found with $TiCl_4$ (42 %).

Scandium triflate ($Sc(OTf)_3$) was chosen because it is a relatively strong Lewis acid, and is much easier to handle than $TiCl_4$ or $SnCl_4$. Upon the addition of the scandium triflate to the reaction mixture, no purple color was observed; however, after 2 days of stirring the reaction became cloudy as a result of the formation of CTV. The yield under these conditions was 40 % which is comparable to that obtained with $TiCl_4$.

2.4. Attempted Synthesis of Calix[4]naphthalene in Ionic Liquids

The synthesis of the *endo*-calix[4]naphthalene **8** is described in Chapter 1. The final step is a $TiCl_4$-mediated cyclocondensation of **20** in refluxing dioxane for 36 hours. Under these conditions the yield of **8** is only 13 %. The low yield of this reaction is unfortunate because the starting material is consumed and it becomes a challenge to find a method of optimizing the cyclocondensation step.

The use of ionic liquids to improve the cyclocondensation of calix[4]naphthalenes was inspired by the synthesis of CTV from veratryl alcohol in [bmim]PF_6 and N_{6444} Imide. CTV is synthesized pure and in general in high yields. These encouraging results suggested

that this method might improve the synthesis of **8**. The similarity of these two syntheses comes from the presumed similarity of the mechanism of formation and the molecular structures of the precursors, veratryl alcohol **29,** and **20**. In both precursors the activating aromatic methoxy and naphthyl hydroxyl groups assist in the Friedel-Crafts type alkylation. The aromatic ring of a nearby monomer acts as the nucleophile, displacing the hydroxy group of the hydroxymethyl side-chain. The result is the formation of methylene-bridged oligomers which under the correct conditions close to form the cyclic calix[4]naphthalenes or CTV (Figure 2.3).

Section 2.3 contains a discussion of several different conditions used to form CTV. Those conditions were evaluated in an attempt to optimize the synthesis of **8** (and **9**); the results are recorded in Table 2.2.

All reactions were performed by adding the Lewis acid to a solution of **20** in the ionic liquid. When vanadyl (IV) acetate was added, the color of the reaction turned green. The reaction mixture was allowed to stir for several days with no reaction observed by TLC. The reaction was then heated first to 50 °C and then to 70 °C, with still no reaction observed. No attempts were made to heat the reaction above this temperature because PF_6^- is known to decompose at higher temperatures.

The attempt to reproduce the previously known conditions for the formation of calix[4]naphthalene, but now in an in ionic liquid was accomplished by adding $TiCl_4$ to the reaction mixture. The addition of $TiCl_4$ caused the same dark purple color change as was seen for the synthesis of CTV. However after inspection it was found that **20** did not react and was recovered unchanged. Again this reaction was attempted at higher temperatures but without success.

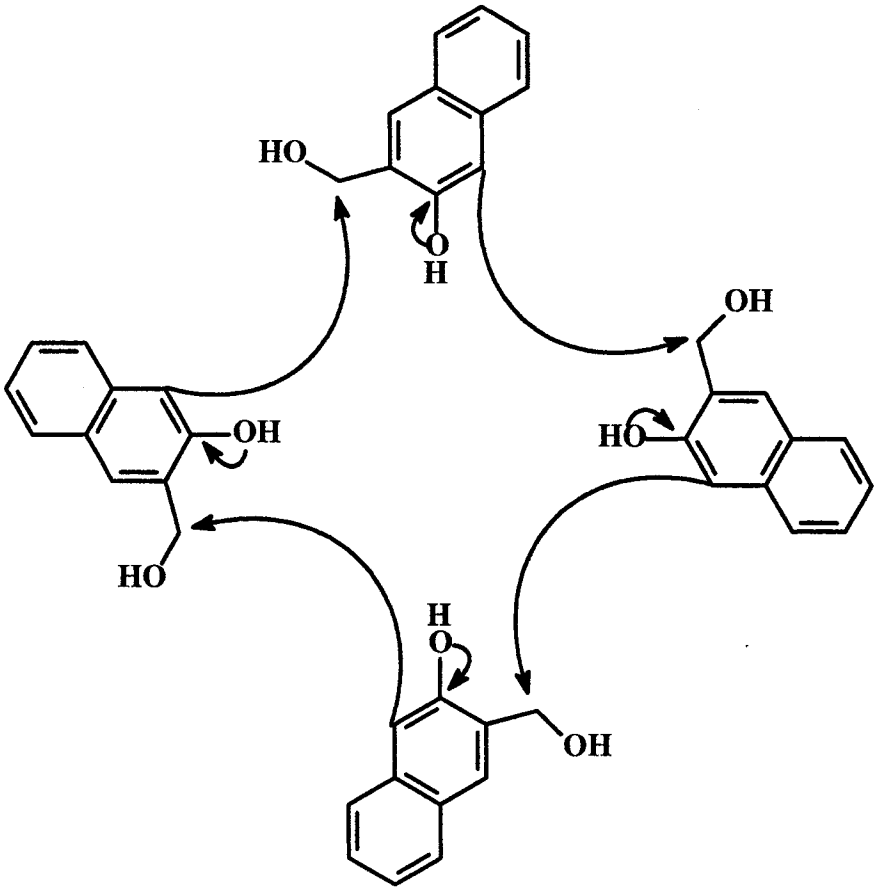

Figure 2.3. Proposed mechanism for the cyclocondensation of 20 to form 8.

$SnCl_4$ and $Sc(OTf)_3$ were also tried at the three different temperatures with no improvement of the results. The final attempt to form calix[4]naphthalene was done using Scott's conditions, again yielding no product. This work provided little hope for improving the efficiency of the one-pot synthesis of **8**. It was hypothesized that the lack of reaction could be due to possible interference from the naphthyl hydroxyl group. It was therefore decided to convert it to the corresponding naphthyl methoxy derivative **32**, and to aim for the synthesis of the tetramethoxy derivative of **33**.

Table 2.2. Results of using ionic liquids and a variety of Lewis acids for the synthesis of calix[4]naphthalene.

Acid	Ionic liquid	Temperature °C	Result
$VO(OAc)_2$	**[bmim]PF_6**	**rt**	**N/R**
$VO(OAc)_2$	**[bmim]PF_6**	**50 °C**	**N/R**
$VO(Oac)_2$	**[bmim]PF_6**	**70 °C**	**N/R**
$TiCl_4$	**[bmim]PF_6**	**rt**	**N/R**
$TiCl_4$	**[bmim]PF_6**	**50 °C**	**N/R**
$TiCl_4$	**[bmim]PF_6**	**70 °C**	**N/R**
$SnCl_4$	**[bmim]PF_6**	**rt**	**N/R**
$SnCl_4$	**[bmim]PF_6**	**50 °C**	**N/R**
$SnCl_4$	**[bmim]PF_6**	**70 °C**	**N/R**
$Sc(OTf)_3$	**[bmim]PF_6**	**rt**	**N/R**
$Sc(OTf)_3$	**[bmim]PF_6**	**50 °C**	**N/R**
H_3PO_4	**N_{6444} Imide**	**50 °C**	**N/R**

The formation of **32** was achieved by methylation of **18** to produce **31**. This is done in a single step. The methylation is then followed by $LiAlH_4$ reduction to give **32** in 82 % yield. This compound was isolated as a pale yellow powder. Compound **32** was then subject to similar conditions as **20** was (Scheme 2.6).

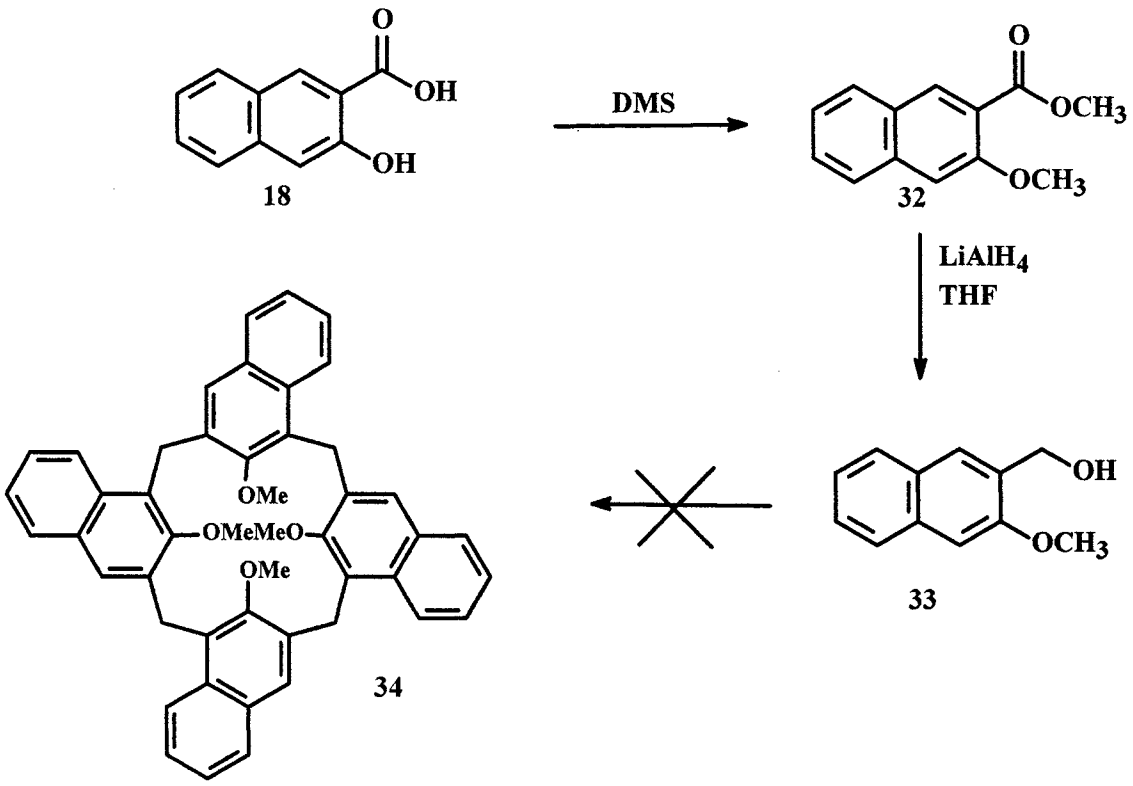

Scheme 2.6. The synthesis of methoxycalix[4]naphthalene (34).

Table 2.3 shows the results of the attempted cyclocondensation of **33**. Using $TiCl_4$ and $SnCl_4$ at the different temperatures both yielded starting materials in approximately 78 %. No other products were found in the ionic liquid which could be identified. With vanadium acetate nothing was extracted from the ionic liquid with ethyl acetate, however when the ionic liquid was dissolved in methanol a light brown-yellow solid could be isolated. It was evident that some reaction did occur, and a new product was found to correspond to one spot on TLC. However, NMR showed no distinguishable peaks. A large number of signals were found in the aromatic region, at around δ = 4 ppm, and another larger number of signals further downfield at δ = 4.5 ppm. These three regions can be related to the protons of the aromatic rings, the methylene bridge and the methoxy respectively; however, the structure of the molecule was not solvable. As the attempt to

synthesize **34** has previously been shown by others in our group to be unsuccessful in organic solvents, it was not a surprise that ionic liquids did not promote this reaction either. The usual method to form a calix[4]naphthalene methoxy ether is by methylation of **8** using CH_3I and NaH.

2.5 Conclusions

The use of an ionic liquid proved successful for the cyclocondensation of the highly reactive veraterol, using different Lewis acids. The results for the synthesis of a calix[4]naphthalene were therefore disappointing. However, they do indicate that there are further investigations required to find a method to improve the cyclocondensation step for the synthesis of **8**. For example, it may be possible to accomplish the synthesis of **8** by a step-wise process in an ionic liquid.

Table 2.3. Results of using ionic liquids and three different of Lewis acids in the attempted synthesis of tetramethoxycalix[4]naphthalene 34.

Acid	Ionic Liquid	Temperature °C	Result
$VO(OAc)_2$	**[bmim]PF_6**	**rt**	**N/R**
$VO(OAc)_2$	**[bmim]PF_6**	**70 °C**	**Insoluble yellow solid product**
$TiCl_4$	**[bmim]PF_6**	**rt**	**N/R**
$TiCl_4$	**[bmim]PF_6**	**70 °C**	**N/R**
$SnCl_4$	**[bmim]PF_6**	**rt**	**N/R**
$SnCl_4$	**[bmim]PF_6**	**70 °C**	**N/R**

2.6. Experimental

General Procedures: All reactions were conducted under Ar or N_2. Organic solutions were concentrated on a rotary evaporator or by vacuum distillation. All compounds were purified by either crystallization, flash chromatography using Merck Silica gel (230-400 mesh) or preparative thin layer chromatography (PLC) plates, which were made from Aldrich Silica gel ((TLC) Standard grade, 2-25μm) with 14% calcium sulphate. Thin layer chromatography was performed on precoated silica gel 60 F_{254} plates (SAI, Inc.).

Materials: All solvents and chemical reagents were purchased from Fluka or Aldrich. Anhydrous $CHCl_3$ and CH_2Cl_2 were obtained from ACS grade chloroform and dichloromethane which had been distilled over calcium hydride. Anhydrous THF was obtained under N_2 by drying ACS grade THF over Na and distilling it from purple sodium benzophenone. Anhydrous ether was obtained by drying ACS grade diethylether over $LiAlH_4$ and distilling.

Instrumentation: Melting points (m.p.) were obtained on a Fisher-Johns apparatus and are uncorrected. ^1H NMR spectral data were collected on a Bruker Avance instrument at 500 MHz using a 16 K data table for a 15.0 ppm sweep width having a digital resolution of 0.321 Hz. Chemical shifts are relative to an internal TMS. Data is presented as follows: chemical shift, multiplicity (s = singlet, d = doublet, dd = doublet of doublets, t = triplet, m = multiplet, q = quartet), coupling constant (*J*, Hz) integration and assignment (H#). The assignments are based on ^1H-^1H Cosy and previously assigned data. ^{13}C NMR spectral data was obtained on a Bruker Avance instrument at 500 MHz using a 16 K data table for a 220 ppm sweep width having a digital resolution of 0.321 Hz. Chemical shifts are relative to the solvent (δ = 77.0 ppm for $CDCl_3$); the assignments are based on CH Hetcor analyses. Low

resolution and high resolution mass spectral data were obtained on a V.G. Micromass (HRMS) 7070 HS instrument. MS data were presented as follows: *m/z*, intensity.

Vanadyl Acetate (30)[62]

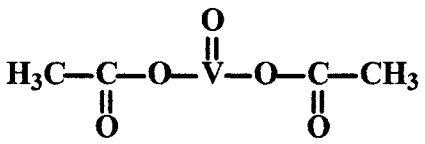

To 50.0 ml of acetic anhydride (0.526 mol) vanadium pentaoxide (18.1 g, 0.990 mmol) was added to form an orange solution. The solution was refluxed for 1 h. The green precipitate was collected using suction filtration and washed several times with dichloromethane and dried under vacuum for 1.5 h (16.7 g, quantitative); decomposition point 270 °C; ms *m/z* (%): 185 (0.8, M^+), 170 (2.6), 143 (1.5), 126 (16), 84 (6), 83 (2.9), 82 (0.9), 67 (8.4), 60 (2.7), 58 (0.9), 43 (26), 42 (3.3), 41 (1), 28 (6), 26 (0.7).

1-*n*-Butyl-3-methylimidazolium chloride ([bmim]Cl) (23)[60]

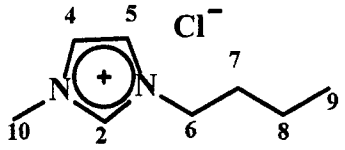

1-Methylimidazole (41.1 g, 0.500 mmol) and 1-chlorobutane (46.3 g, 0.500 mmol) were combined in a Schlenk tube set with a reflux condenser, and heated to 100 °C for 5 d. The reaction formed two layers, which slowly merged into a single layer.

The resulting liquid product was cooled, forming a white solid. The solid was then filtered using suction filtration and washed with diethyl ether. The solid was then dissolved in anhydrous acetonitrile (dried over CaH_2). Anhydrous diethyl ether (dried over $LiAlH_4$) was added, forming two layers. The solution was then refrigerated for several hours until

clear colorless crystals formed. The crystals were collected by suction filtration and washed with 3 x 100 ml portions of diethyl ether. Crystals were then dried and sealed under vacuum until use (72.5 g, 83.0%); ^{1}H NMR ($CDCl_3$) δ = 0.98 (t, J = 7.2 Hz, 3H, H-9), 1.40 (m, 2H, H-8), 1.91 (m, 2H, H-7), 4.13 (s, 3H, H-10), 4.33 (t, J = 7.2 Hz, 2H, H-6), 7.29 (s, 2H, H-4 or H-5), 7.38 (s, 2H, H-4 or H-5) 10.98 (s, 1H, H-2); ^{13}C NMR δ= 13.6 (C-9), 19.7 (C-8), 32.4 (C-7), 36.8 (C-6), 50.1 (C-10), 121.7 (C-4 or C-5), 123.3 (C-4 or C-5), 138.9 (C-2); ms *m/z* (%) 139 (M^+ 2.6), 124 (21), 123 (8), 97 (34), 81 (50), 56 (16), 41 (46), 35 (6).

1-Butyl-3-methylimidazolium hexafluorophosphate ([bmim]PF_6) (24)[60]

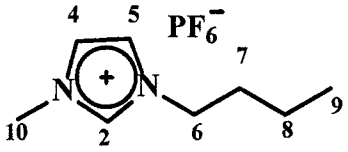

[Bmim]Cl (10.32 g, 59.07 mmol) was dissolved in water (95 ml) and cooled to 0 °C. Hexafluorophosphoric acid (60 % weight in water, 9.49 g, 65.0 mmol) was then added dropwise and allowed to stir for 16 h.

Two layers formed overnight. The top aqueous layer was decanted, and the lower ionic liquid was washed with 10 x 40 ml of water. The resulting clear liquid was placed under vacuum at 45 °C for 48 h. The ionic liquid (8.7 g, 52 %) was sealed under vacuum until use; ^{1}H NMR (acetone-d_6) δ = 0.95 (t, J = 7.2 Hz, 3H, H-9), 1.39 (m, 2H, H-8), 1.94 (m, 2H, H-7), 4.06 (s, 3H, H-10), 4.37 (t, J = 7.2 Hz, 2H, H-6) 7.71 (s, 2H, H-4 or H-5), 7.76 (s, 2H, H-4 or H-5), 8.99 (s, 1H, H-2); ^{13}C NMR (acetone-d_6) δ = 13.2 (C-9), 19.5 (C-8), 32.2 (C-7), 35.9 (C -6), 49.8 (C-10), 122.9 (C-4 or C-5), 124.2 (C-4 or C-5), 136.8 (C-2).

Tri-*n*-butylhexylammonium iodide salt (26)[61]

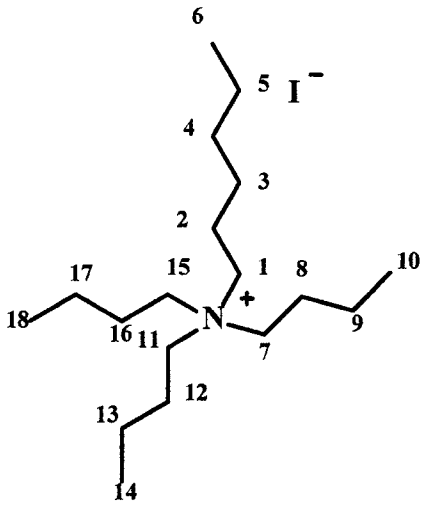

A mixture of 1-iodohexane (16.7 g, 78.8 mmol) and tributylamine (7.70 g, 41.5 mmol) was prepared and heated to 85.9 °C for 5 d. The orange-colored solution was cooled to yield a deep red gummy solid. The product was then was washed with 2-butanone (2 x 50 ml). The deep red-orange malleable solid was dried under vacuum to give **26** as a crusty, orange solid (7.90 g, 48.0 %): m.p. 53-56 °C; ^{1}H NMR ($CDCl_3$) δ = 0.91 (t, J = 7.0 Hz), 3H, H-6), 1.01 (m, 9H, H-10, H-14, H-18), 1.39 (m, 12H, H-3, H-4, H-5, H-9, H-13, H-17), 1.70 (m, 8H, H-2, H-8, H-12, H-16), 3.75 (m, 8H, H-1, H-7, H-11, H-15); ^{13}C NMR ($CDCl_3$) δ = 13.88 (C-6), 14.00 (C-10, C-14, C-18), 19.92 (C-9, C-13, C-17), 22.54 (C-5), 24.40 (C-4), 24.48 (C-3), 26.20 (C-2), 31.33 (C-8), C-12, C-16), 59,39 (C-7, C-11, C-15), 59.55 (C-1); ms *m/z* (%) 142 (M^+ 100), 184 (3.1), 170 (28), 128 (22), 127 (14), 100 (32), 84 (5), 71 (1), 57(38), 43 (25).

Bis(trifluoromethanesulfonyl)amide lithium salt (27)[61]

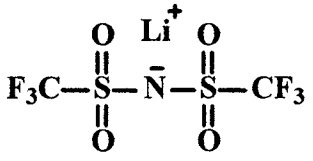

Under Ar, bistrifluoromethanesulfonamide (1.10 g, 3.91 mmol) was dissolved in anhydrous THF (5 ml). The reaction was cooled to -78 °C and *n*-butyllithium (0.229 g, 3.91 mmol) (1.6 M in hexane) was added dropwise over several min. Once addition was complete the resulting solution was stirred for 5 min and was allowed to warm to rt. The solvent THF and hexanes were removed under vacuum and the product residue (salt) was sealed until use. As a result of the instability of this product no spectral or physical data were collected.

Tributylhexylammonium ion with bis(trifluoromethanesulfonyl)amide (N6444 Imide) (28)[61]

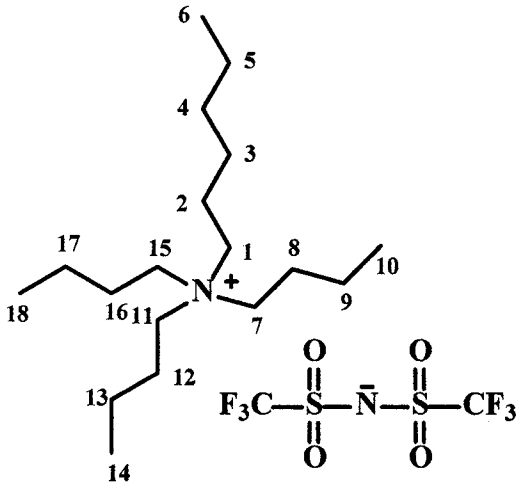

A solution of **27** (1.41 g, 3.55 mmol) was dissolved in water (5 ml). A second solution of **26** (1.12 g, 3.91 mmol) was dissolved in 0.8 ml of water and added to the first solution. The resulting orange solution was stirred at rt for 3 h, at which time two layers could be seen to form. The top aqueous layer was decanted and the bottom pale orange ionic liquid was washed with water (2 x 5 ml), then dried under vacuum for 48 h; ^{1}H NMR ($CDCl_3$) δ = 0.90 (t, J = 6.6 Hz, 3H, H-6), 1.00, (m, 9H, H-10, H-14, H-18), 1.39 (m, 12H,

H-3, H-4, H-5, H-9, H-13, H-17), 1.57 (m, 8H, H-2, H-8, H-12, H-16), 3.15 (m, 8H, H-1, H-7, H-11, H-15).

Cyclotriveratrylene (31)[29, 30]

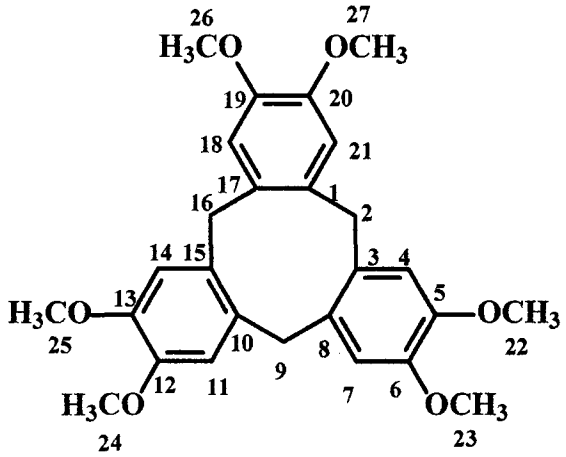

A) Under anhydrous conditions $TiCl_4$ (0.610 g, 3.23 mmol) was added by syringe solution of 3,4-dimethoxybenzyl alcohol (**29**) (0.500 g, 3.00 mmol) in [bmim]PF_6 (1.01 g, 3.56 mmol) and stirred vigorously. After several min the mixture turned dark purple and became a thick slurry. After 2 h the ionic liquid was dissolved in 10 ml of methanol and the white crystals precipitated out of the methanol and were collected via suction filtration and dried under vacuum for 3 h (0.45 g, 42 %); m.p. 215-217 °C; ^{1}H NMR ($CDCl_3$) δ = 3.55 (d, 3H, H_a-2 H_a-9 H_a-16), 3.83 (s, 18H, H-22, H-23, H-24, H-25, H-26, H-27), 4.77 (d, 3H, H_b-2, H_b-9, H_b-16), 6.83 (s, 6H, H-4, H-7, H-11, H-14, H-18, H-21); ^{13}C NMR δ = 36.7 (C-2, C-9, C-16), 56.3 (C-22, C-23, C-24, C-25, C-26, C-27), 113.4 (C-3, C-8, C-10, C-15, C-7), 132.0 (C-4, C-7, C-14, C-18, C-21), 148.0 (C-6, C-6, C-12, C-13, C-19, C-20); ms *m/z* (%): 450 (87, M^+), 419 (22.7), 405 (16.9), 404 (7.2), 372 (231), 299 (100), 268 (32.6), 253 (6.14), 212 (6.1), 187 92.4), 151 (72.1), 137, (10.2).

B) Under anhydrous conditions vanadyl acetate (0.600, 3.24 mmol) was added to a solution of **29** (0.500 g, 3.00 mmol) in [bmim]PF_6 (1.00 g, 3.52 mmol) and was stirred vigorously for 7 h at 50 °C (Moens' conditions). The reaction mixture was then dissolved in dichloromethane and vanadyl acetate was recovered and reused. The dichloromethane was then evaporated and the residue was the washed in MeOH to remove the ionic liquid. The white crystals were collected by suction filtration and dried under vacuum for 3 h to afford 0.38 g (85 %) of **31** whose spectral properties were identical to those obtained using method A.

C) Under anhydrous conditions $SnCl_4$ (0.410 g, 3.23 mmol) was added by syringe to a solution of **29** (0.500 g, 3.00 mmol) and [bmim]PF_6 (1.09 g, 3.84 mmol) and stirred vigorously for 6-7 h at rt. The ionic liquid was then dissolved in MeOH and the white crystals of 31 precipitated out of the MeOH were collected by suction filtration and dried under vacuum for 3 h to afford 0.31 g, (68 %) of **31** whose spectral properties were identical to those obtained using method A.

D) Under anhydrous conditions $Sc(OTf)_3$ (0.100 g, 0.200 mmol) was added to a solution of **29** (0.500 g, 3.00 mmol) in [bmim]PF_6 (1.00 g, 3.52 mmol). The reaction was stirred vigorously at room temperature for 48 h. The ionic liquid was then dissolved in MeOH and the white precipitate which formed was collected using suction filtration. The crystals were dried under vacuum for 3 h which afford 0.18 g, (40 %) of **31** whose spectral properties were identical to those obtained using method A.

Methyl -3-hydroxy-2-naphthoate (19)

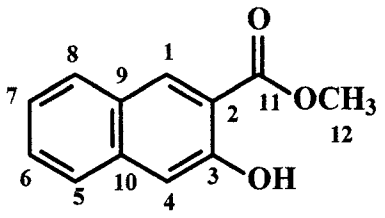

Concentrated sulfuric acid was added to a solution of 3-hydroxy-2-naphthoic acid (50.0 g, 266 mmol) (**18**) in MeOH (270 ml) at rt. The reaction mixture was then refluxed for 8 h. The reaction mixture was cooled to rt to form a yellow solid which was filtered, washed with aqueous 10 % $NaHCO_3$ to give 52.12 g (97 %) of **19**, whose spectral properties were identical to those reported by Ashram.[6]

3-(Hydroxymethyl)-2-naphthol (20)

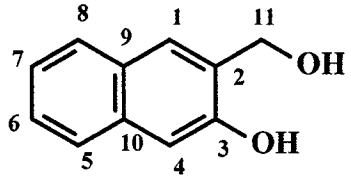

A solution of methyl 3-hydroxy-2-naphthoate (**19**) (2.04 g, 10.1 mmol) in anhydrous THF (50 ml) was added at rt to a suspension of LiAlH (0.705 g, 18.6 mmol) in dry THF (30 ml) over 30 min, and the mixture was stirred at rt for 3 h. The reaction was quenched by the slow addition of cold water, followed by cold brine, and then the mixture was treated with aqueous 10 % HCl at 0 °C. The THF was partially evaporated under vacuum; the product was then extracted from the aqueous layer, three times using 15-ml portions of diethyl ether. The ether was dried using $MgSO_4$, filtered and the solvent was evaporated to give a pale yellow solid 1.37 g (78 %) of **20** which could be crystallized for

analysis from ethanol-water, m.p. 186-188 °C; (lit. m.p. 185°C)[28]. The spectral properties of **20** are identical to those reported by Ashram.[6]

Methyl -3-methoxy-2-naphthoate (32)

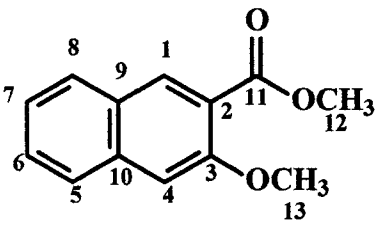

To a suspension of 3-hydroxy-2-naphthoic acid (14.0 g, 72.0 mmol) in dichloromethane (350 ml) were added water (200 ml), phase-transfer catalyst (Adogen^R, 5 ml) and dimethyl sulphate (52 ml). The mixture was stirred vigorously, and aqueous 10 % NaOH (180 ml) was added dropwise, over 30 min. The reaction was then allowed to stir for an additional 3 h. The water was decanted off the dichloromethane, and the aqueous layer was extracted with dichloromethane. After drying the combined organic layers with $MgSO_4$, and filtering, the solvent was then removed under vacuum. The residue dimethyl sulphate was removed by vacuum distillation. The yellow product was then purified by flash chromatography using ethyl acetate-hexane (10:40) to yield **32** as an oily yellow product (11.3 g, 73 %). Whose spectral data are identical to those reported by Ashram.[6]

3-Hydroxymethyl-2-methoxynaphthalene (33)

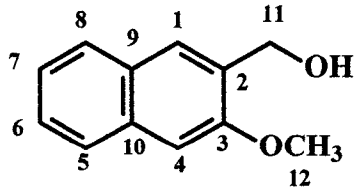

A solution of methyl-3-methoxy-2-naphthoate (**18**) (5.47 g, 25.3 mmol) in anhydrous THF (50.0 ml) was added at 0 °C to a suspension of LiAlH (1.40 g, 37.3 mmol)

in dry THF (30.0 ml) over 20 min, and the mixture was stirred as rt for 3 h. The reaction was quenched by the slow addition of cold water, followed by cold brine, and then the mixture was treated with aqueous 10 % HCl at 0 °C. The THF was partially evaporated under vacuum; the product was then extracted from the aqueous layer three times using 3 x 20 ml of diethyl ether. The ether was dried using $MgSO_4$, filter and the solvent was evaporated to give a pale yellow solid which was purified using flash chromatography using ethyl acetate-hexane (30:70) to give **33** as a white solid (3.90 g, 82 %) whose spectral properties were reported by Ashram.[6]

Calix[4]naphthalene (8)

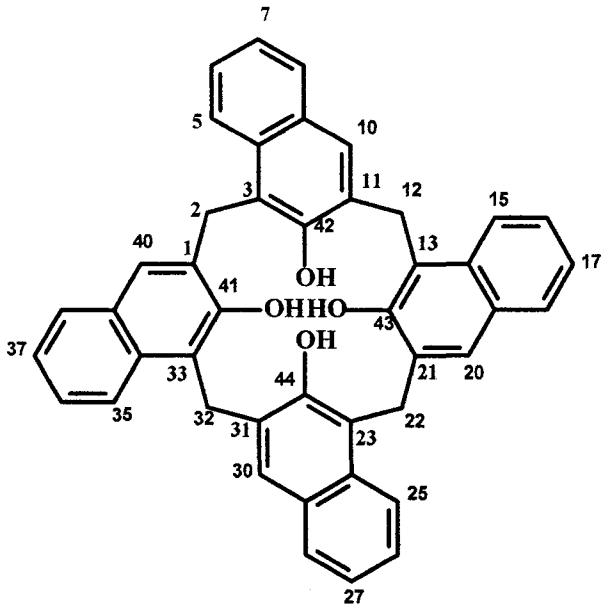

Typical reaction conditions: under anhydrous conditions a Lewis acid such as $TiCl_4$ (1.15 g, 2.59 mmol) was added to a solution of **20** (0.420 g, 2.43 mmol) in [bmim]PF_6 (4.00 g, 14.1 mmol) and was stirred vigorously for 7 h at rt (or temperature indicated in Table 2.2). The reaction mixture was then extracted with ethyl acetate. The ethyl acetate was then evaporated and the residue was washed in MeOH to remove the ionic liquid. The white crystals were collected by suction filtration and dried under vacuum for 3 h to afford

0.340 g (81 %) of **20** whose spectral properties were identical to those of the starting material.

Tetramethoxycalix[4]naphthalene (34)

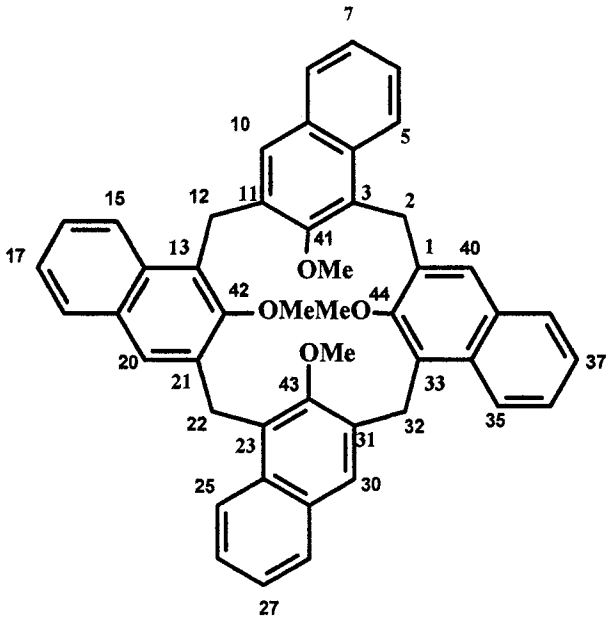

Typical reaction conditions: under anhydrous conditions a Lewis acid such as $TiCl_4$ (1.15 g, 2.59 mmol) was added to a solution of **33** (0.169 g, 2.43 mmol) in [bmim]PF_6 (1.00 g, 3.55 mmol) and was stirred vigorously for 8 h at rt (or temperature indicate in Table 2.3). The reaction mixture was then extracted with ethyl acetate. The ethyl acetate was then evaporated and the residue was the washed in MeOH to remove the ionic liquid. The white crystals were collected by suction filtration and dried under vacuum for 3 h to afford 0.132 g (78 %) of **33** whose spectral properties were identical to those of the starting material.

Chapter 3

An Attempted Synthesis of Calix[4]naphthalene using a Florisil^{R}-Mediated Cyclocondensation

3.1. Introduction

The first calix[4]azulene reported was by Asao *et al.*[7] [1.1.1.1] (1,3)-methoxyazulenophane (**10**), which consists of four molecules of 2-methoxyazulene linked at the 1- and 3-positions by methylene bridges (Figure 1.7). The synthesis of **10** (Scheme 3.1) was achieved by a stepwise process.[7] Paraformaldehyde was reacted with 2-methoxyazulene **35** in the presence of acetic acid to give the dimeric product **36** in 92 % yield. Product **36** was then subjected to a Vilsmeyer formylation reaction to yield 59 % of the dialdehyde **37**, which in turn, was reduced using DIBAH to give the bishydroxymethyl compound **38** in 87 % yield. Subunits **36** and **38** were then reacted together to give a complex mixture. The cyclic calix[4]azulene **10** was isolated from the mixture in 20 % yield and was found to be in the 1,3-alternate conformation.

K10 montmorillonite (which is a sedimentary clay, high in aluminum silicates, which has been treated with an acid) has been used in the synthesis of macrocyclic molecules such as porphyrins.[64] The clay is highly acidic. Colby and Lash[8] used K10 montmorillonite as a catalyst for the cyclocondensation of azulene with paraformaldehyde, but found however, only trace amounts of the calix[*n*]azulene.

They did however report a successful synthesis of the nonfunctionalized calix[4]azulene (**11**)[8] which involved a one-pot cyclocondensation of azulene and paraformaldehyde in the presence of Florisil^{R} (Scheme 3.2) to give a 74 % yield of the blue-green solid, **11**.

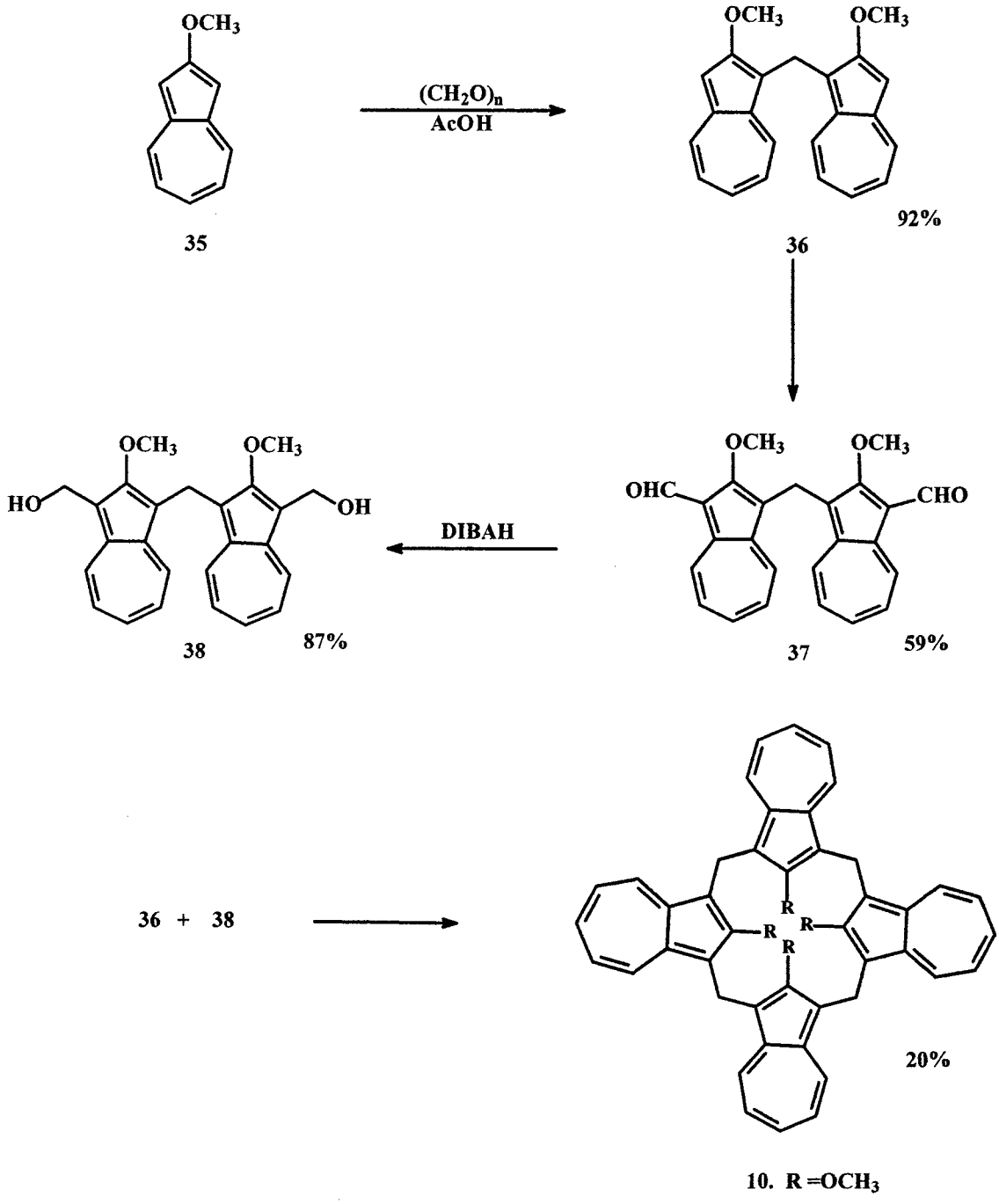

Scheme 3.1. The synthesis of [1.1.1.1] (1, 3)-methoxyazulenophane (10).

Florisil^{R} is a mildly acidic synthetic magnesium silicate ($MgO{\cdot}3.75SiO_2{\cdot}H_2O$),[65] which is commonly used as a filtration aid. However, Colby and Lash's cyclocondensation of azulene and paraformaldehyde used Florisil^{R} as a catalyst. These conditions were milder than the traditional one-pot syntheses of calix-type compounds, however, they did not allow for the formation of any other calixazulene product in the presence of other carbonyl compounds such as acetone or hexachloroacetone. The mechanism for this synthesis of calix[4]azulene is not completely understood. Nonetheless, it was of interest to see if Florisil^{R} could be used in the cyclocondensation of other molecules to form calix-type compounds, such as the calix[4]naphthalenes of interest to us.

3.2. Attempted Synthesis of CTV and Calix[4]naphthalene Using a Florisil^{R}-Mediated Cyclocondensation

Colby and Lash's conditions were repeated to form **11**. Their results were easily reproduced in our lab affording a 78 % yield of the blue-green solid, **11**. The ^{1}H NMR spectra of calix[4]azulene (Appendix C) showed no impurities. The LCMS-APCI showed a major peak at m/z = 561 corresponding to a $[M + 1]^{=}$ ion of **11**. The MS was conducted in the positive ionization mode, so the major peak is consistent, with the predicted structure.

The cyclocondensation of azulene and paraformaldehyde, in the presence of Florisil^{R}, provided a potential new method to try to optimize the synthesis of calix[4]naphthalene **8** and a new method for the synthesis of CTV.

As noted previously, CTV was easily formed using ionic liquids and several different Lewis acids (Chapter 2). Therefore, veratryl alcohol (**29**) was subjected to the

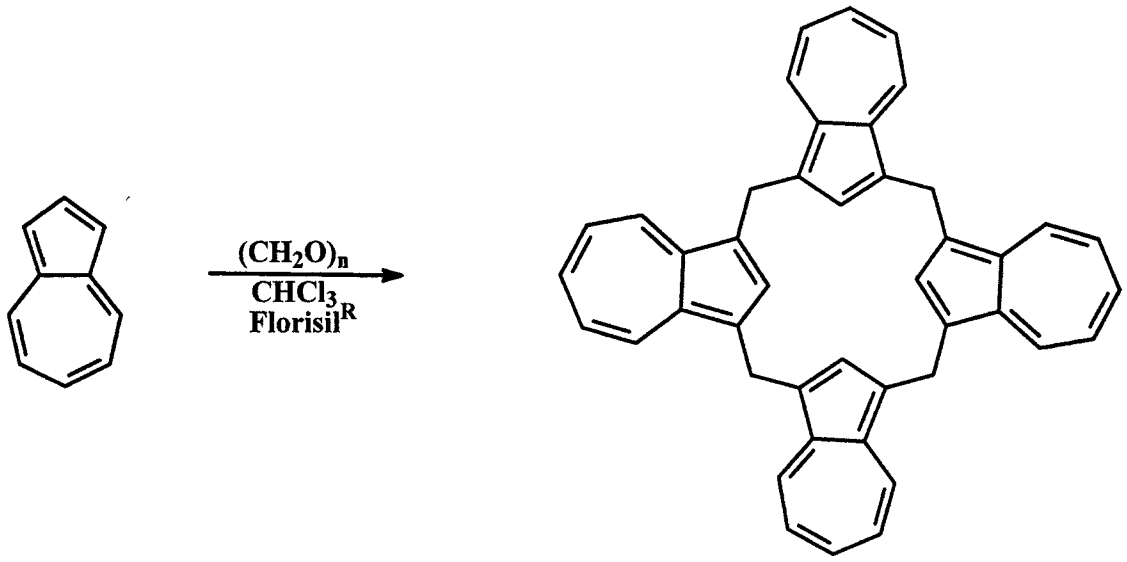

11

Scheme 3.2. The synthesis of calix[4]azulene (11).

conditions Colby and Lash used in the formation of **11**. The reaction was allowed to stir for several hours at room temperature with no change observed by TLC. The reaction was then allowed to continue stirring for up to three days at room temperature; TLC continued to indicate only the presence of starting material. The reaction was then heated to reflux for an additional three days, with still no observed change by TLC. Approximately 95 % of the starting material was recovered.

Veratryl alcohol, with two *ortho-para* directing methoxy groups on the aromatic ring, is a highly reactive molecule. However, Florisil^R was not a strong enough catalyst to allow for the cyclocondensation of **29** to form **31**. The attempted cyclocondensation of **29** failed and provided little insight on Colby and Lash's conditions, and whether or not it

would be useful in the synthesis of other macrocyclic compounds such as calixnaphthalenes and calixarenes.

The first attempt to synthesize **8** using the Florisil^{R}-mediated method was performed by reacting 2-naphthol and paraformaldehyde, in dioxane. The reaction was allowed to stir for 20 minutes before a sample was taken for TLC, at which point all of the starting material had been consumed. The isolated and purified product was the dimer **41** in 98 % yield (Scheme 3.3). The dimer was not an unexpected product, as it is a well-known condensation product when 2-naphthol is reacted with paraformaldehyde.

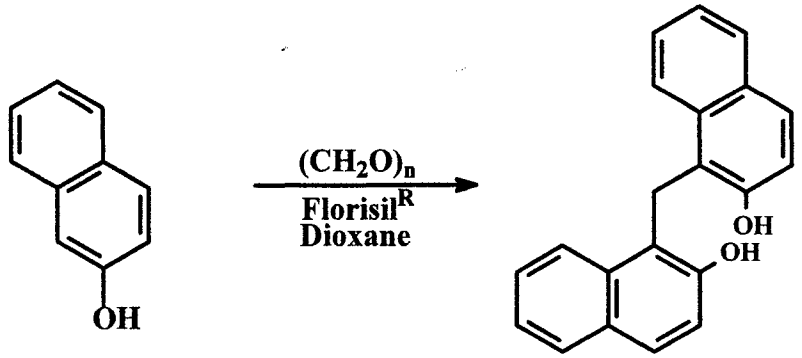

40 **41**

Scheme 3.3. The synthesis of naphthol dimer 41.

The dimer, however, in our case was not the desired compound; we decided to investigate the cyclocondensation of hydroxymethylnaphthoate **20** in the presence of Florisil^{R} to form **8**. Unfortunately, the reaction of **20** did not result in formation of the desired product. Instead, the hydroxymethyl group was oxidized to the corresponding aldehyde in an approximately 30 % yield. The remaining unreacted starting material was recovered (64 %). The reaction was repeated and allowed to continue for several hours, however no improvement in the yield was found. With the same reaction components the

reaction was heated to reflux in dioxane for a period of 6 days with only mild improvement observed in the yield of the oxidation product. No cyclocondensation products were observed.

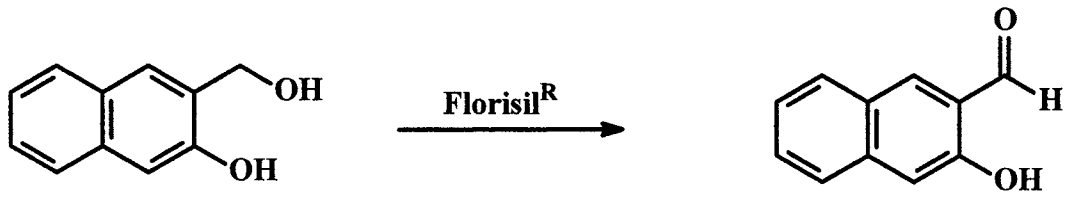

20 **42**

Scheme 3.4. The synthesis of the 2-hydroxy-3-naphthaldehyde (42).

The exact role of the paraformaldehyde in the cyclocondensation of azulene to form **11** is not well understood; however, the presence of paraformaldehyde may be a factor in the formation of a cyclic product. This led to an investigation of the cyclocondensation of **20** in the presence of paraformaldehyde.

Parformaldehyde and **20** were then combined under conditions similar to conditions which were used in the attempt to cyclocondense paraformaldehyde with 2-naphthol. The reaction was allowed to stir at room temperature for approximately 30 minutes, during which time the starting material was consumed. The purified product turned out to be another dimer (**43**) (Scheme 3.5). The structure of the product was determined by ^{1}H NMR data and mass spectroscopy.

It was then considered that the Florisil^R alone might not be sufficient to affect the cyclocondensation of **20** to form **8**. This hypothesis was evaluated by the addition of a Lewis acid to the Florisil^R-containing reaction conditions. The Lewis acids employed were similar to those used in Sections 2.3 and 2.4 of this thesis. The results are recorded in Table 3.1.

product **42** only was observed with no cyclic product being observed. This experiment was then repeated using different Lewis acids.

It becomes obvious that the condition which allows for the formation of **11** is not a general procedure that can be applied to similar molecules. In the case of the precursor used for the attempted synthesis of calix[4]naphthalenes, the Florisil^{R} acts as a mild oxidation reagent. As such, this reaction could be useful in systems as a mild selective oxidant of an alcohol to form the corresponding aldehyde.

3.3. Conclusions

Colby and Lash's conditions did not result in the desired cyclocondensation for the formation of calix[4]naphthalene. When these conditions were repeated using $CHCl_3$ as the solvent for the cyclocondensation of calix[4]naphthalene no reaction occurred because the starting material **20** was not soluble in this solvent system. The Colby and Lash's conditions were then modified using dioxane so that the **20** would dissolve and react, however this still did not produce the desired result, the only product observed being aldehyde **42**. Colby and Lash's original conditions are an effective way to synthesize calix[4]azulene but the reaction seems to be unique for the formation of **11**, and has shown little potential for the cyclocondensation of other calix-type molecules. It however, provided us with a mild method to produce **43**, which could be a useful intermediate for the synthesis of other calixnaphthalenes.

In the next chapter a detailed investigation into some of the properties of calix[4]azulene is discussed. The complexation of calix[4]azulene with C_{60} is examined using both NMR techniques and uv-visible spectroscopy.

3.4. Experimental

Calix[4]azulene (11)[8]

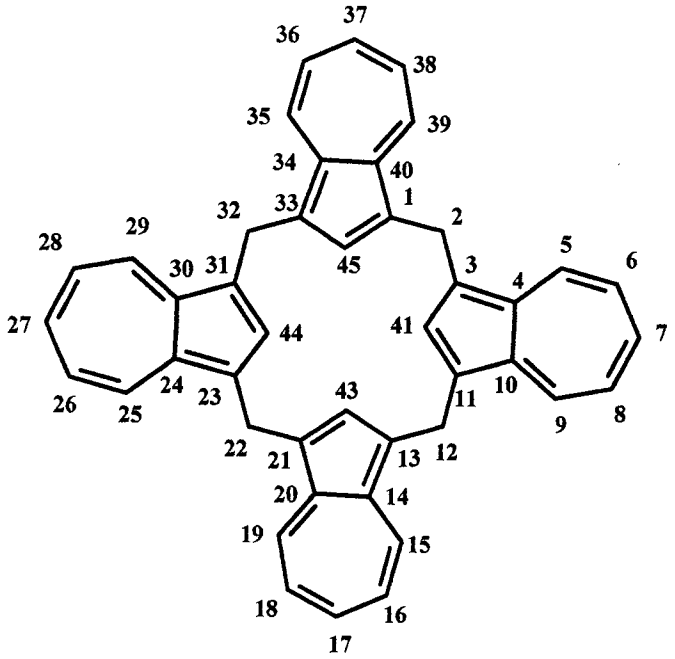

Azulene (0.496 g, 3.87 mmol) was added to a mixture of Florisil^{R} (20.1 g) in chloroform (100 ml). Paraformaldehyde (0.48 g) was then added to the purple mixture and the reaction was allowed to stir at rt for 90 min. The reaction turned to a blue-green color. The mixture was diluted with dichloromethane (750 ml). The Florisil^{R} was removed by suction filtration and the solvent was removed under vacuum to afford 0.42 g (78%) of a blue-green solid, whose m.p. and spectral properties where identical to those reported by Colby and Lash.[8]

Bis[2-hydroxy-1-naphthyl]methane (41)

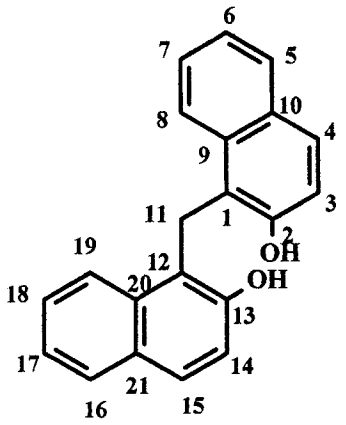

To a solution of paraformaldehyde (0.48 g) and Florisil^{R} (20 g) in chloroform (100 ml) 2-naphthol (0.505 g, 3.75 mmol) was added and was allowed to stir at rt for 30 min. The solution was then diluted with of dichloromethane (300 ml). The Florisil^{R} was removed by suction filtration and the solvent removed under vacuum to give a pale brown solid. The solid was purified using flash chromatography (35% ethyl acetate in hexanes) to afford **41**, (0.68g, 98 %);(lit. m.p.197-199 °C.)[6] m.p.198-200°C, ^{1}H NMR (acetone-d_6) δ = 4.98 (s, 2H, H-11), 7.18 (t, J = 7 Hz, 2H, H-7, H-18), 7.27 (t, J = 7 Hz, 2H, H-6, H-17), 7.31 (d, J = 9 Hz, 2H, H-,4 H-15), 7.65 (d, J = 9 Hz, 2H, H-3, H-14), 7.70 (d, J = 8Hz, 2H, H-8, H-19), 8.40 (d, J = 8.5 Hz, 2H, H-5, H-16), 9.09 (s, OH); ^{13}C NMR (acetone-d_6) δ = 21.74 (C-11), 118.86 (C-4, C-15), 120.37 (C-2, C-13), 123.39 (C-7, C-18), 124.99 (C-5, C-16), 126. 64 (C-6, C-17), 128.86, (C-3, C-14), 129.2 (C-8, C-19), 130.32 (C-9, C-20), 135.15 (C-10, C-21), 152.75 (C-1, C-12); ms *m/z* (%) 300 (M^{+}, 6), 281 (15), 239 (2.1), 156 (21), 144 (100), 128 (27), 115 (16), 89 (3).

Bis[3-hydroxymethyl-2-hydroxy-1-naphthyl]methane (43)

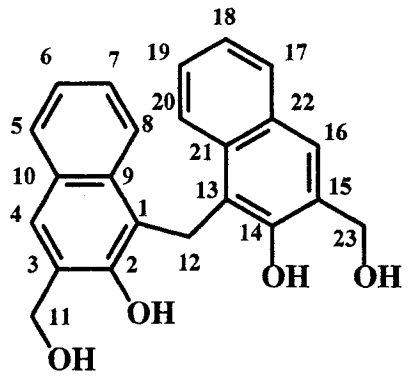

Compound **20** (0.380 g, 2.13 mmol) was added to a solution of paraformaldehyde (0.130 g) and Florisil^R (10.0 g) in dioxane (55.0 ml) and was allowed to stir at rt for 5 h; an additional 0.21 g of paraformaldehyde was then added. The reaction was then allowed to stir for an additional 18 h. The solution was diluted with dioxane (300 ml), and the Florisil^R was removed by suction filtration and the solvent was removed under vacuum to give a red brown solid. The solid was purified using flash chromatography (50 % ethyl acetate in hexanes) to afford **43** (0.214 g 56%); m.p. 210-214°C; ^{1}H NMR δ = 4.49 (s, 2H, H-12), 5.03, (s, 4H, H-11, H-23), 5.27 (s, 2H, CH_2OH), 7.19 (m, 2H, H-7, H-19), 7.26 (m, 2H, H-7, H-18) 7.59 (s, 2H, H-4, H-14), 7.68 (d, J = 8.5 Hz, 2H, H-8, H-20), 8.30 (d, J = 8.5 Hz, 2H H-5, H-17), 9.14 (s, 2H, OH); ms *m/z* (%) 360 (M^+, 10) 322 (21), 296 (6.7), 239 (3), 186 (45), 174 (38), 128 (100), 115 (24), 89 (5.).

2-Hydroxy-3-naphthaldehyde (42)

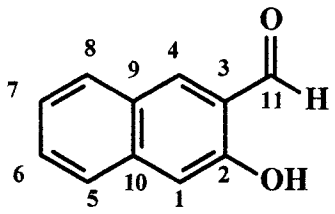

A) Compound **20** (0.670 g, 3.76 mmol) was added to a solution of 20.0 g of Florisil^R in 100 ml of dioxane and was allowed to stir at rt for 4 h. The Florisil^R was removed by filtration, the filtrate was collected and the solvent was removed under vacuum. The resulting yellow residue was purified using flash chromatography (30% ethyl acetate in hexanes). The product **42** was a bright yellow solid (0.18 g, 28 %); (lit. m.p. 93-94°C)[37] m.p. 92-94 °C; ^{1}H NMR δ = 7.29 (s, 1H, H-4), 7.38 (t, J = 7.5 Hz, 1H, H-6), 7.57 (t, J = 7.5 Hz, 1H, H-5), 7.72 (d, J = 8.5 Hz,1H, H-5), 7.87 (d, J = 8.5 Hz, 1H, H-8), 8.16 (s, 1H, H-1), 10.10 (s, 1H, **OH**), 10.32 (s, 1H, **CHO**); MS *m/z* (%) 172 (M^+, 100), 171 (43), 142 (3), 126 (12), 115 (44), 89 (6).

B) Compound **20** (0.550 g, 3.08 mmol) was added to a solution of Florisil^R (18.4 g) in dioxane (100 ml) and was heated to reflux and allowed to stir for 5 d. The Florisil^R was removed by filtration, the filtrate was collected, and the solvent was removed under vacuum. The resulting yellow residue was purified using flash chromatography (30% ethyl acetate in hexanes). The product **42** was a bright yellow solid (0.16 g, 31 %), which was identical to the product obtained from procedure A.

C) Compound **20** (0.650 g, 3.73 mmol) was added to a solution of $VO(OAc)_2$ (1.31 g, 7.08 mmol) and of Florisil^R (21.5 g) in dioxane (100 ml) and was allowed to stir at rt for

12 h. The Florisil^R was removed by filtration, the filtrate was collected and the solvent was removed under vacuum. The resulting yellow residue was purified using flash chromatography (30% ethyl acetate in hexanes) to afford **42** (0.19 g, 29 %).

D) Compound **20** (0.540 g, 3.03 mmol) was added to a solution of $TiCl_4$ (0.20 ml, 1.82 mmol) and Florisil^R (19.4 g) in dioxane (80.1 ml), and was heated to reflux and allowed to stir for 36 h. The Florisil^R was removed by filtration, the filtrate was collected and the solvent was removed under vacuum. The resulting brown residue was purified using flash chromatography (30% ethyl acetate in hexanes), to afford **42** as a bright yellow solid (0.18 g, 34 %).

E) Compound **20** (0.510 g, 3.86 mmol) was added to a solution of $Sc(OTf)_3$ (100 mg, 0.20 mmol) and Florisil^R (19.4 g) in dioxane (80.4 ml) and was heated to reflux and allowed to stir for 12 h. The Florisil^R was removed by filtration, the filtrate was collected and the solvent was removed under vacuum. The resulting yellow residue was purified using flash chromatography (30% ethyl acetate in hexanes) to afford **42** as a bright yellow solid (0.09 g, 18 %).

F) Compound **20** (0.350 g, 1.96 mmol) was added to a solution of *p*-toluenesulfonic acid (0.37g, 0.19 mmol) and Florisil^R (15.8 g) in dioxane (55.2 ml), and was heated to reflux and allowed to stir for 12 h. The Florisil^R was removed by filtration, the filtrate was collected and the solvent was removed under vacuum. The resulting yellow residue was purified using flash chromatography (30% ethyl acetate in hexanes) to afford **42** as a bright yellow solid (0.06 g, 17.8 %).

Chapter 4
A Study of Supramolecular Complexation between Calix[4]azulene and C_{60}

4.1. Introduction

Supramolecular chemistry[65] involves non-covalent bonding interactions which construct units, or adducts, which may further associate to form larger species. The formation of these adducts may occur with a high degree of control.[66] The operation of enzymes which perform many different and complicated functions, require that a substrate first attach itself into an active pocket of the enzyme forming an enzyme-substrate complex. The enzyme acts as a host molecule, which contains a concave surface into which a convex substrate or guest molecule can fit. When the guest is encapsulated by the host this forms an inclusion complex which is a classic type of supramolecular complex.

A large number of complexes between macrocyclic compounds and guest species such as metallic ions or neutral organic molecules have been reported in the literature.[67-69] One such example is the complex which forms between a calixarene and C_{60},[68] as described in the first chapter of this thesis. Such supramolecular complexes are held together by one, or a combination, of the following types of noncovalent bonding interactions:[66]

a. Hydrogen Bonding. Hydrogen bonding is an attraction between a hydrogen atom and a heteroatom, such as oxygen or nitrogen, having a free lone pair of electrons. Hydrogen bonding is a very important form of noncovalent bonding in biology. Watson and Crick proposed that hydrogen bonding was responsible for the formation of DNA base pairs.[66] It is then the steric effects created by the base pairing that creates the

familiar double helix (Figure 4.1).

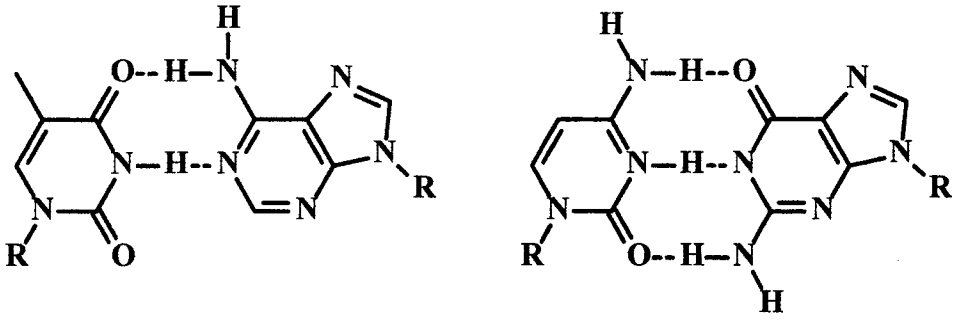

Thyamine **Adenine** **Cytosine** **Guanine**

R = Deoxyribose

Figure 4.1. The hydrogen bonding in DNA base-paring.

b. Electrostatic Interactions. Electrostatic interactions are the attractions between permanent charges within a species e.g. charged ions, or the dipoles formed in heteroatomic bonds. These interactions include ion-ion interactions, ion-dipole interactions and dipole-dipole interactions (Figure 4.2).

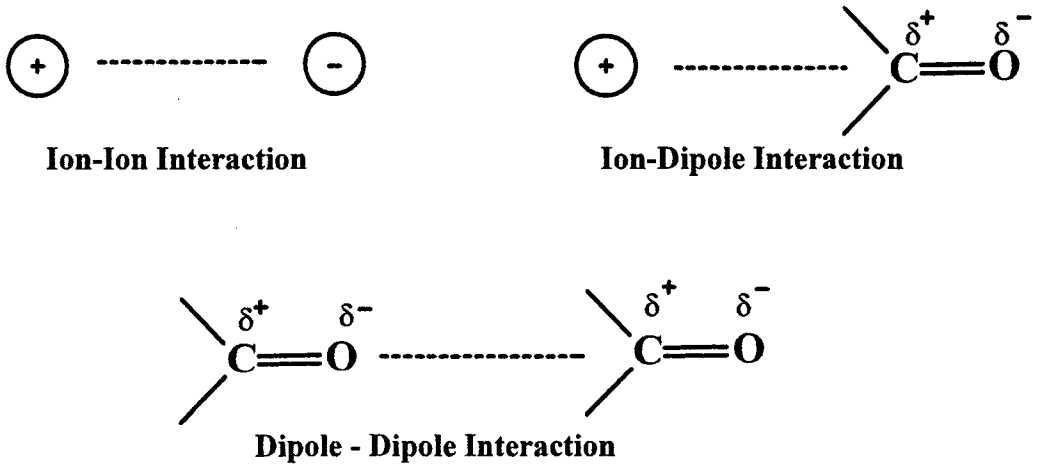

Ion-Ion Interaction **Ion-Dipole Interaction**

Dipole - Dipole Interaction

Figure 4.2. Electrostatic interactions.

c. Van der Waals Forces. Van der Waals forces include London dispersion forces and forces of attraction with permanent dipoles. London forces are result of all the electrons with in a molecule being displaced forming a dipole. These interactions occur when two molecules (or more) develop instantaneous dipoles and the two (or more) dipoles become aligned in such a way that the electron clouds react in an attractive manner. Forces which are associated with permanent dipoles are the result of an electron pair within a molecular bond being displaced as a result of electronegativity differences between the two atoms of the bond.[71]

d. π-π Interactions.* π-π* interactions only occur in systems which contain double bond π-orbitals. There are two ways in which π-π* interactions are commonly described in aromatic systems. The first occurs when two aromatic rings are parallel to each other such that the π-systems are facing each other; this is known as a "*face to face*" interaction (Figure 4.3). The second occurs when two rings are orthogonal to each other; this is known as a "*face to edge*" interaction (Figure 4.3). In 1990, Hunter and Sanders[72] described the "*face to face*" interaction as being slightly misaligned and that the two π-systems are not directly on top of each other. In this argument π-π* interactions occur when the attractive interaction between the π-electrons and the σ-framework is more favourable than the repulsive contribution of the π-electrons. This suggests that this form of interaction is not a π-π* interaction but is in fact a π-σ interaction (Figure 4.4).

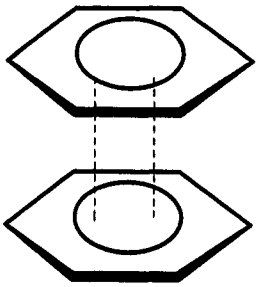

Figure 4.3. A $\pi - \pi^*$ interaction.

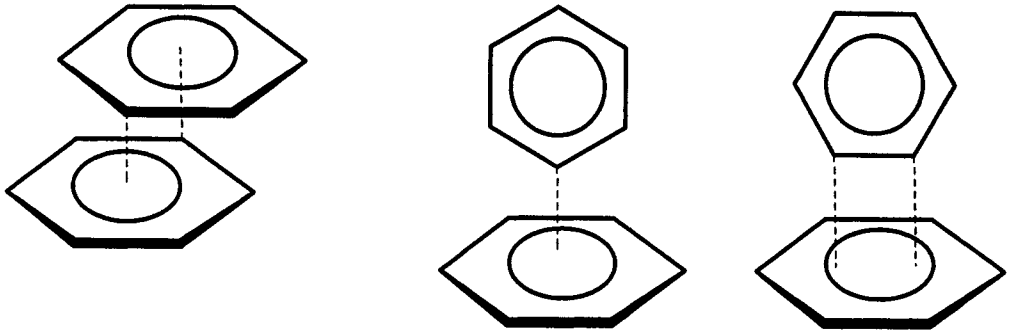

Face - Face Interaction **Face - Edge Interactions**

Figure 4.4. $\sigma - \pi$ interactions.

e. Charge Transfer. The conceptual basis for charge transfer complexes was pioneered by Mulliken in 1952. Mulliken proposed that charge transfer complexation was the result of electron delocalization between the filled molecular orbitals of a "donor" moiety into an empty acceptor molecular-orbital of appropriate symmetry in the acceptor moiety. The donor acceptor interaction is weak relative to covalent bonds and is characterized by a parameter H_{DA}. H_{DA} is a measure of the electronic coupling in the donor-acceptor complex in energy units. The presence of charge transfer complexation is often signalled by the presence of a new absorption band in the uv-vis and near IR spectra

of donor-acceptor charge transfer complexes assignable to a photo induced electron transfer between the donor-acceptor pair.[73]

f. Hydrophobic or Solvophobic Effects.[75] These effects are based on the observation that solvent molecules pack more tightly around a solute than around other solvent molecules. The solvophobic effect occurs as a result of mixing two solutions containing two different solutes: one of the solutions contains a host molecule which contains a cavity occupied by solvent molecules, and the other solution contains a guest molecule which is surrounded by solvent molecules. When the two solutions are mixed together the solvent within the cavity of the host is displaced and the solvent around the guest rearranges as an inclusion complex is formed (Figure 4.5). The solvent then arranges around the complex or is displaced into the bulk solvent as a result of which entropy of the system is increased.

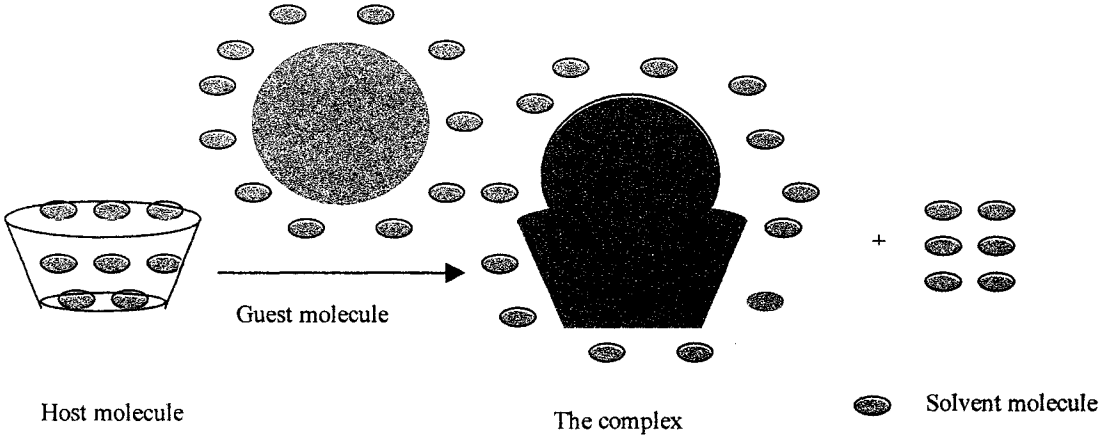

Figure 4.5. The solvophobic effect.

4.1.1. C_{60}

C_{60} is an exceptionally well-studied molecule.[36] It can undergo chemical modification such as the addition of *N,N*–dimethylethylenediamene across the 6,6'-

position ring junction of two six-membered rings.[76] It is spherical and is an electron-deficient system which can bind to electron-rich molecules. The shape of C_{60} makes it an ideal guest molecule for macrocyclic hosts with the appropriately-sized and shaped cavity.[75] Many supramolecular complexes have been reported between C_{60} and macrocyclic hosts, such as CTV,[77] calixarenes,[67] homooxacalixarenes,[67] resorcairenes,[67] calix[4]naphthalenes,[68] hexahomotrioxacalix[3]naphthalene[69] and substituted corannulenes.[78]

The uv-vis spectrum of C_{60} in several solvents has been documented.[79, 80] It has a large absorbance between 440 nm and 690 nm, with several shoulders which have been assigned as singlet transition bands. It has a λ_{max} of approximately 540 nm. Changes in the absorbance spectrum of C_{60} can indicate the formation of a complex.

4.1.2. Determining the Stoichiometry and K_{assoc} of a Supramolecular Complex

The stoichiometry of a complex is the ratio of guest-to-host molecules and must be determined before the association constant (K_{assoc}) (Equation 1.1) can be determined. K_{assoc} is a direct measure of the Gibbs free energy for formation of a supramolecular complex (Equation 1.2 and 1.3) using Equation 4.1, where ΔG^0 is defined as the change in Gibbs free energy, and R is defined as the ideal gas constant.

$$\Delta G^0 = -RT\ln K_{assoc} \qquad (4.1)$$

One common method to determine the stoichiometry of a complex is the continuous variation method (Job's method).[82, 83] A series of solutions containing both

guest and host in varying ratios are prepared. These solutions must cover the entire range of mole fractions (χ) of host or guest. The concentrations of the guest and host are varied such that the total concentration ([H] + [G]) remains constant.

These solutions are then analyzed by uv-vis and/or by NMR spectroscopic methods. The product of the change in absorbance and the mole fraction at a given wavelength is plotted against the mole fraction of the guest. For NMR the change in the chemical shifts ($\Delta\delta$) multiplied by the moles concentration of the host [H] or the guest [G] is plotted against the mole fraction of the host [H] or of the guest [G]. When a reaction occurs between the guest and the host the resulting curve cannot be modelled as a linear combination of the individual spectra of the host and guest. A simple 1:1 complex will generate a Job plot in the form of a symmetrical hyperbolic function with the maximum centered at the mole fraction 0.5. A complex with greater than a 1:1 ratio of host to guest (or guest to host), shows a more complex curve.[83] The data used to determine the stoichiometry can theoretically be used to extract K_{assoc}, however, there are too many unknown parameters, such as in uv-vis determination, the extinction coefficient (ε) of the possible species may not be known. Therefore Job data are not the most reliable for the determination of the K_{assoc} and if possible a second independent experiment should also be conducted.

A titration experiment[80] is often used to experimentally determine the equilibrium constant for a reaction, from the changes observed in absorption spectra, or the changes observed in chemical shifts. These types of experiments involve the sequential addition of one compound to the solution of the second. The concentration of the first compound remains constant while the concentration of the compound being added increases. From

this data several methods have been used to calculate the K_{assoc}.

One such treatment is the Benesi-Hildebrand[83-85] protocol which is applicable to both NMR and uv-vis spectroscopic methods (Equations 4.2a and 4.2b). For the NMR method, Equation 4.2a applies:

$$\mathbf{1/\Delta\delta = 1/(\Delta\delta_o \bullet \mathit{K}_{assoc} \bullet [G]) + 1/\Delta\delta_o} \qquad \mathbf{(4.2a)}$$

Equation 4.2a is a form of the Benesi-Hildebrand formula where $\Delta\delta = (\delta_{observed} - \delta_{free})$. In a titration experiment conducted with **11** and C_{60}, the changes in chemical shift, $\Delta\delta$, is measured with respect to a representative signal in the ^{1}H NMR spectra of **11** as C_{60} is added; $\Delta\delta_o = (\delta_{complex} - \delta_{free})$ cannot be determined directly when the exchange or equilibrium between host and guest and host:guest complex is rapid; [G] = equilibrium concentration of the "free" or uncomplexed guest (C_{60}) *i.e.* [G] = [G^o] – [HG] (where [G^o] = initial concentration of guest, and [HG] = concentration of the host:guest complex at equilibrium). A plot of $1/\Delta\delta$ *vs* 1/[G] will give a straight line whose slope = $1/(\Delta\delta_o \bullet K_{assoc})$ and intercept = $1/(\Delta\delta_o)$, therefore, dividing the intercept by the slope will give a value for K_{assoc}. (Note: $\Delta\delta_o$ is also referred to as $\Delta\delta_{max}$ or δ_∞ by other authors.) Alternatively, in order to avoid an extrapolation to obtain the value for the intercept, Equation 4.2a can be multiplied by $(\Delta\delta \bullet K_{assoc} \bullet \Delta\delta_o)$ to give Equation 4.2b:

$$\mathbf{\Delta\delta_o \bullet \mathit{K}_{assoc} = \Delta\delta / [G] + \Delta\delta \bullet \mathit{K}_{assoc}} \qquad \mathbf{(4.2b)}$$

Rearranging Equation 4.2b gives 4.2c, which is the Scatchard [86] or Forster-Fyfe[87] equation:

$$\mathbf{\Delta\delta / [G] = -\Delta\delta \bullet \mathit{K}_{assoc} + \Delta\delta_o \bullet \mathit{K}_{assoc}} \qquad \mathbf{(4.2c)}$$

A plot of $\Delta\delta$ / [G] *vs* $\Delta\delta$ gives – K_{assoc} directly from the slope, thus not requiring a value for the intercept which is potentially subject to large errors. However, in many cases with limited amounts of host or guest compounds available to a researcher thereby precluding an intensive study, the two methods do not differ significantly

Since [G] is difficult to measure, Equations 4.2a-c can be simplified by the assumption that [G] = [G^o]. This assumption is valid when K_{assoc}• [G] << 1 *i.e.* when complexation is weak, and so, plotting 4.2a-4.2c using [G^o] instead of [G] can be used to obtain K_{assoc}.[86] There are other treatments which could be employed to more accurately determine K_{assoc}, such as the iterative Rose-Drago approach.[86] Another is to employ an equimolar dilution method[88] where the concentrations of host and guest are always equal *i.e.* [H] = [G], of course with the understanding that there is only 1:1 complexation occurring. Recently, Goswani and coworkers[88] used such an approach to study molecular recognition of some xanthine alkaloids in which K_{assoc} was determined using Horman and Dreux's equation 4.2d,[88] where a = $\Delta\delta$ / $\Delta\delta_o$

$$\boldsymbol{K_{assoc} = a/\{(1-a)^2\,[c]\}} \qquad \textbf{(4.2d)}$$

and [c] = concentration of host or guest (which are equal under the equimolar conditions). Due to time constraints however, these latter procedures were not employed and are not discussed any further in this thesis.

For the uv-vis titration experiment, the form of the Benesi-Hildebrand equation is 4.2e. This expression holds for the case in which the absorbance of a solution of a host molecule (A_H) is measured as a function of added guest, against a reference solution of the host alone (A_H^o). The initial (uncomplexed) concentrations of host and guest are [H^o] and [G^o] and the equilibrium concentrations of host, guest and host:guest complex are

[H], [G] or [HG] (assuming only 1:1 complex formation) respectively. Furthermore, this equation assumes that [H] = [H°] *i.e.* when the condition [H°] >> [G°] is employed, since [H] is not easy to measure directly (*alternatively, if [G°] >> [H°] is employed instead, the appropriate equations can use [G] = [G°],*). The path length is *b*, and $\Delta\varepsilon_{HG}$ = (ε_{HG} • [HG] – ε_H • [HG] – ε_G • [HG]) where ε_H is the molar extinction coefficient of the host, ε_G is that of the guest and ε_{HG} is that of the host:guest complex:

$$b/\Delta A = 1/([H^\circ] \bullet K_{assoc} \bullet \Delta\varepsilon_{HG} \bullet [G^\circ]) + 1/([G^\circ] \bullet \Delta\varepsilon_{HG}) \quad \textbf{(4.2e)}$$

Multiplying Equation 4.2e by [G°] gives 4.2f . A straight-line "double reciprocal"

$$([G^\circ] \bullet b)/\Delta A = 1/([K_{assoc} \bullet \Delta\varepsilon_{HG} \bullet [H^\circ]) + 1/\Delta\varepsilon_{HG} \quad \textbf{(4.2f)}$$

plot of ([G°] • *b*)/ΔA (or simply *b*/ΔA) on the *y*-axis *versus* 1/([H°]) on the *x*-axis gives a slope and intercept which, according to Equation 4.2f will afford K_{assoc} by dividing the intercept on the *y*-axis of the resulting linear regression analysis by the slope.

Use of the Scott equation (4.2g) avoids the extrapolation needed to determine the intercepts on the *y*-axes in both cases. It is obtained directly by multiplying Equation 4.2f by [H°]:

$$([G^\circ] \bullet [H^\circ] \bullet b)/\Delta A = 1/([K_{assoc} \bullet \Delta\varepsilon_{HG}) + [H^\circ]/(\Delta\varepsilon_{HG}) \quad \textbf{(4.2g)}$$

There are other limitations to the use of such plots, and these have been extensively reviewed elsewhere.[86]

In Chapter One of this thesis, the complexes formed between calix[4]naphthalenes[4] and C_{60} and the complexes formed between selected calixarenes[31-33,36] and C_{60} were introduced. Calix[4]azulene (**11**) resembles calix[4]naphthalene (**8**) in its topology; it is composed of azulene rings linked by methylene bridges connected to the 1,3-positions of the azulene rings.[8] The azulene subunits of **11** (like the naphthol

subunits of **8**) are composed of two fused rings to create a Huckel $2n$ +2 aromatic compound. The two compounds do have some significant differences: **8** has C_4 symmetry whereas **11** shows C_{4v} symmetry; also **11** has no functional groups while **8** contains a hydroxy group on each naphthalene unit. Our group has been studying supramolecular complexation between calix[4]naphthalenes and C_{60}[4,68,71,78] and was interested in evaluating the novel calix[4]azulene for this kind of study. In this chapter we examine the complexation products of C_{60} and **11** using two different spectroscopic methods.

4.2. Synthesis and Characterization of 11

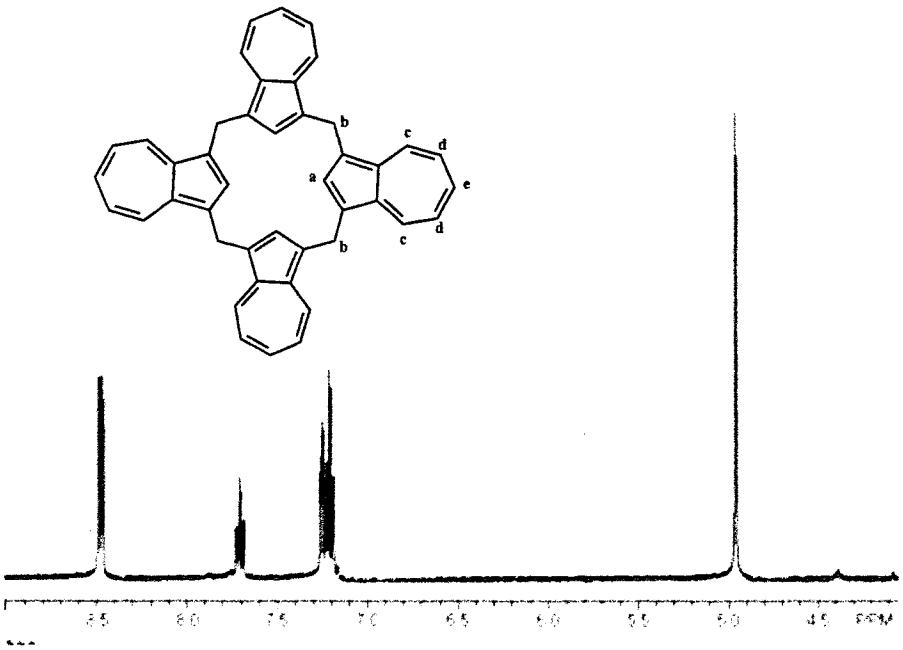

Figure 4.6. NMR spectrum of calix[4]azulene (1.03 mM) in CS_2. This NMR was run on a Bruker 500 MHz spectrometer using a Teflon® insert with a capillary tube filled with chloroform-d_1. The proton lettering scheme and assignment are also illustrated. Assignments can be seen in Section 3.4.

The synthesis of calix[4]azulene was conducted as reported by Colby and Lash.[8] Figure 4.6 shows the ^{1}H NMR spectrum of calix[4]azulene in CS_2 using a specially-designed insert which allows for the use of a sealed capillary tube containing $CDCl_3$ as an internal NMR lock. The peak assignments are given in Section 3.4 and illustrated in Figure 4.6.

4.2.1 Determining the Absorption Structure of 11

Calix[4]azulene dissolved in CS_2 is bright blue. Uv-vis spectral data shown in Figure 4.7 shows the very different absorption spectra of calix[4]azulene and C_{60}. The absorbance spectrum of calix[4]azulene shows a broad band envelope that extends from approximately 490 nm to 790 nm, with a λ_{max} at 632 nm. The absorbance spectrum of C_{60} shows a absorbance band envelope from approximately 440 nm to 690 nm, with a λ_{max} of 540 nm. There are three main features within the calix[4]azulene absorbance spectra above 490 nm, the first being at 634 nm, the second at 696 nm, and the third at 774 nm.

Comparison of the uv-vis spectrum of calix[4]azulene with that of azulene (Figure 4.8), shows a notable difference in that calix[4]azulene absorbs at lower energy wavelengths in the visible region. The band envelope of the azulene spectrum stretches from approximately 482 to 726 nm, whereas the calix[4]azulene spectrum shows a band envelope from approximately 500 to 800 nm (*vide supra*). The absorbance bands of calix[4]azulene and azulene are, however, similar in structure (Figure 4.8). There are regions of the visible spectrum where the absorbances of azulene are similar to those of calix[4]azulene. For calix[4]azulene these peaks are at 632, 700, and 768 nm, whereas for azulene, these peaks show up at 586, 652 and 706 nm. The peaks observed in the spectrum of azulene have already been assigned previously to the disallowed $S_0 \rightarrow S_1$

transition.[89] The corresponding observed absorbances in the spectrum of calix[4]azulene can therefore also be assigned to the $S_0 \rightarrow S_1$ absorption, by analogy.

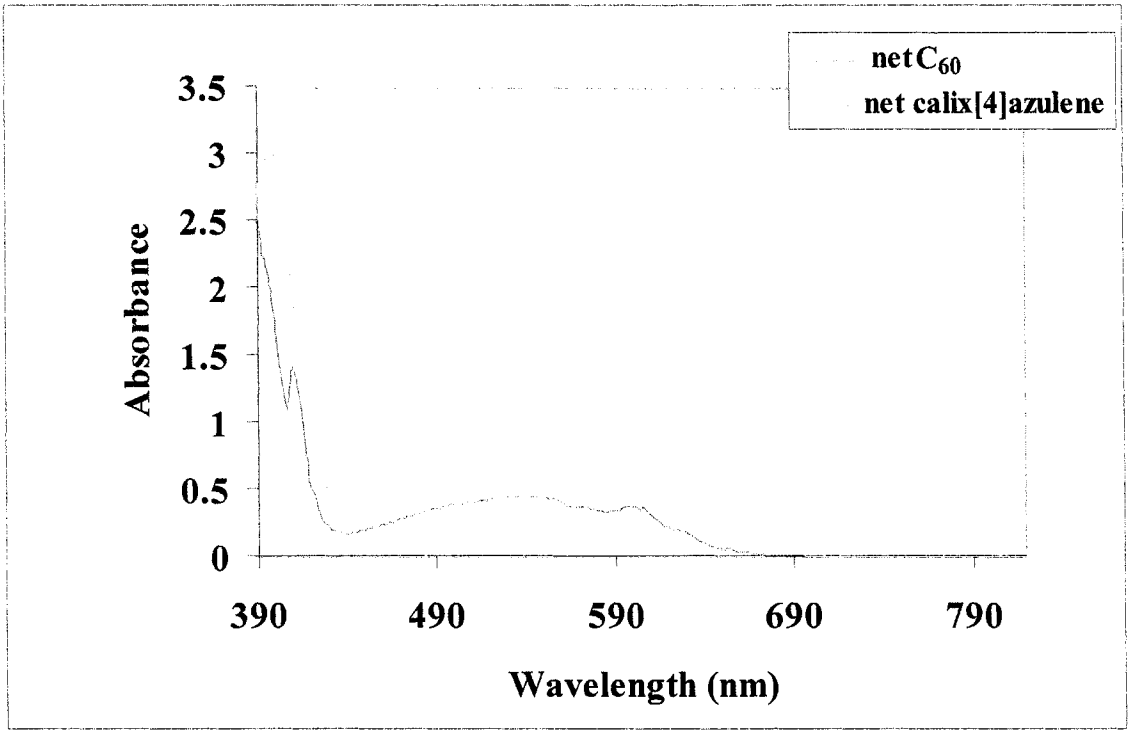

Figure 4.7. The UV-visible spectrum of calix[4]azulene (1.03 mM) and C_{60} (0.938 mM) in CS_2, at 298K. "Net" refers to the calculation in which the absorbance value for the blank (air) is subtracted from the absorbance value of the individual solution being measured. Air was used as the blank as a way to help detect any problems with the solvent, such as absorbing impurities in CS_2.

4.3. Supramolecular Binding by UV-Visible Spectroscopy and ^{1}H NMR Spectroscopy

4.3.1. UV-Visible Studies-General Observations

Upon mixing solutions of C_{60} and calix[4]azulene, the color of the solution changed from the initial magenta for pure C_{60} and blue for pure calix[4]azulene, respectively, to a final grey-blue solution. The uv-vis spectra plotted as a function of the ratio of **11** to C_{60} are shown in Figures 4.9 and 4.10. The observed spectral changes cannot be accounted for by merely a linear combination of the reagents. At low ratios of **11** to C_{60} the observed spectra are consistent with C_{60} as the dominant species. An increase in the ratio of **11** results in a diminishing of the C_{60} absorbance and a growth of a new absorption band at longer wavelengths.

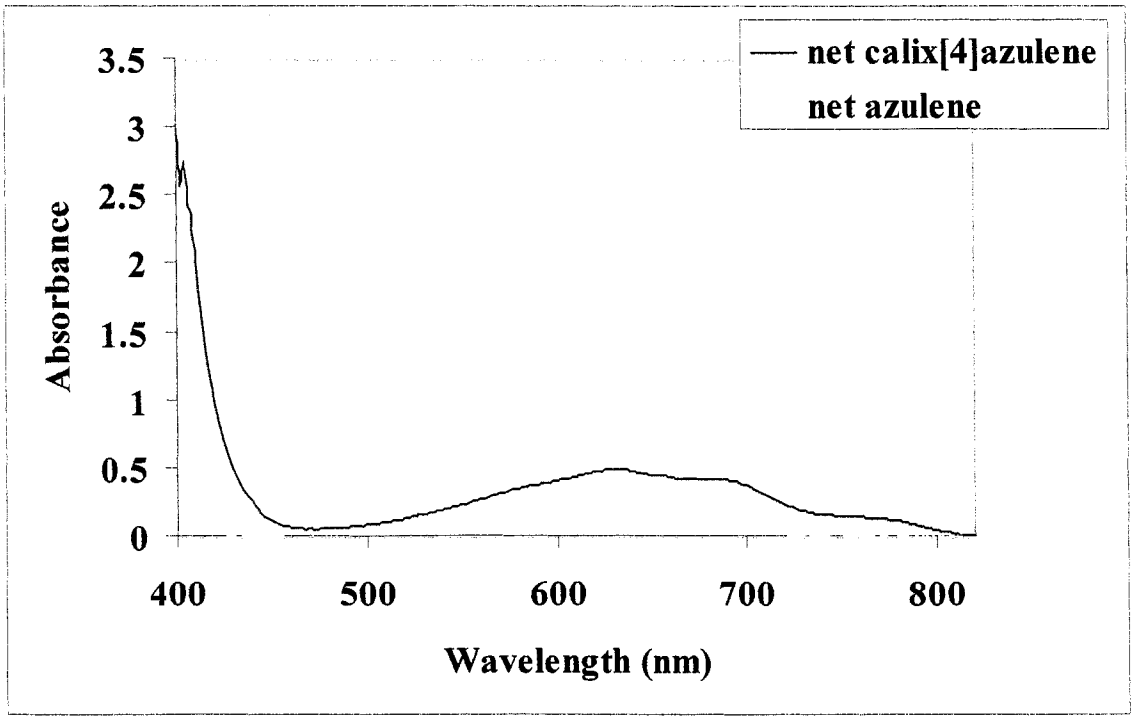

Figure 4.8. Absorbance spectra of calix[4]azulene (1.03 mM) and azulene (1.49 mM). Both compounds were measured CS_2 solvent.

As the concentration of C_{60} is increased, a new band formation is observed between 490 nm and 590 nm. All the spectra cross at two points in the absorbance curves: at 440 nm and 574 nm. These two isosbestic points can be interpreted as an indication of a complex (or complexes) being formed. The presence of a second isosbestic point may indicate that a more complicated complex than a simple 1:1 complex is being formed.

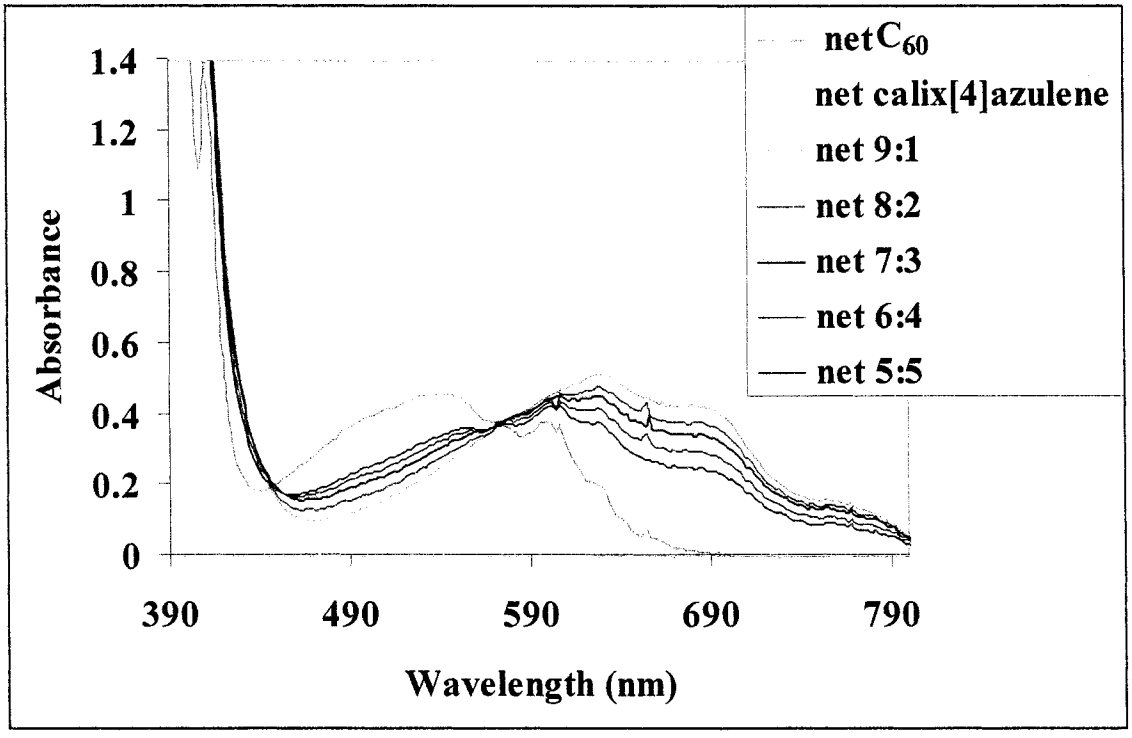

Figure 4.9. Absorbance spectra from a continuous variation experiment in CS_2 where the mole ratios of calix[4]azulene to C_{60} range from 1:1 to 9:1. The original solutions were 1.03 mM for calix[4]azulene and 0.938 mM for C_{60}. The correct concentrations for each sample can be found in Appendix C. "Net" refers to the calculation in which the absorbance value for the blank (air) is subtracted from the absorbance value of the individual solution being measured.

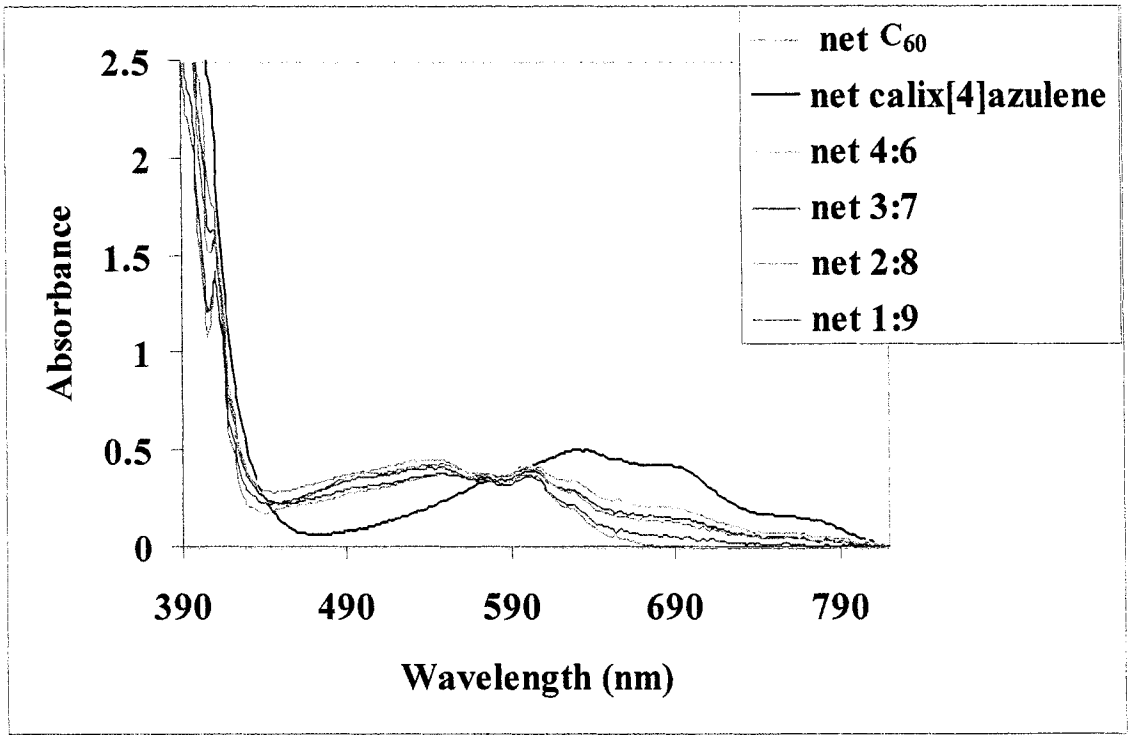

Figure 4.10. Absorbance spectra from a continuous variation experiment in CS_2 where the mole ratios of calix[4]azulene to C_{60} range from 1:9 to 4:6. The original solutions were 1.03 mM for calix[4]azulene and 0.938 mM for C_{60}. The correct concentrations for each sample can be found in Appendix C. "Net" refers to the calculation in which the absorbance value for the blank (air) is subtracted from the absorbance value of the individual solution being measured.

4.3.2. NMR Studies-General Observations

Upon mixing solutions of **11** and C_{60} there are only very small chemical shift changes in the proton resonances of **11** as the ratio of C_{60} to **11** increases. These shift changes are a result of the change in environment due to complexation with the C_{60}. The chemical shifts are an average of the chemical environment of the protons. When **11** complexes with C_{60}, the π-electron clouds of the C_{60} are introduced into the environment of **11**, thereby changing its electric and magnetic fields. This can then induce a shift in the position of the proton signals. As well, there is the possibility of several species being present which may also create a change in the chemical shifts. The trends are summarized in Tables 4.1, 4.2 and 4.3. Table 4.1 shows the dependency of the chemical shifts of **11** itself, using three commonly-used NMR solvents.

Table 4.1. ^{1}H NMR chemical shifts of H_a-H_e of calix[4]azulene in different solvents.[1]

solvent	H_a ppm	H_b ppm	H_c ppm	H_d ppm	H_e ppm
CS_2	**7.248**	**4.958**	**8.466**	**7.208**	**7.703**
Toluene-d_8	**6.433**	**4.172**	**7.708**	**6.324**	**6.787**
Benzene-d_6	**6.923**	**4.204**	**7.743**	**6.336**	**Nd[2]**

As can be seen in Tables 4.2 and 4.3, the observed changes in chemical shifts could indicate the presence of two-step equilibria for example, the one shown in Equation 4.3b where 11 is in excess:

$$\mathbf{11} + \mathbf{C_{60}} \rightleftharpoons \mathbf{11{:}C_{60}} \qquad \textbf{(4.3a)}$$

$$\mathbf{11} + \mathbf{11{:}C_{60}} \rightleftharpoons \mathbf{(11)_2{:}C_{60}} \qquad \textbf{(4.3b)}$$

Or when C_{60} is in excess (Equations 4.3c):

[1] See Figure 4.6 for the assignment of the protons.
[2] Nd: Not determined.

$$\mathbf{11} + C_{60} \rightleftharpoons \mathbf{11{:}}C_{60} \qquad \textbf{(4.3a)}$$

$$\mathbf{11{:}}C_{60} + C_{60} \rightleftharpoons \mathbf{11{:}}(C_{60})_2 \qquad \textbf{(4.3c)}$$

The changes in the NMR data in CS_2 solution appear larger than in benzene solution. Both C_{60} and calix[4]azulene are more soluble in CS_2 than in benzene, ie. 62 mg calix[4]azulene will dissolve in 1 ml of CS_2 whereas only 37 mg of calix[4]azulene will dissolve in 1 ml of benzene. However in both case the chemical shifts are very small and have errors of ± 0.0005, which make interpretation of this data difficult.

Table 4.2. Changes in chemical shifts in CS_2 as the mole ratio of calix[4]azulene to C_{60} changes.

Ratio of **11** to C_{60}	Δ ppm H_a	Δ ppm H_b	Δ ppm H_c	Δ ppm H_d	Δ ppm H_e
9:1	**0.000**	**0.001**	**0.002**	**0.001**	**0.002**
8:2	**0.002**	**0.002**	**0.002**	**0.001**	**0.002**
7:3	**0.003**	**0.003**	**0.004**	**0.003**	**0.003**
6:4	**0.005**	**0.002**	**-0.003**	**0.002**	**0.002**
5:5	**0.002**	**0.001**	**0.001**	**0.001**	**0.001**
4:6	**0.003**	**0.002**	**0.002**	**0.001**	**0.002**
3:7	**0.003**	**0.002**	**0.002**	**0.001**	**0.002**
2:8	**0.003**	**0.002**	**0.002**	**0.001**	**0.001**
1:9	**0.002**	**0**	**0.002**	**-0.002**	**0.001**

Table 4.3. Changes in chemical shifts in benzene-d_6 as the mole ratio of calix[4]azulene and C_{60} changes.

Ratio of **11** to C_{60}	Δ ppm H_a	Δ ppm H_b	Δ ppm H_c	Δ ppm H_d	Δ ppm H_e
9:1	**0.000**	**0.000**	**0.000**	**0.000**	-
8:2	**0.000**	**0.000**	**0.001**	**0.001**	-
7:3	**0.000**	**0.000**	**0.001**	**0.001**	-
6:4	**0.000**	**0.000**	**0.000**	**0.000**	-
5:5	**-0.003**	**-0.002**	**-0.002**	**-0.002**	-
4:6	**-0.003**	**-0.002**	**-0.002**	**-0.002**	-
3:7	**-0.002**	**-0.001**	**-0.001**	**-0.001**	-
2:8	**-0.001**	**-0.001**	**-0.001**	**0.000**	-
1:9	**-0.003**	**0.000**	**-0.001**	**-0.001**	-

The chemical shift changes noted in Tables 4.2 and 4.3 are not straightforward to interpret, partly because the values are very small and contain relatively large errors. The formation of a 1:1 complex would be expected to show upfield shift increases until a 1:1 ratio of the guest to the host is reached. On either side of this ratio there would be a mixture of multiple species, including the complexed and uncomplexed guest, or host, which would cause a decrease in the magnitude of the upfield shift. The data in Table 4.2 and 4.3 differ from the results expected for a 1:1 complex and therefore make it difficult to form a simple conclusion about the structure of the adduct.

The observed changes in chemical shifts could indicate the presence of a two-step equilibrium (Equation 4.4). A Job plot of the data from Table 4.2 is shown as Figure 4.10. This plot is not a simple hyperbola, but rather suggests a bimodal distribution. It appears that there are two maxima at 0.25 and 0.75 mole fraction of C_{60}. However, due to the large error limit values, the data are not reliable enough to unequivocally discriminate between such 1:1 and 2:1 complexes. Also, since the solubility of **11** in CS_2 or benzene-d_6 is low, potential larger chemical shifts could not be determined using more concentrated solutions than the ones used in these experiments. No further NMR studies were conducted with this system.

$$\mathbf{[G] + [H] \rightleftharpoons [G \cdot H] + [H] \rightleftharpoons [G \cdot 2H]} \qquad \mathbf{(4.4)}$$

Molecular modeling calculations using Spartan Pro[10] of **11** in the absence of guest molecules, based upon the AM1 semi empirical methods, showed the lowest energy

conformation to be *pinched cone* (Figure 4.12). However, a docking calculation with C_{60} clearly revealed the optimized lowest energy conformation of the calix[4]azulene in the 1:1 complex to be a C_{4v}–symmetrical *cone* (figure 4.13). Similar molecular modelling of the $(\mathbf{11})_2$:C_{60} complex reveals the structure shown in Figure 4.14.

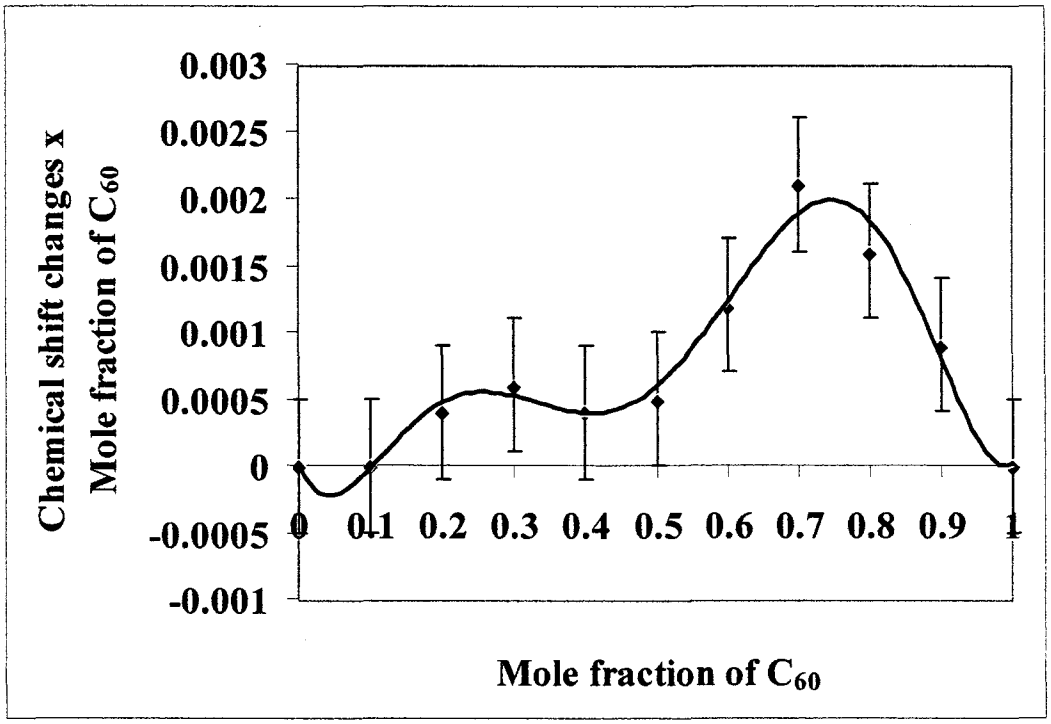

Figure 4.11. Job plot of the chemical shift change for the methylene signal of calix[4]azulene in CS_2 as the mole fraction of C_{60} increases.

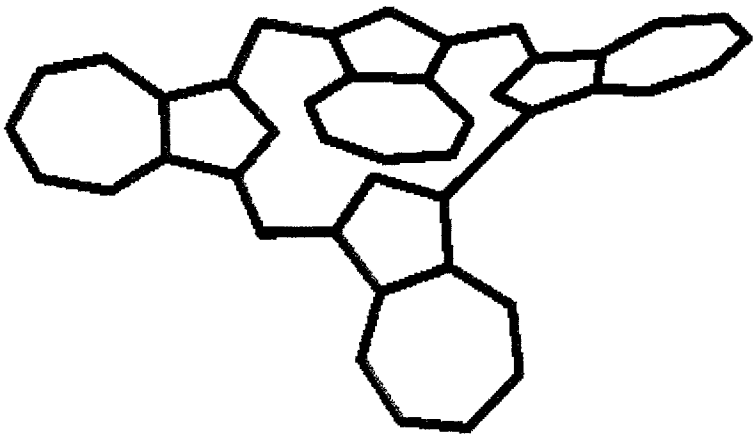

Figure 4.12. ***Pinched cone*** **conformer of calix[4]azulene.** This is the minimum energy conformer as determined by molecular modeling with PC Spartan Pro molecular modeling program. Note: Hydrogen atoms have been omitted for clarity.

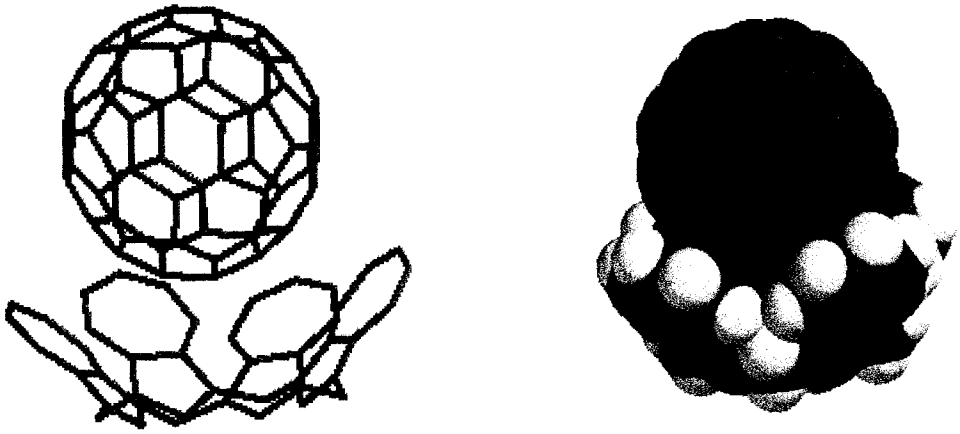

Figure 4.13. **The 1:1 C_{60}: calix[4]azulene complex as generated using the PC Spartan Pro molecular modeling program.** Note: Hydrogen atoms have been omitted for clarity on the structure on the left but not on the space-filling structure on the right.

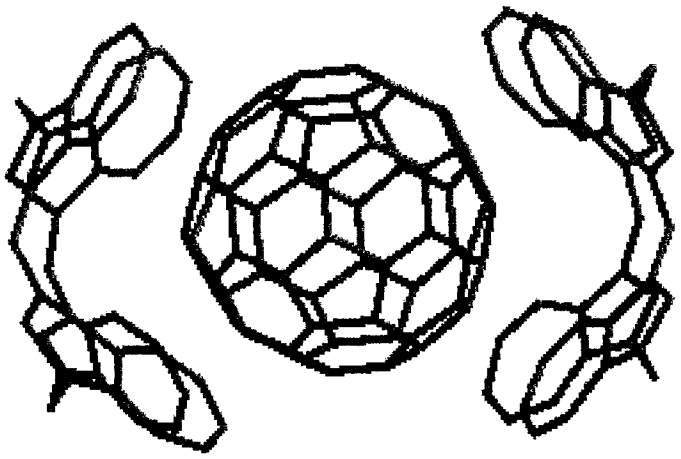

Figure 4.14. The 2:1 calix[4]azulene:C_{60} complex as generated using the PC Spartan Pro V.5.0 molecular modeling program. (Note: Hydrogen atoms have been omitted for clarity.)

4.4. Evidence for Supramolecular Complexation between C_{60} and 11

4.4.1. Equilibrium Constants by UV-Visible Spectroscopy

4.4.1.b. Determining the Stoichiometry of the Calix[4]azulene:C_{60} Complex by UV-Visible Spectroscopy

The absorbance spectra of pure calix[4]azulene and C_{60} in CS_2 were previously shown in Figure 4.7. This figure also shows isoabsorptive points[1] at 444 nm and 580 nm. Figure 4.9 shows the uv-vis absorbance spectra when the mole ratio of calix[4]azulene to C_{60} is varied from 5:5 to 9:1. The isosbestic points observed in the continuous variation analysis are found at 440 nm and the second at around 574 nm. There is an observed shift

from the isoabsorptive points of the individual compounds and the isosbestic points of analysis which are greater than the expected experimental error. If no complexation occurred between the two solutes in this experiment the isosbestic points would be found at the same wavelengths as the isoabsorptive points.

Figure 4.10 shows the absorbance spectra recorded when the calix[4]azulene:C_{60} mole ratio is varied from 1:9 to 4:6, the range in which [**11**] << [C_{60}]. Only one isosbestic point can be observed. The second isobestic point which had been observed for the higher mole fractions (9:1 to 1:1) of calix[4]azulene was not observed. This does not necessarily indicate that no complex was formed; it instead indicates that at low calix[4]azulene concentrations, there may be different species present than those which may be present at the higher calix[4]azulene concentrations. In turn, this suggests that the complex formed is more complicated than a simple 1:1 complex.

With each increase of the mole fraction of C_{60}, the band envelopes change in both shape and intensity. The absorptions between 440 and 574 nm increase in intensity, whereas those at greater than 574 nm decrease in intensity. However, the changes in absorbance between each change in mole ratio are not linearly related. The non-linear increase in absorbance is an indication of a change in the nature of the species in solution, such as the formation of a complex.

A specific wavelength at a significant distance from the isobestic point was chosen to be plotted using the Job method to help determine the stoichiometry. Figure 4.14 shows the Job plot of using the uv-vis data at 520 nm. The shape of the Job plot does not contain a maximum at 0.5, but shows an apparent maximum when the mole fraction

[1] The isoabsorbtive point is a wavelength where the absorption spectra of two species cross. At this wavelength the two species have the same extinction coefficients

of **11** is 0.7, which gives the hyperbola an apparent skewed shape. This suggests higher order binding between calix[4]azulene and C_{60}. This is a similar conclusion derived from to the Job plots which were obtained from the NMR experiments (*vide supra*, Figure 4.11).

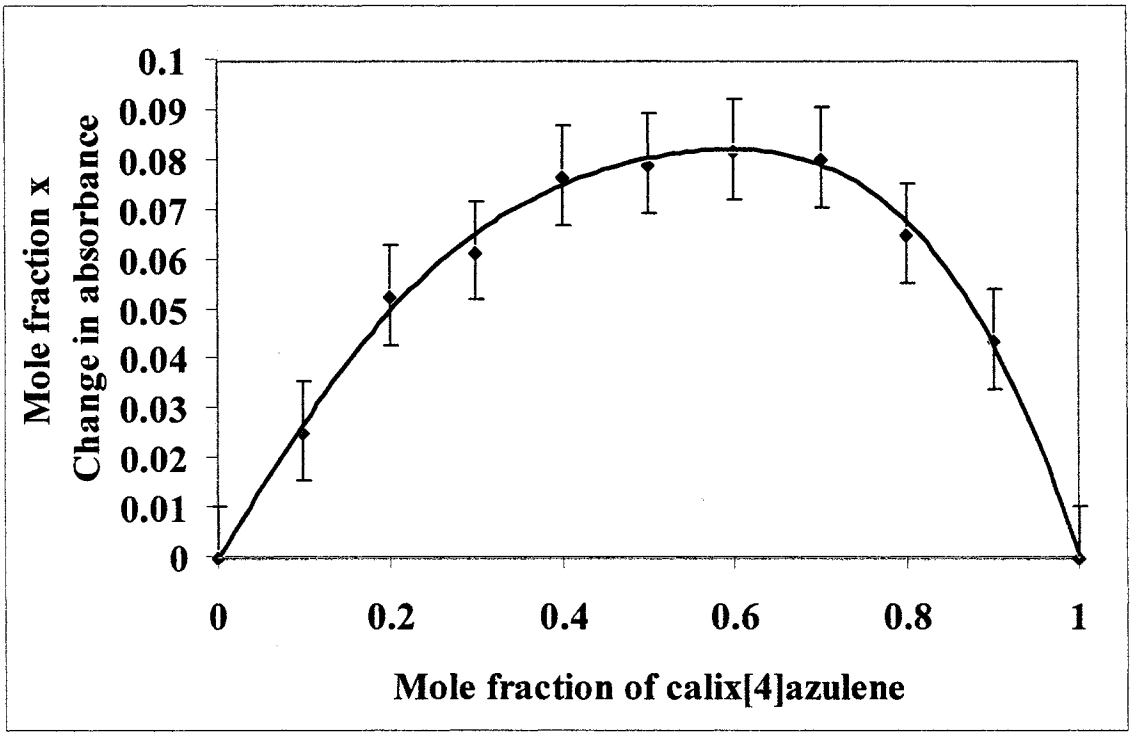

Figure 4.15. Job plot of calix[4]azulene vs C_{60} at 520 nm in CS_2. The line of best fit has no meaning and is shown for clarity only.

4.5. Determining K_{assoc} of C_{60} with Calix[4]azulene (11)

In order to determine the K_{assoc} values for each of the two complexes, an experiment was devised to examine each individual complex with the least amount of interference from the other complex.

Two individuals titrations were performed. The first was the addition of aliquots of a stock calix[4]azulene solution in CS_2 into a stock solution in CS_2 of C_{60}. A second

stock solution of C_{60} in CS_2 was used as the blank, with equivalent amounts of CS_2 being added to correct for dilution. This allowed us to study the formation of the first complex, by observing the absorbance of the 1:1 complex. The second titration was performed by the addition of aliquots of a stock solution of C_{60} into a stock solution of calix[4]azulene, again both host and guest being in CS_2 solution. This allowed us to potentially observe the absorbance of any higher-order binding complex, such as a 2:1 complex, since the calix[4]azulene host is always in excess.

The data from each of the titrations were plotted using the Benesi-Hildebrand treatment, from which the K_{assoc} were calculated. Figure 4.16 shows the absorbance changes from the first titration while Figure 4.17 shows the corresponding Benesi-Hildebrand plot. Figure 4.18 shows the absorbance spectra obtained from the second titration while Figure 4.19 shows the respective Benesi-Hildebrand plot. The calculated K_{assoc} was found to be approximately 3,000 M^{-1} for the formation of the suggested 2:1 complex.

The Benesi-Hildebrand plot depicted in Figure 4.17 gave a slope of 1.02×10^{-6} ($\pm$ 5.35×10^{-8}) and an intercept value of -0.0018 ($\pm$ 4.01×10^{-4}) with a correlation coefficient of R = 0.989. The slope and intercept yield K_{assoc} = 1770 (3.11×10^{-5}) M^{-1} and $\Delta\varepsilon$ = -600 $M^{-1}cm$ ($\pm$ 130). If these values are meaningful they can be tested by introducing the values into Equation 4.4 which is derived from Equation 4.2b.

$$\Delta A = [G^\circ] \bullet [H^\circ] \bullet K_{assoc} \bullet \Delta\varepsilon / (1 + K_{assoc} \bullet [H^\circ]) \qquad (4.5)$$

As can be seen in Figure 4.20, this is not the case. The bottom curve in Figure 4.20 is the result of using the calculated K_a and $\Delta\varepsilon$ from the Benesi-Hildebrand analysis,

the straight line was created directly from the experimental data. By observation, one can tell that the fit resulting from the Benesi-Hildebrand is inadequate for this system. The magnitude of the errors associated with the analysis of these plots has been previously discussed by Traylor *et al.*[90] Accordingly, for the Benesi-Hildebrand analysis to be applicable, $K > 1000$ and $\Delta\varepsilon > 150$ are necessary.[91] Saturation behavior in ΔA vs $[C_{60}]$ keeping [**11**] constant and ΔA vs [**11**] keeping $[C_{60}]$ constant, is an experimental requirement of the system which severely restricts the ranges of $[C_{60}]$ and [**11**] which could be explored.

The calculations reported in this section, in particular those shown in Figure 4.17 were undertaken by A. Bishop and Professor D. Thompson, MUN.

4.6 Conclusions

The experimental data and calculation show that the newest cavity-containing hydrocarbon macrocycle, calix[4]azulene, is an effective host for C_{60}. In CS_2 solution it apparently forms a complex with C_{60}, with higher host ratios. The uv-vis data showed an increased absorptivity of the adduct over the absorbance of **11** itself. Furthermore, the Job plot suggests sequential 1:1 and 2:1 complexation. The chemical shifts differences although small, appear to support this contention. Numerical analysis of spectroscopic data using the Benesi-Hildebrand protocol is unreliable in this system as the required limiting criteria are not met and as a result, the extraction of K_{assoc} from the uv-vis data was not meaningful. Further experiment, such as a Hill analysis and other titrations, will be required to exhaustedly evaluate the nature of the complexation properties of calix[4]azulene with C_{60}.

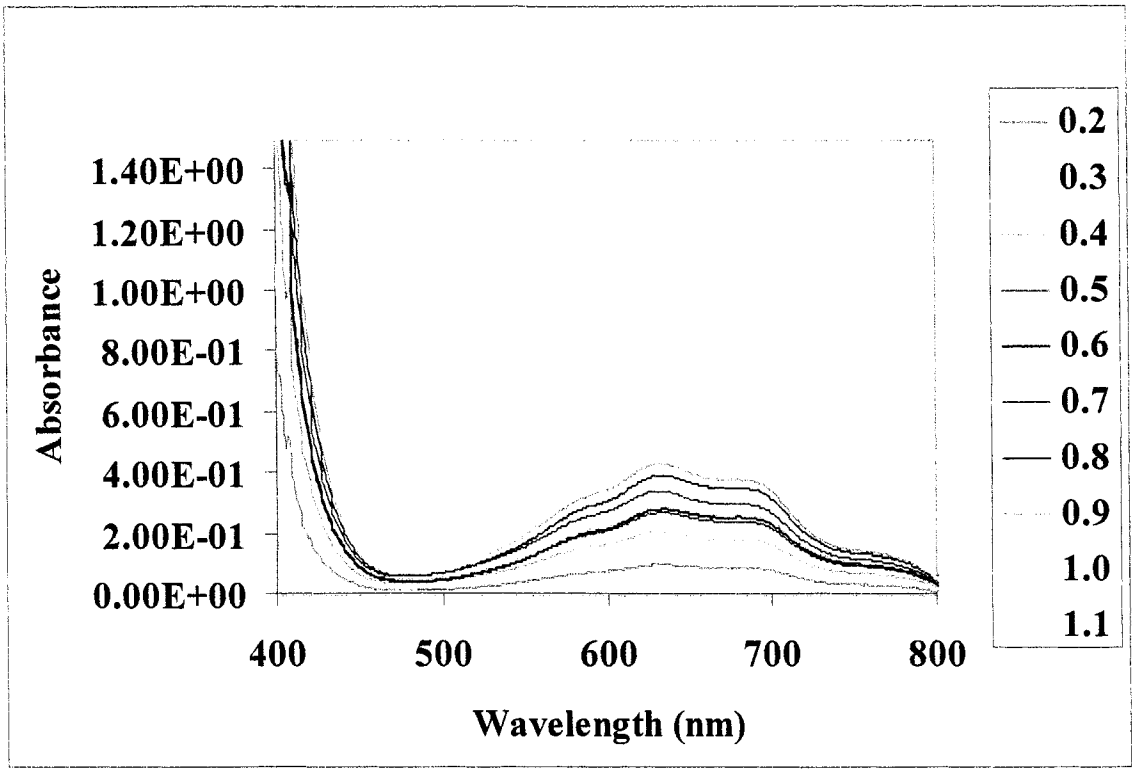

Figure 4.16. The absorbance spectra from the titration of calix[4]azulene into a solution of C_{60} The original concentrations were 1.00 mM for calixazulene and 1.01 mM for C_{60}. The concentration of individual samples can be found in Appendix C, Table C.7. The aliquots added were 0.10ml and the legend notes the total amount of the calix[4]azulene solution added to the C_{60} solution to give a total volume of 3.8 ml.

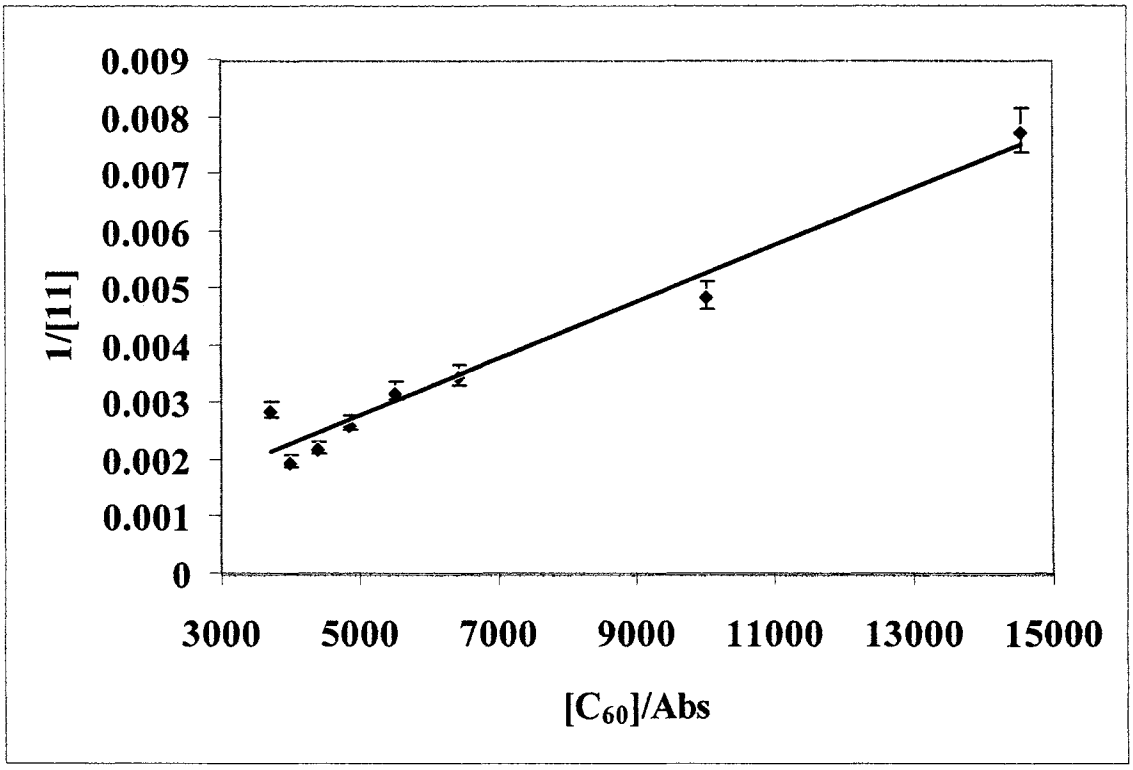

Figure 4.17. The Benesi-Hildebrand plot at 650 nm of the titration of calix[4]azulene into a solution of C_{60} and CS_2, obtained from the absorbance spectra shown in Figure 4.16.

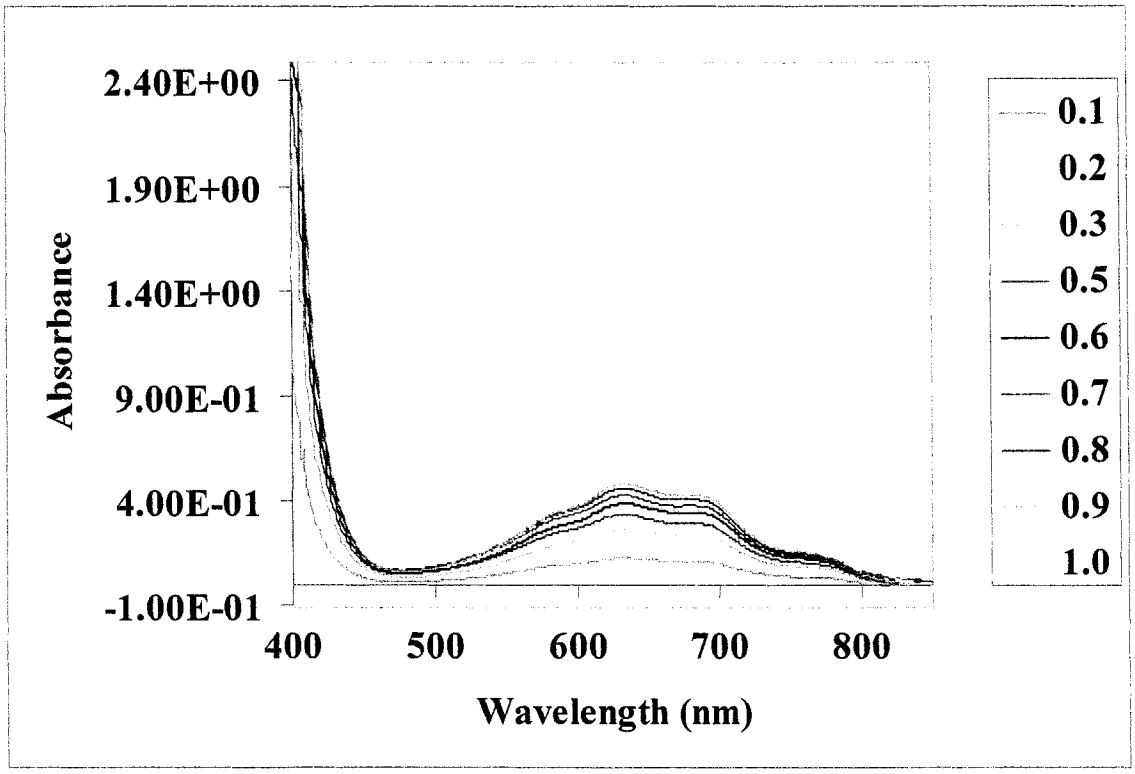

Figure 4.18. The absorbance spectra from the titration of C_{60} into a solution of calix[4]azulene. The original concentrations of solutions were 0.9977 mM for C_{60} and 1.065 mM for **11**. The concentration of individual samples can be found in Appendix C, Table C.8. The aliquots added were 0.10ml and the legend notes the total amount of the calix[4]azulene solution added to the C_{60} solution.

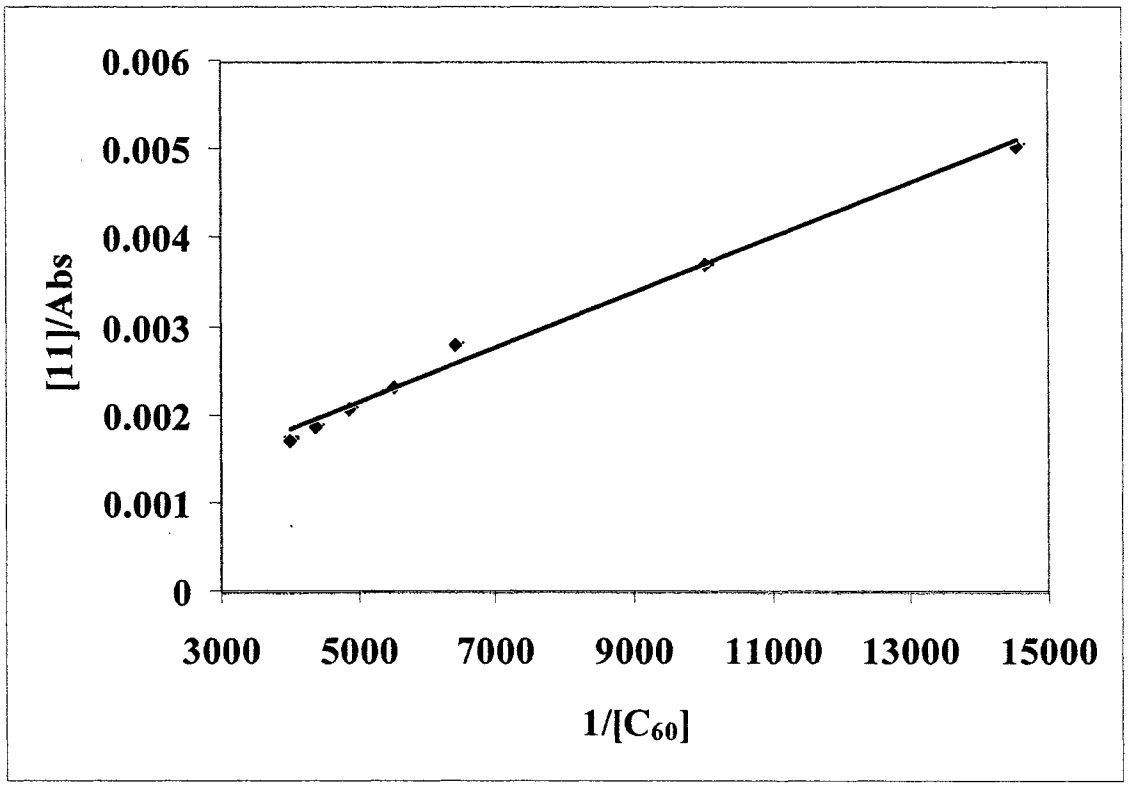

Figure 4.19. The Benesi-Hildebrand plot at 650 nm of the titration of C_{60} into a solution of calix[4]azulene and CS_2, obtained from the absorbance spectra shown in Figure 4.18.

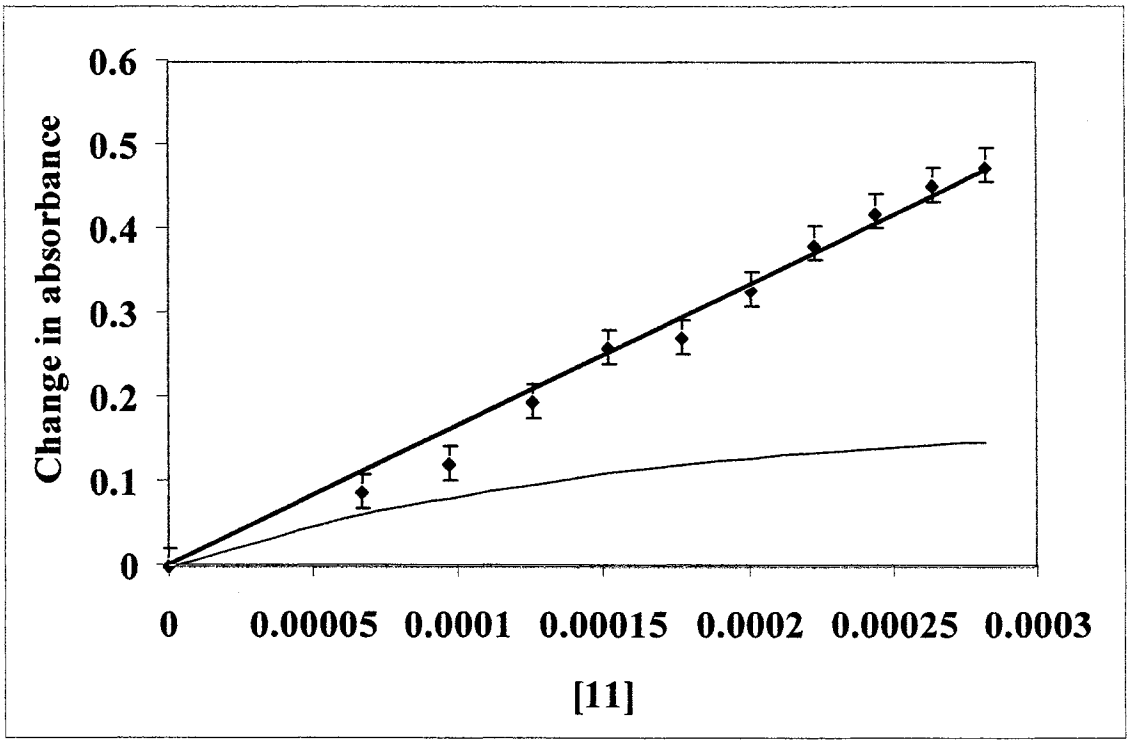

Figure 4.20. Plot of ΔA vs [11]- *top*: experimental data; *bottom*: data calculated from Equation 4.5.

4.7. Experimental

Azulene, formaldehyde, buckminsterfullerene (C_{60}) and Florisil^{R} were all purchased from Aldrich and were used as received. All calculations of data and graphs plotted were performed using Microsoft Excel spreadsheets. The spreadsheet accepted as input a table of mole ratios of calix[4]azulene to C_{60} and the observed variable (change in chemical shift or change in absorbance at a given wavelength), and then multiplied the two variables together for a Job plot. Job plots and Benesi-Hildebrand plots were plotted from the calculated data. From these plots the stoichiometry, K_{assoc} and $\Delta\varepsilon$ were calculated for complexation in both solvents. Solvents used for NMR and uv-vis experiment were HPLC grade.

Synthesis of Calix[4]azulene

Experimental

Calix[4]azulene was synthesized using a similar method as that described by Colby and Lash.[8] The methodology for this synthesis is described in Section 3.4 of this thesis.

NMR Experiments

All ^{1}H NMR data were collected on a Bruker Avance Instrument at 500 MHz using a 16 K data table for a 10.0 ppm sweep width having a digital resolution of 0.321 Hz. The solvents used were CS_2 (99.9%) and benzene-d_6 (99.6%). NMR in CS_2 were performed using an concentric-coaxial Teflon® insert with a Microbore™ capillary tube filled with chloroform-d_1 with 5 % TMS to allow for chemical lock and give a reference peak. A 10.0 ml solution of 1.03 mM calix[4]azulene and a 10.0 ml solution of 0.938 mM C_{60} in CS_2 were prepared. These two solutions were then used to prepare a series of nine

separate 1.00 ml solutions of varying mole ratios (9:1, 8:2, 7:3, 6:4, 5:5, 4:6, 3:7, 2:8, 1:9 calix[4]azulene:C_{60}), which were placed in NMR tubes. A sample of the pure calix[4]azulene solution was also placed in a NMR tube. A ^{1}H NMR spectrum for each solution was taken, and then carefully worked up on WinNuts NMR data processing program. This experiment was then repeated in benzene-d_6 without the insert (see Appendix C).

UV-vis experiment

Ultraviolet-visible spectral data were collected on an Hewlett Packard Diode array Spectrophotometer 8452A using HP 89532A General Scanning Software. The same series of solutions as were used in the NMR experiments were used for the uv-vis experiment. Samples of the C_{60} solution and CS_2 blank were placed in NMR tubes. A specially-designed holder was employed which enabled the NMR tubes to be placed in the path of the light source of the diode-array spectrometer. The holder consisted of a 1cm x 1cm x 4 cm Teflon^R block into which a 3-mm wide x 3.2 cm "widow" was cut into the block and thus constituted the window through which the light from the diode array spectrometer passed. The block also had an approx 5-mm hole drilled into the top so that the NMR tube could fit snugly into it. The path length of the solution contained in the NMR tube "cuvette" was therefore approximately 3 mm (interior diameter of the NMR tube). This set-up allowed for both the ^{1}H NMR and uv-vis determinations to be conducted without the need for removing the solutions in each case, and thus minimizing the volumes of deuterated solvents and quantities of materials required.

This experiment was repeated in benzene-d_6 (see Appendix C). All experiments used air as the reference, so that any absorbing impurities in the solvent could be

detected. The UV-vis experiments were repeated before and after the NMR experiments. The solution used to collect the uv-vis spectra of azulene was a 1.16 mM azulene solution in CS_2 (Figure 4.8). The uv-vis spectrum of azulene was collected using the same procedure as described above.

The titration experiments were done on a Cary instrument. The first titration was done by placing 2.70 ml of a 1.00 mM solution of C_{60} in CS_2 in two more conventional, 1 cm x 1 cm cuvettes, a second solution of 1.00 mM calix[4]azulene was added to one of the cuvettes in 100 μl aliquots, with an absorbance reading taken between each of the eleven additions. The second cuvette was used as the reference and received 100 μl aliquots of solvent to correct for the dilution. The second titration was done by placing 2.70 ml of a 1.00 mM solution of calix[4]azulene in CS_2 in two 1 cm x 1 cm cuvettes. A second solution of 1.00 mM C_{60} was added into one of the cuvettes in 100 μl aliquots, with an absorbance reading taken between each of the eleven additions. The second cuvette was used as the reference and received 100 μl aliquots of solvent to correct for the dilution.

Chapter 5

An Examination of the Supramolecular Complexation Stoichiometry of *tert*-Butylmethoxycalix[*n*]arenes and C_{60}

5.1. Introduction

Tert-butylcalix[6]arene[32] (**12**) forms a 2:1 complex with C_{60}, whereas *tert*-butylcalix[8]arene[33] (**13**) forms a 1:1 complex, as described in Chapter 1 of this thesis. In the investigation of the complexation properties of calix[4]azulene with C_{60} a novel method of conducting the ^{1}H NMR determinations was used which allowed the use of the nonpolar solvent, CS_2. The methyl ether derivatives **44** and **45** of calixarenes, **12** and **13,** respectively were synthesized (Figure 5.1).[91] The ether derivatives were then investigated to characterize their colligative and spectroscopic properties, and finally to characterize their host-guest complexation properties with C_{60}.

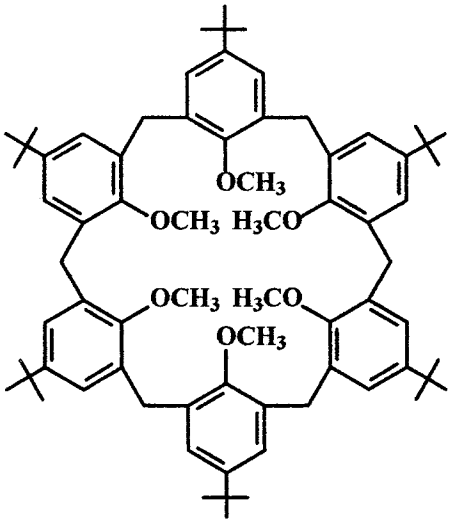

44

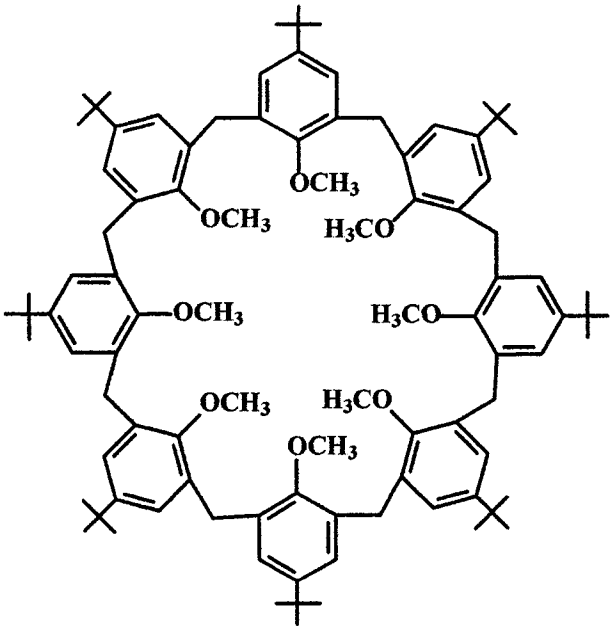

45

Figure 5.1. ***Tert*-butylmethoxycalix[6]arene and *tert*-butylmethoxycalix[8]arene.**

5.2. Characterization of *tert*-butylmethoxycalix[6]arene (44) and *tert*-butylmetoxycalix[8]arene (45)

The NMR data for **44** and **45** can be found in Section 5.3 of this thesis. Figures 5.2 and 5.3 are the absorbance spectra of **44** with C_{60} and **45** with C_{60}. The absorbance spectrum of C_{60} has been described in Chapter 4 of this thesis; neither **44** nor **45** show significant absorptions in the visible region ($\lambda > 350$ nm) at room temperature in CS_2 solution. CS_2 itself has a uv-vis cut-off at $\lambda < 340$ nm which precludes a determination of the uv spectrum for **44** and **45** at these wavelengths.

5.3. Supramolecular Binding by UV- Visible and ^{1}H NMR Spectroscopy

5.3.1. UV-Visible Spectroscopic Studies – General Observations

Upon mixing a solution of C_{60} (deep purple) with the solution of **44** (colorless) a pale purple solution resulted. A similar colored solution was observed when a solution of C_{60} was mixed with the solution of **45** (clear, colorless). The uv-vis spectra plotted as a function of the ratio of **44** and **45** respectively to C_{60} are shown in Figures 5.2 and 5.3. The observed spectral changes beyond $\lambda = 340$ nm cannot be modeled as a linear combination of the two reagents in either case. At low ratios of **44** the observed spectra are consistent with C_{60} being the dominant species. When the experiment was repeated with **45**, the low ratios of the host also produced spectra which are consistent with C_{60} being the dominant species. In both cases, the increase in the host mole fraction results in a decrease in the C_{60} absorbance. The spectra do not show equal decreases in absorption with each change in mole fraction, therefore the data cannot be discussed as simple dilution effect.

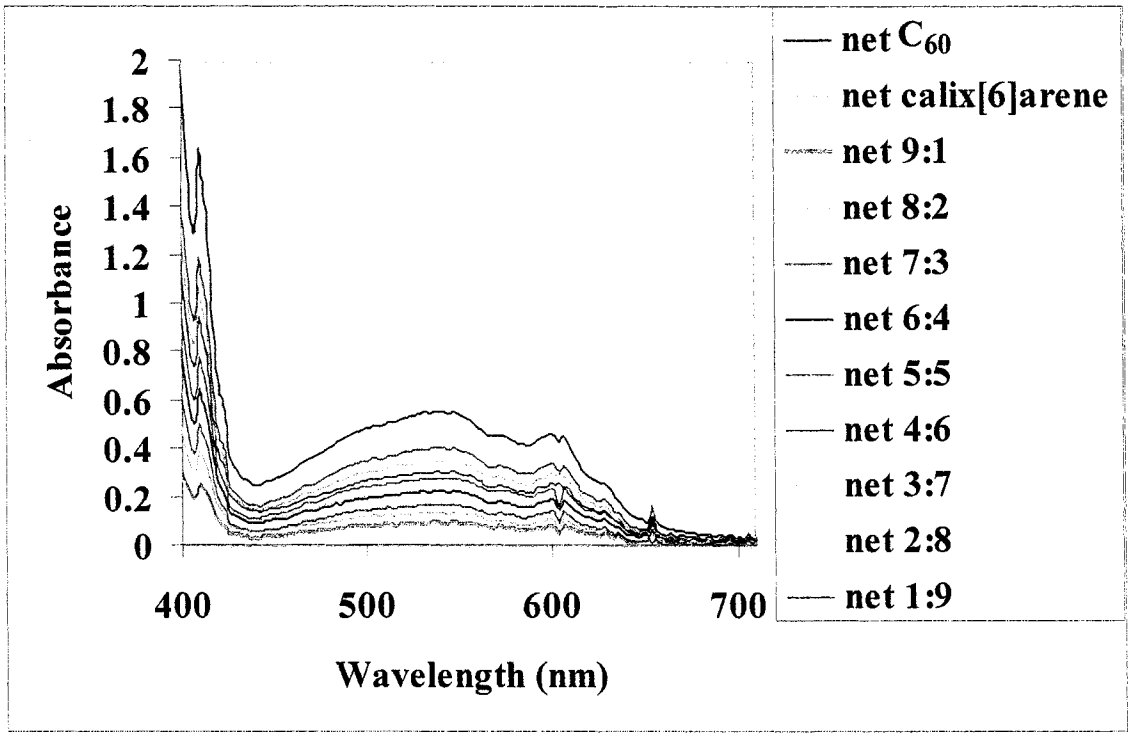

Figure 5.2. Absorbance spectra from the continuous variation experiment for 44 and C_{60}. The original solutions were 1.40 mM for **44** and 0.911 mM for C_{60}. The concentration of individual samples can be found in Appendix D, Table D.1. The net is defined the same as in Figure 4.9.

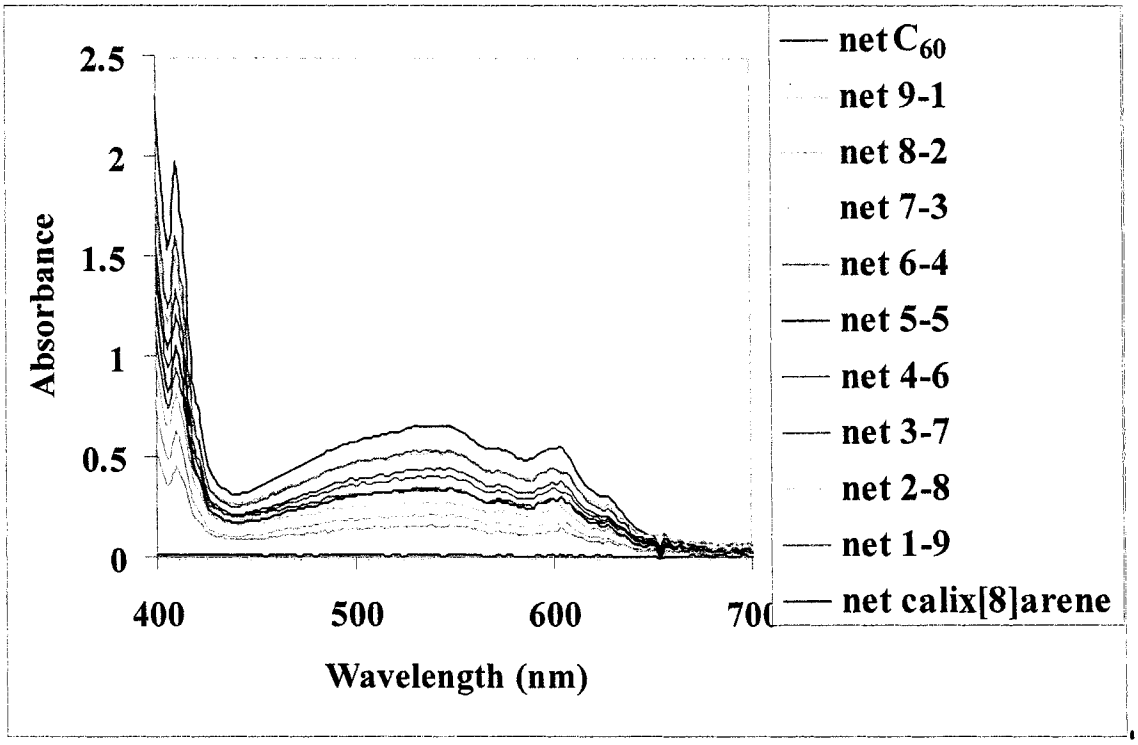

Figure 5.3. Absorbance spectra from the continuous variation experiment for 45 and C_{60}. The original solutions were 0.953 mM for **45** and 1.00 mM for C_{60}. The concentration of individual samples can be found in Appendix D, Table D.2. The net is defined the same as in Figure 4.9.

These spectra were then mathematically transformed by multiplying each spectrum by the difference in absorption between the individual absorption and the absorption of C_{60} at 450 nm, to show the differences between the C_{60} absorbance spectrum and the individual absorbance spectra at each molar fraction. Figures 5.3 and 5.4 show the changes in shape of the band envelope as the mole fractions of **44** or **45** increases, respectively.

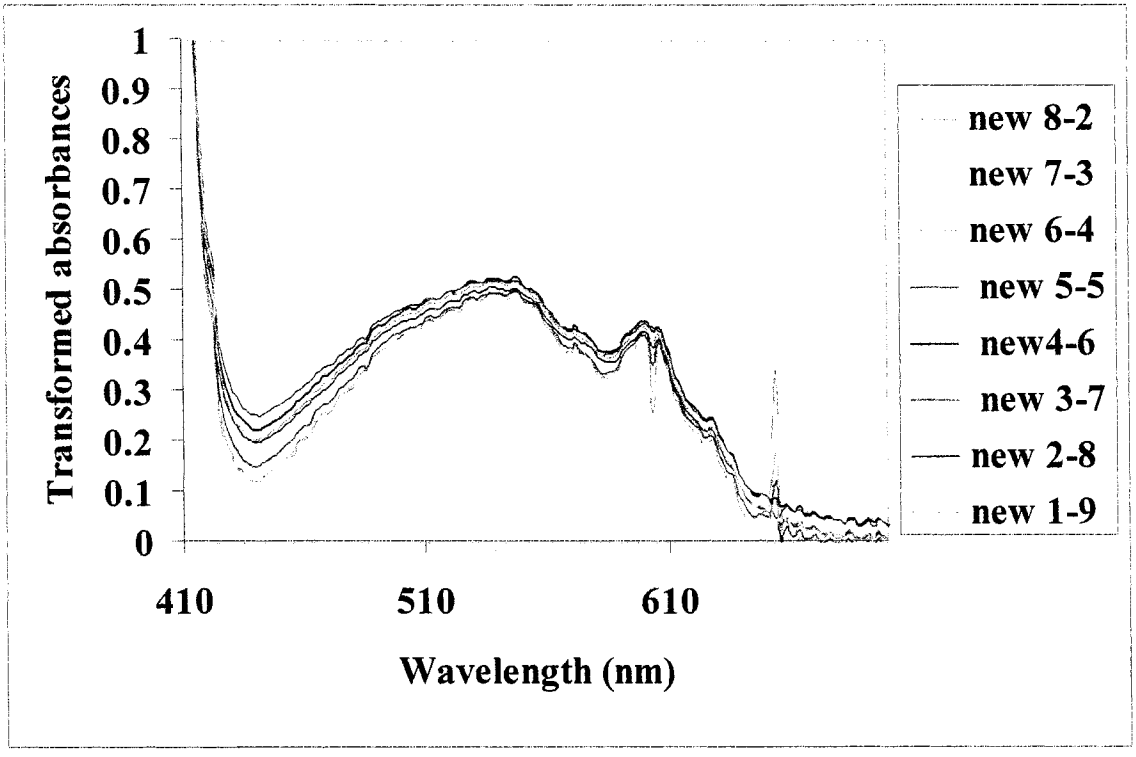

Figure 5.4 Mathematically transformed absorbance of 44 in CS_2.

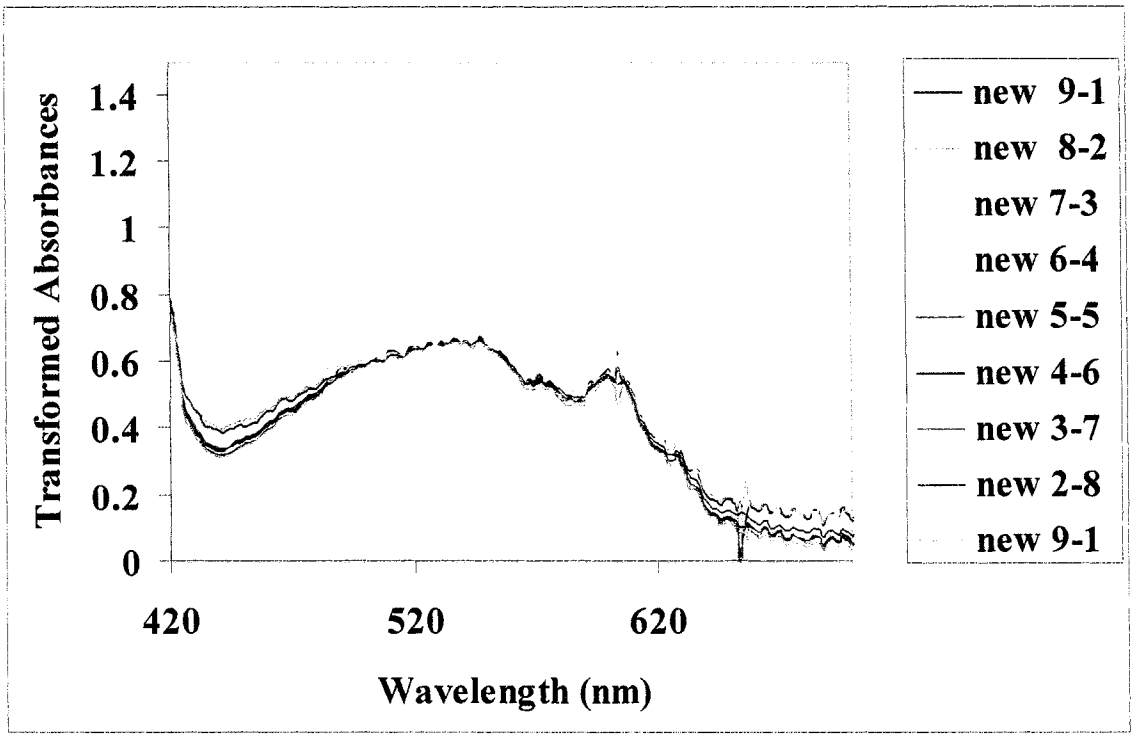

Figure 5.5 Mathematically transformed absorbance of 45 in CS_2.

5.3.2. NMR Studies – General Observations

The ^1H NMR data collected for calix[4]azulene in CS_2 showed the greatest change in chemical shifts ($\Delta\delta$), and therefore data for both **44** and **45** in CS_2 were also collected. Upon mixing of **44** and C_{60} there are chemical shift changes in the proton resonance as the ratio of C_{60} to **44** increases. These shifts are the result of change in the chemical and magnetic environment of the protons of **44**. These data are summarized in Table 5.1. The observations which were made for **45** are similar to those for **44,** and are summarized in Table 5.2. The changes in the chemical shifts are small and contain relatively large errors and therefore not straightforward to interpret. Similar to calix[4]azulene a mixture of multiple species may be present which may decrease the magnitude of any chemical shift changes from the complexation of calix[*n*]arene with

C_{60}. The data in both experiments were not consistent with the strict formation of a dominant 1:1 complex. Quantitative studies to characterize the complexation of C_{60} with **44** and **45** are outlined below.

Table 5.1. Changes in chemical shifts in CS_2 as the ratio of 44 to C_{60} changes.

Ratio of **44** to C_{60}	Δ ppm *t*-butyl	Δ ppm aromatics	Δ ppm methylene	Δ ppm methoxy
1:0	**1.423**	**3.219**	**4.082**	**7.169**
9:1	**-0.001**	**0.000**	**-0.002**	**-0.001**
8:2	**0.000**	**0.001**	**0.000**	**0.001**
7:3	**0.001**	**0.001**	**0.001**	**0.002**
6:4	**0.001**	**0.001**	**0.001**	**0.002**
5:5	**0.002**	**0.001**	**0.001**	**0.002**
4:6	**-0.001**	**-0.001**	**0.000**	**0.001**
3:7	**0.000**	**0.001**	**0.003**	**0.002**
2:8	**0.001**	**0.001**	**0.000**	**0.001**
1:9	**0.002**	**0.002**	**0.002**	**0.003**

Table 5.2. Changes in chemical shifts in CS_2 as the ratio of 45 to C_{60} changes.

Ratio of **45** to C_{60}	Δ ppm *t*-butyl	Δ ppm aromatics	Δ ppm methylene	Δ ppm methoxy
1:0	**1.069**	**6.923**	**4.036**	**3.413**
9:1	**-0.005**	**-0.005**	**-0.004**	**-0.006**
8:2	**-0.001**	**-0.001**	**-0.001**	**-0.001**
7:3	**0.001**	**0.001**	**0.000**	**0.000**
6:4	**0.003**	**0.002**	**0.001**	**0.001**
5:5	**0.001**	**0.000**	**0.000**	**0.000**
4:6	**0.000**	**-0.001**	**-0.001**	**-0.001**
3:7	**0.000**	**0.000**	**0.000**	**0.000**
2:8	**0.000**	**0.000**	**0.001**	**0.001**
1:9	**0.003**	**0.001**	**0.001**	**0.001**

5.3.3. Determining the Stoichiometry of the 44:C_{60} complex and the 45:C_{60} Complex by UV-visible Spectroscopy

Figure 5.2. shows absorbance spectra from the continuous variation experiment in which the ratio of C_{60} to **44** was varied from 9:1 to1:9. As the mole fraction changes for calix[*n*]arene - from 0.0 to 1.0, the absorbance changes show the decreasing C_{60} characteristics.

The absorbances at 520 nm for both compounds were plotted using the Job method, and are illustrated in Figures 5.6 and 5.7. The resulting plots could not be modeled as a linear combination of reagents. The resulting curves show a maximum at around 0.7 for **44** and 0.6 for **45** which gives the hyperbola a skewed shape. These data suggest a possible multi-step equilibrium process. A multi-step equilibrium suggests higher order binding between calix[*n*]arene and C_{60}, as described for calix[4]azulene in equations 4.3a –4.3c.

5.4. Conclusions

As a result of the data limitations such as small absorption changes and small chemical shift it is difficult to interpret the data and come to a solid conclusion of the structure of the adduct formed between **44** or **45** and C_{60}. Further investigation into to the stoichiometry of these complexes was not attainable. Further investigation into the complexation properties of **44** and **45** are necessary. The experiments necessary to complete this study include, repeating the Job analysis using other solvents such as benzene or toluene. As well a detailed examination of the overall K_{assoc} of these compounds would help to identify the nature of the complexes being formed. This examination can be carried out with the use of a Benesi-Hildebrand study along with a Hill analysis.

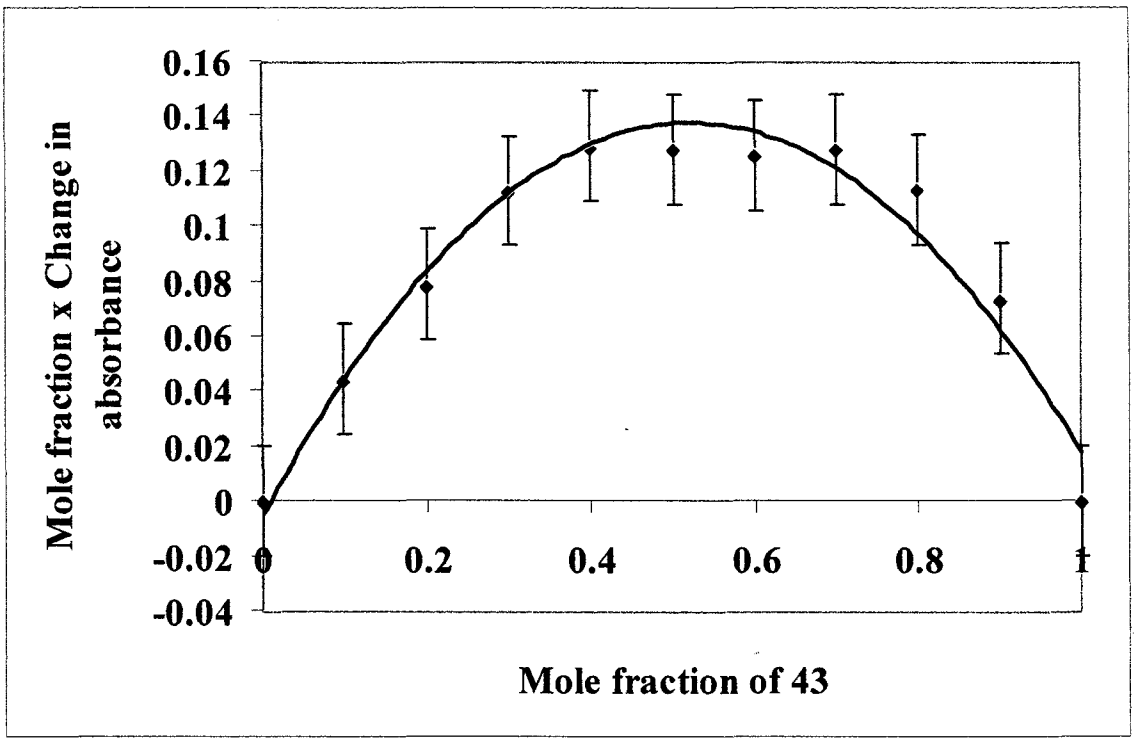

Figure 5.6 Job plot of 44 with C_{60} in CS_2 at 520 nm.

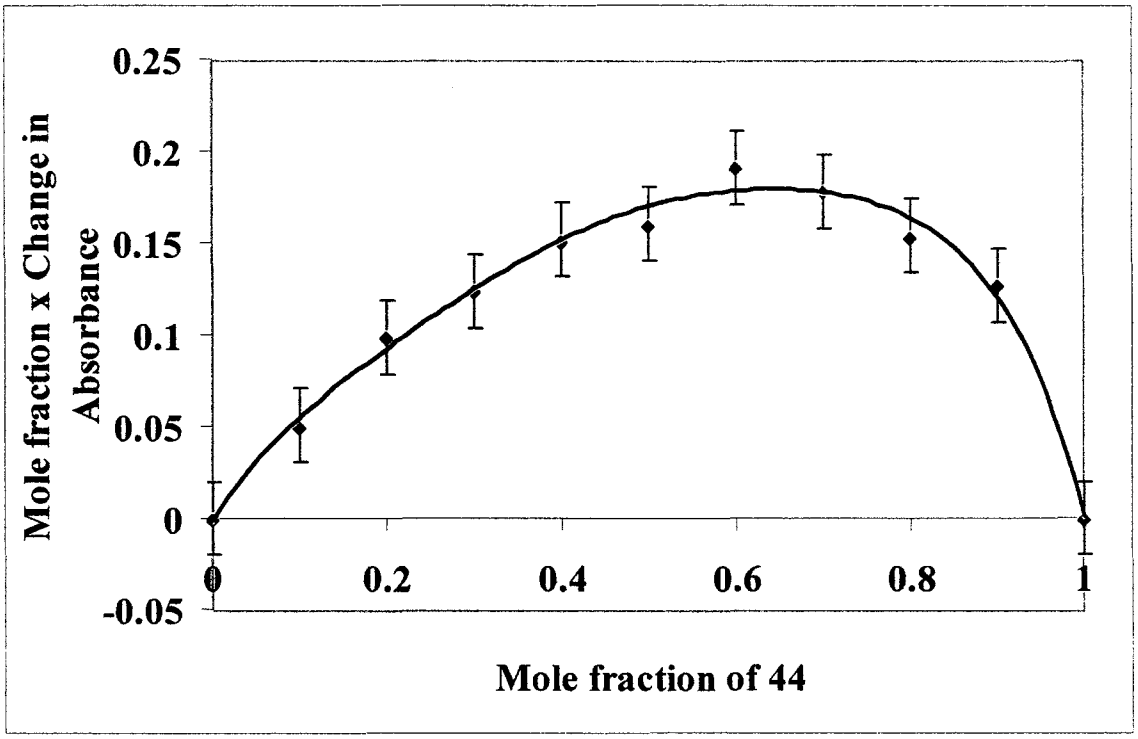

Figure 5.7 Job plot of 45 with C_{60} in CS_2 at 520 nm.

5.4. Experimental

5,11,17,23,29,35-Hexa-*t*-butyl-37,38,39.40,41,42-hexahydroxycalix[6]arene, 5,11,17,23,29,35,41,46-octa-*t*-butyl-49,50,51,52,53,54,55,56-octahydroxycalix[8]arene, iodomethane (CH_3I), sodium hydride (NaH) in 60% mineral oil and C_{60} were all purchased from Aldrich and used as received. Tetrahydrofuran (THF) purchased form Aldrich was distilled over sodium before use. All calculations were done as previously described for the calix[4]azulene experiments, in Section 4.7.

5,11,17,23,29,35-Hexa-*tert*-butyl-37,38,39,40,41,42-hexamethoxycalix[6]arene (44)

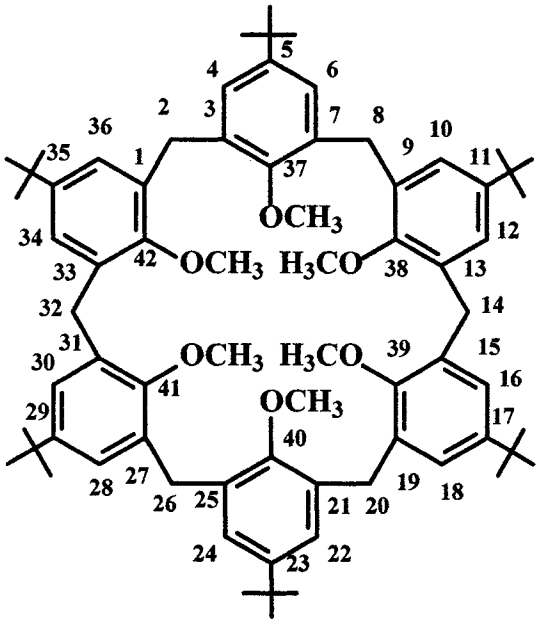

Compound **44** was synthesized using a method similar to that described by Gutsche and Lin.[91] A solution of 1.10 g, (1.13 mmol) of p-*tert*-butylcalix[6]arene, 1.21 g (46.7 mmol) of NaH and 9.33 g (65.9 mmol) of CH_3I was refluxed in DMF (5 ml) and anhydrous THF (50 ml) for 20 h. The THF was evaporated under vacuum, and the grey solid residue was washed with water to remove DMF before being collected by suction filtration. The residue was then crystallized in methanol and dichloromethane to afford

1.11g (94 %) of **44** as colorless crystals; lit. m.p. 380-381 °C;[87] ^{1}H NMR ($CDCl_3$): δ = 1.42 (s, 54H, H-*tert*-butyl), 3.22 (s, 18H, OCH_3), 4.08 (s, 12H, H-2, H-8, H-14, H-20, H-36, H-32), 7.17 (s,12H, H-4, H-6, H-10, H-12, H-16, H-18, H-22, H-24, H-28, H-30, H-34, H-36).

5,11,17,23,29,35,41,47-octa-*tert*-butlyl-49,50,51,52,53,54,55,56-octamethoxy-calix[8]arene (45)

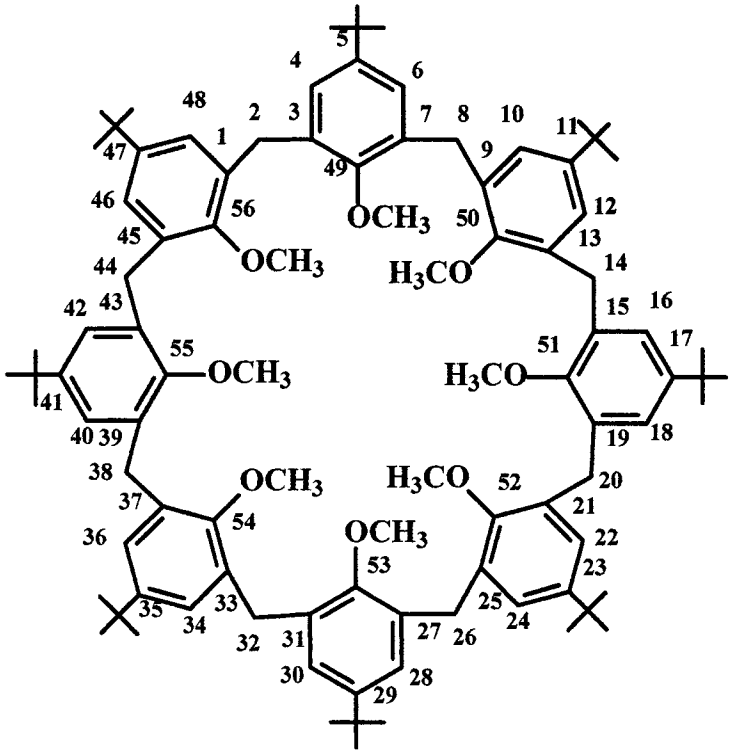

Compound **45** was synthesized using a method similar to that described by Gutsche and Lin.[91] A solution of 1.31 g (1.01 mmol) of *p-tert*-butylcalix[8]arene, 1.21 g (46.7 mmol) of NaH, and 9.33 g (65.9 mmol) of CH_3I was refluxed in DMF (5 ml) and anhydrous THF (50 ml) for 20 h. The THF was evaporated under vacuum and the yellow solid residue was washed with water to remove DMF and was then collected by suction filtration. The residue was crystallized in methanol and dichloromethane to afford 1.34 g (94%) of **45** as colorless crystals; lit m.p. 411-412 °C;[87] The ^{1}H NMR ($CDCl_3$): δ = 1.07 (s, 72H, H-*tert*-butyl), 3.41 (s, 24H, OCH_3), 4.04 (s, 16H, H-2, H-8, H-14, H-20, H-26,

H-32, H-38, H-44), 6.92 (s, 16H, H-4, H-6, H-10, H-12, H-16, H-18, H-22, H-24, H-28, H-30, H-34, H-36, H-40, H-42, H-46, H-48).

^{1}H NMR Titration Experiments

The ^{1}H NMR experiments were conducted using the same equipment and software as described in the calix[4]azulene experiment, Section 4.7.

A 10.0 ml solution of 1.40 mM of **44** and a 10.0 ml solution of 0.911 mM of C_{60} in CS_2 were prepared. These two solutions were then used to prepare a series of nine solutions of varied mole ratio (9:1, 8:2, 7:3, 6:4, 5:5, 4:6, 3:7, 2:8, 1:9) of **44** to C_{60}, which were then each placed in separate NMR tubes. A sample of the solution of the pure **44** was also placed in a NMR tube. ^{1}H NMR spectra were determined for each solution.

A 10.0 ml solution of 0.950 mM of **45** and a 10.0 ml solution of 1.00 mM of C_{60} in CS_2 were prepared. These two solutions were then used to prepare a series of nine solutions of varied mole ratio (9:1, 8:2, 7:3, 6:4, 5:5, 4:6, 3:7, 2:8, 1:9) of **45** to C_{60} which were then each placed in separate NMR tubes. ^{1}H NMR spectra were determined for each solution.

UV-Visible Titration Experiments

The UV-visible experiments were conducted as described for the calix[4]azulene experiment (Section 4.7), using the same equipment and software. The same series of solutions used in the NMR experiment were used in the uv-vis experiment. A sample of the pure C_{60} solution and a sample of blank CS_2 were also placed in NMR tubes. Each sample was measured to give Figures 5.2 and 5.3. The uv-vis experiments were repeated before and after the NMR experiments.

References

1. C. D. Gutsche, *Calixarenes Revisited,* Monographs in Supramolecular Chemistry, J. F. Stoddard (Ed.), Royal Society of Chemistry, Cambridge, 1998.
2. C. D. Gutsche, *Aldrichim. Acta.* 1995, **28**, 3.
3. M. M. Olmstead, G. Sigel, H. Hope, X. Xu and P. P. Power, *J. Am. Chem. Soc.* 1985, **107**, 8087.
4. S. Mizyed, Ph.D. Dissertation, *Complexation Studies of Calixnaphthalenes and Hexahomotrioxacalixnaphthalenes with [60]Fullerene*, Memorial University of Newfoundland, St. John's, Newfoundland, Canada, 2001.
5. S. R. Izatt, R. T. Hawkins, J. J. Christensen and R. M. Izatt, *J. Am. Chem. Soc.* 1985, **107**, 63.
6. M. Ashram, Ph.D. Dissertation, *Synthesis of calix[4]naphthalenes and their properties,* Memorial University of Newfoundland, St. John's Newfoundland, Canada, 1997.
7. T. Asao, S. Ito and N. Morita, *Tetrahedron Lett.* 1988, **29**, 2839.
8. D. A. Colby and T. D. Lash, *J. Org. Chem.* 2002, **67**, 1031.
9. S. Shinkai, S. Mori, H. Koreishi, T. Tsubaski and O. Manabe, *J. Am. Chem. Soc.* 1986, **108**, 2409.
10. These calculations were performed using the programs implemented in PC SPARTAN Pro 5.0 from Wavefunction Inc., Irving, CA 92612.
11. P. E. Georghiou and Z. Li, *Tetrahedron Lett.* 1993, **34**, 2887.
12. N. Ehlinger, S. Lecocq, R. Perrin and M. Perrin, *Supermol. Chem.* 1993, **2**, 71.

13. C. D. Gutsche, B. Dhawan. J. A. Levine, K. H. No and L. J. Bauer, *Tetrahedron Lett.* 1983, **39**, 409.

14. S. Kanamathareddy, C.D. Gutche, *J. Am. Chem. Soc.* 1993, **115**, 6572.

15. G. D. Andreetti, F. Ugozzoli, F. A., Casnati, E., Ghidini, A., Pochini and R. Ungaro, *Gazz. Chim. Ital.* 1989, **199**, 47.

16. *Calixarenes 2001*, Kluwer Academic publishing. Dordrecht/ Boston/London, 2001, 291-292, *and references therein.*

17. C.D. Gutsche, A.Gutsche and A. I.Karauvov, *J. Incl. Phenom.* 1985, 3.

18. A. Zinke and E. Ziegler, *Ber.* B74, 1941, 1729.

19. C.D. Gutsche, M. Iqbal and D. Stewart, *J. Org. Chem.* 1986, **51**, 742.

20. B, Botta, M. C. Digiovanni, G. D. Monache, M. C. De Rosa, E. Gacs-Baitz, M. Botta, F. Corelli, A. Tafi, A. Santini, E. Benedetti, C. Pedone and D. Misiti, *J. Org. Chem.* 1994, **59**, 1532.

21. A. Wolff, B. Böhmer, W. Vogt, F. Ugozzoli, and G. D. Andreetti, *J. Org. Chem.* 1990, **55**, 5665.

22. D. K. Fu, F. Xu and T. M. Swager, *J. Org. Chem.* 1996, **61**, 802.

23. B.T. Hayes and R. F. Hunter, *Chem. Ind.* 1954, **193**.

24. V. Böhmer, K. Jung and M. Schon and A. Wolff, *J. Org. Chem.* 1992, **57**, 790.

25. V. Böhmer, P. Chim and H. Kammerer, *Makromol. Chem.* 1979, **180**, 2503.

26. V. Böhmer, F. Marschollek and L. Zette, *J. Org. Chem.* 1987, **52**, 3200.

27. V. Böhmer, L. Merkel and V. Kunz, *J. Chem. Soc., Chem. Commun.* 1987, 896.

28. G. D. Andreetti, V. Böhmer, J. G. Jordon, M. Tabatabai, F. Ugozzoli, W. Vogt and A. Wolff, *J. Org. Chem.* 1993, **58**, 4023.

29. H. WaffenSchmidt, Dissertation RWTH Aachem Germany, 2000. *Referenced in* P. Wassercheid, W. Keim, *Angew. Chem. Int. Ed.* 2000, **39**, 3772-3789

30. J. L. Scott, D. R. MacFarlane, C. L. Raston and C. M. Teoh, *Green Chem.* 2000, **2**, 123-126.

31. C. L Raston, J. L Atwood, P. J. Nichols and I. B. N. Sudria, *J. Chem. Soc,. Chem. Commun.* 1996, 2615.

32. J. L. Atwood, L.J. Barbour, C.L.Raston and I. B. N. Sudria, *Angew. Chem. Int. Ed. Engl.* 1998, **37**, 981.

33. R. M. Williams and J. W. Verhoeven, *Rec. Trav. Chim. Pays-Bas.*1992, **111**, 531.

34. J. L. Atwood, G,A. Koustanis and C. L. Raston, *Nature.* 1994, **368**, 229.

35. T. Suzuki, K. Nakashima and S. Shinkai, *Chem. Lett.* 1994, 699.

36. R. Taylor (Ed.), *The Chemistry of Fullerenes*, Advanced Series in Fullerenes, Vol. 4, World Scientific Publishing Co. Pte. Ltd., Singapore, 1995, *and references therein.*

37. *The Merck Index,* 7th ed., Merck & Co., Inc. Rahway, N.J., U.S.A., 1960.

38. P. Walden *Bull. Acad. Imper. Sci* (St. Peterburg), 1914, 1800; cited in S. Sugden and H. Wilkins. *J. Chem. Soc.* 1929, 1291-1298.

39. P. Wassercheid and W. Keim, *Angew. Chem. Int. Ed.*, 2000, **39**, 3772-3789.

40. R. Sheldon, *Chem. Commun.* 2001, 2399-2407.

41. S. V. Volkov, *Chem. Soc. Rev.*, 1990, **19**, 21-28.

42. J. S. Wilks, J. A. Levisky, R.A. Wilson and C. L. Hussy, *Inorg. Chem.* 1982, **21**, 1263-1264.

43. K. R. Seddon, *J. Chem. Tech. Biotechnol.* 1997, **68**, 351- 356.

44. H. Füllbier, *Electrochim. Acta.* 1992, **37**, 379-383.

45. P. Bonhôte, A.P. Dias, N. Papgeorgiou, K. Kalyanasundaram and M. Gratzel, *Inorg. Chem.* 1996, **35**, 1168-1178.

46. A. A. Fannin Jr., D.A. Florean, L. A. Kiny, J. S. Landers, B. J. Piersma, D. J. Stech, R. C. L. Vagnn, J. S. Wilkes and J. L. William. *J. Phys. Chem.* 1984, **88**, 2614-2621.

47. M. Freemantle, May 15, 2000, *C&EN.* 37-50.

48. T. Welton, *Chem. Rev.* 1999, **99**, 2071-2083.

49. C. J. Adams, M. J. Earle, G. Roberts and K. R. Seddon, *Chem. Commun.* 1998, 2097.

50. M. J. Earle, P. B. McCormac and K.R. Seddon, *Green Chem.* 1999, **1**, 23.

51. E. G. Kunt, *Chemtech.* 1987, 570.

52. G. W. Parshall, *J. Am. Chem. Soc.* 1972, **94**, 8716.

53. J. G. Knifton, *J. Mol. Catal.* 1987, 43.

54. Y. Charvin, L. Massman and H. Olivier, *Angew. Chem, Int. Ed. Engl.* 1995, **34**, 2698.

55. D. A. Z. Suarez, J. E. L. Dullin, S. Einloft, R. F. Desouza and J. Dupon, *Polyhedro.,* 1996, **15**, 1217.

56. A. J. Carmichael, M. J. Earle, J. D. Holbrey, P. B. McCormac and K. R. Seddon, *Org. Lett.* 1999, **1**, 7, 997-1000.

57. Y. Chaurvin, B. Gilber and I. Guibord, *J. Chem. Soc. Chem. Commun.* 1990, 1715.

58. Y. Chaurvin, S. Eiloft and H. Olivier, *Int. Eng. Chem. Res.* 1995, **34**, 1144.

59. J. S. Wilkes, J. A. Levisky, R. A. Wilson and C. L. Hussey, *Inorg. Chem.* 1982, **21**, 1263-1264.

60. C. M. Gordon, J. D. Holbrey, A. R. Kennedy and K. R. Seddon, *J. Matter. Chem.* 1998, **8**, 2627-2639.

61. J. Sun, M. Forsyth and D. R. MacFarlane, *Ionics*. 1997, **3**, 356.

62. B. M. Choudary, M. L. Kantam, V. Neeraja, T. Bandyopadhyay and P. N. Reddy, *Journal of Molecular Catalysis A: Chemical*. 1999, **140**, 25.

63. N. M. Przhiyalgovskaya and G.T.Mondodoev, *Zh. Obshch. Khimi.* 1964, **34**, 5, 1570.

64. M. Onaka, T. Shinoda, Y. Izumi and E. Nolen, *Tetrahedron Lett.* 1993, **34**, 2625.

65. H.-J. Schneider and A. K. Yatsimirsky, *Principles and Methods in Supramolecular Chemistry.* Wiley, Chichester, 2000.

66. B. Dietrich, P.Viout and J.-M. Lehn, *Macrocyclic Chemistry*. VCH, Weinheim, 1993, *and references therein.*

67. J. Wang, S.G. Bodie, W.H. Watson and C.D. Gutche, *J. Org. Chem.* 2000, **65**, 8260 *and references therein.*

68. P. E. Georghiou, S. Mizyed and S. Chowdhury, *Tetrahedron Lett.* 1999, **40**, 611.

69. S. Mizyed, M. Ashram, D.O. Miller and P.E. Georghiou, *J. Am. Chem. Soc. Perkin Trans 2*. 2001, 1916.

70. J. D. Watson and F. H. C. Crick. *Nature*, 1953, **171**, 737. *Referenced in:* D. P. Snustad, M. J. Simmons and J. B. Jenkins, *Principles of Genetic.,* Wiley, Weinheim, 1997.

71. B. D. Beer, P. A. Gale and D. K. Smith, *Supramolecular Chemistry*. Oxford, 1999.

72. C. A. Hunter and J. K. M. Saunders, *J. Am. Chem. Soc.* 1990, **112**, 5527.

73. R. H. Petrucci, W.S. Harwood and F.G. Herring, *General Chemistry, Principles and Modern Applications.* 8th ed., Prentie Hall Inc., Upper Saddle River, 2002. *and refereces therein.*

74. H. S. Frank and M.W. Evans, *J. Phys. Chem.* 1945, **13**, 507.

75. F. Diederich and M.G. Lopiz, *Chem Soc. Rev.* 199, **28**, 263.

76. G. J. Ferrandi, *Elements of Inorgainc Photochemistry*. John Wiley & Sons Inc., New York, 1998 *and references therein.*

77. J. W. Steed, P.C. Junk, J. L. Atwood, M. J. Burnes, C.L. Raston and R. S. Burkhalter, *J. Am. Chem. Soc.* 1994, **116**, 10346.

78. S. Mizyed, P. E. Georghiou, M. Bancu, B. Cuadra, A.K. Rai, P. Cheng and L.T. Scott, *J. Am. Chem. Soc.* 2001, **123**, 51, 12270.

79. S. H. Gallagher, R. S. Armstrong, P. A. Lay and C. A. Reed, *J. Phys. Chem.* 1995, **99**, 5817.

80. S. Leach, M. Vervloet, A. Deprès, E. Bréheret, J. P. Hare, T. J. Dennis, H. W. Kroto, R. Taylor and D. R. M. Walton, *Chemical physics*. 1992, **160**, 451.

81. L. Fielding, *Tetrahedron*. 2000, **56**, 6151 and *references therein.*

82. V. M. S. Gil, N.C. Oliveira, *J. Chem. Ed.* 1990, **67**, 6, 473.

83. H. A. Benesi and J.H. Hildebrand, *J. Am. Chem. Soc.* 1949, **71**, 2703.

84. R. Mathur, E. D. Becker, R. B. Bradley and C. N. Li, *J. Phys. Chem.* 1963, **67**, 2190.

85. M. W. Hanna and A. L. Ashbaugh, *J. Phys. Chem.* 1964, **68**, 811.

86. H. Tsukube, H. Furuta, Y. Takeda, Y. Kudo, Y. Inue, Y. Liu, H. Sakamoto and K. Kimura, *"Determination of Stability Constants"* in *Comprehensive Supramolecular Chemistry.* J. E. D. Davies and J. A. Ripmeeter (Ed.), Elsevier Science Ltd. Oxford UK, 1996 *and reference therein.*

87. I. Horman and B. Dreux, *Anal. Chem.* 1983, **55**, 1219.

88. S. Gosami, A. K. Mahapatra and R. J. Mukherjee, *J. Chem. J. Soc., Perkin trans.* **1** 2001, 2717.

89. N. J. Turro, *Modern Molecular Photochemistry.* University Science Books, Sausalito, California, 1991, *and references therein.*

90. T. G. Traylor, S. Tsuchiya, D. Campbell, M. Mitchell, D. Stynes and N. Koga, *J. Am. Chem. Soc.* 1985, **107**, 604.

91. C. D. Gutsche and L.-G. Lin, *Tetrahedron.* 1986, **42**, 6, 1633.

Appendix A

^{1}H NMR of Selected Compounds from Chapter 2

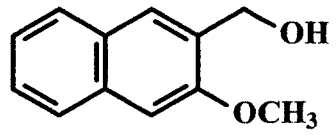

19

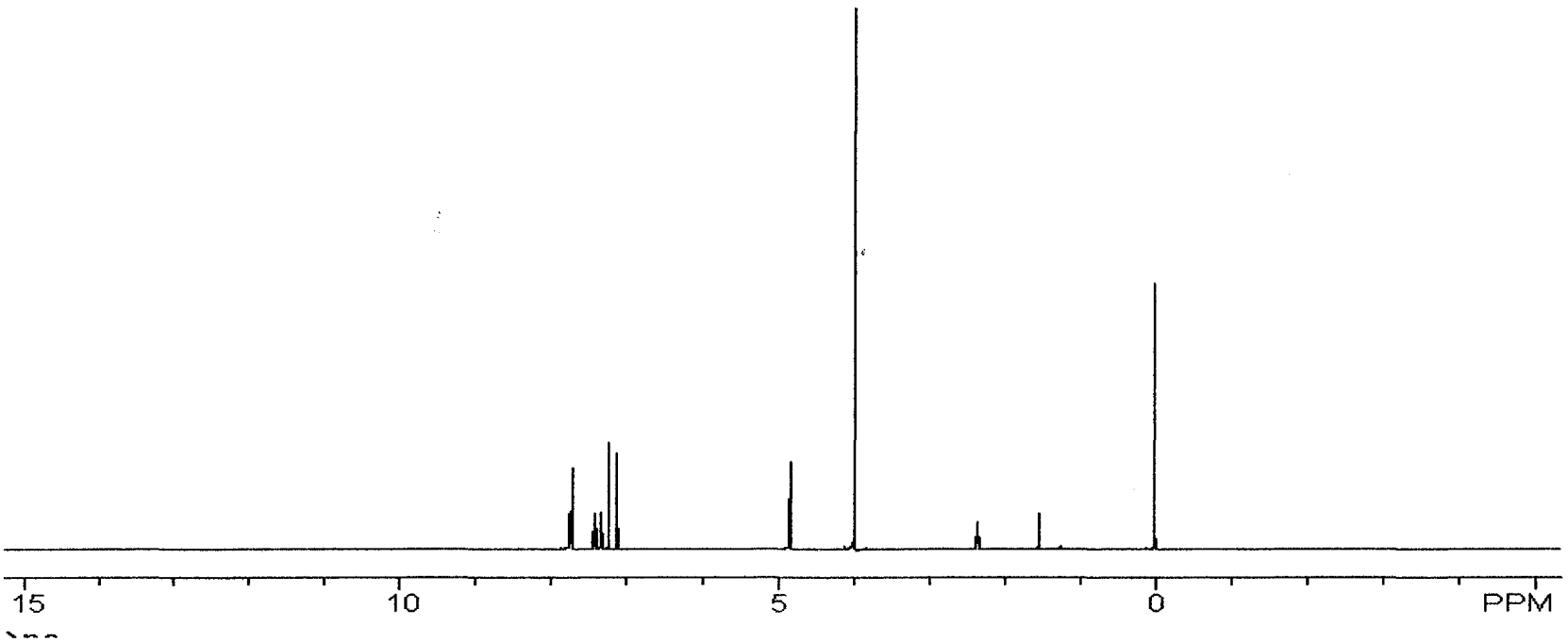

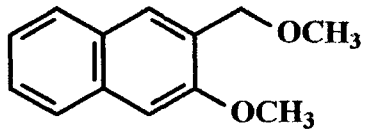

32

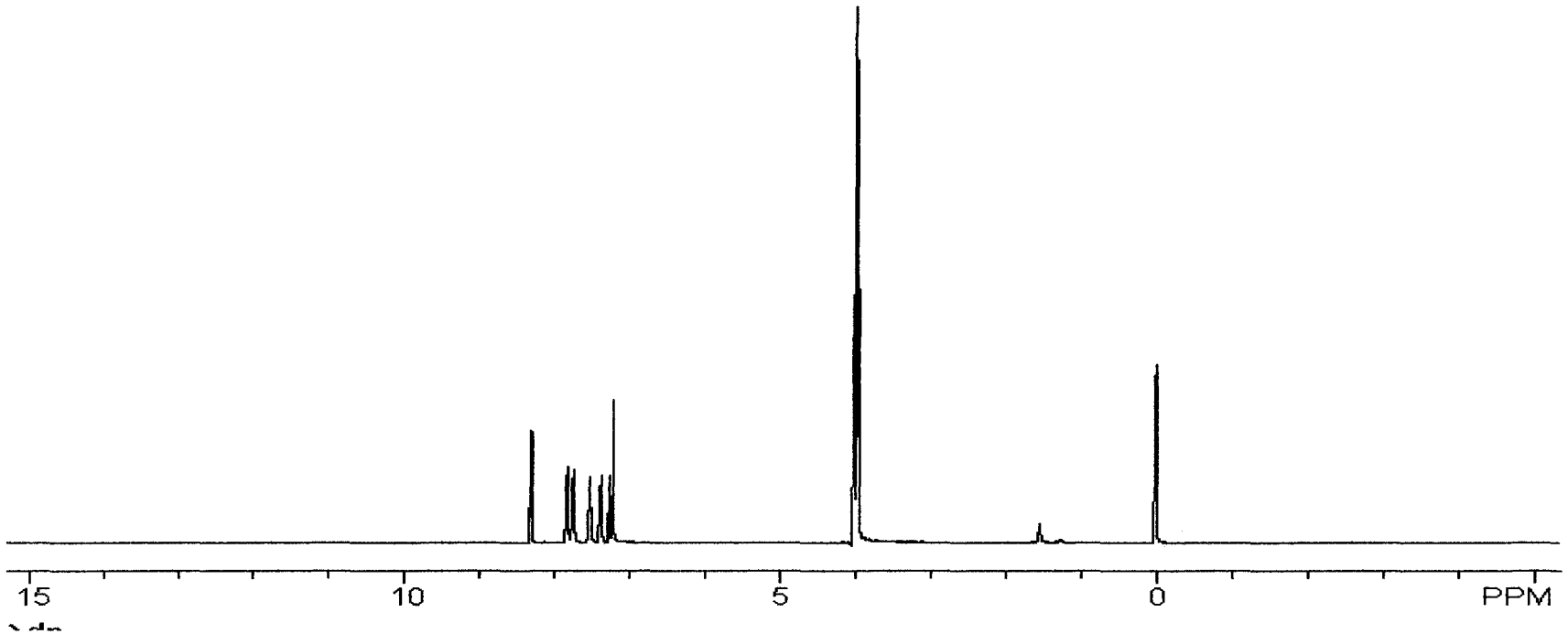

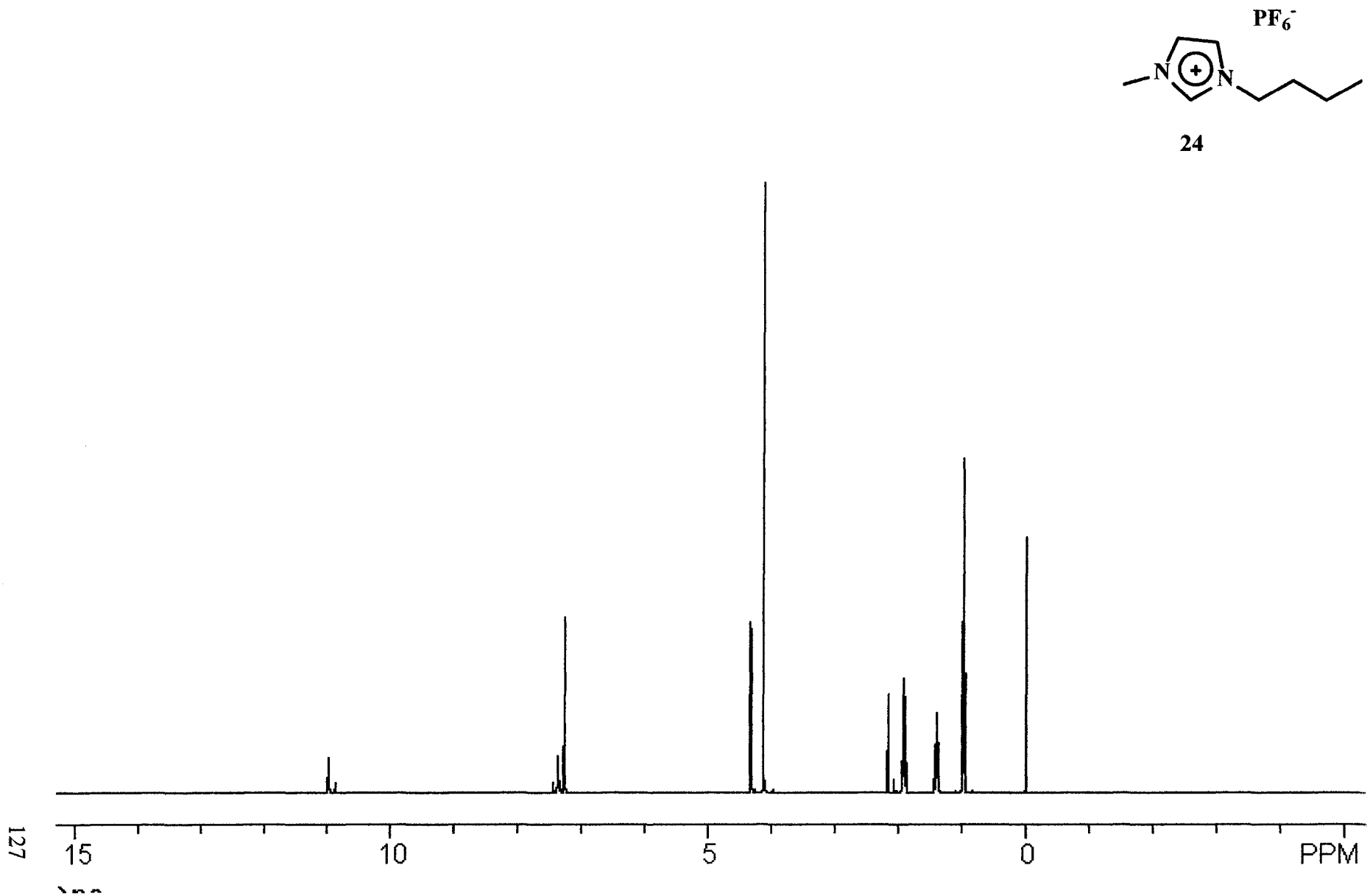
PF6-
N
N
24
127
15
10
5
0
PPM

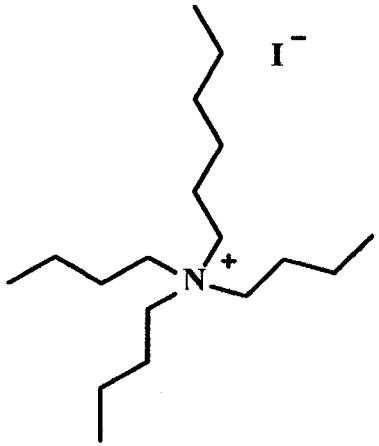

26

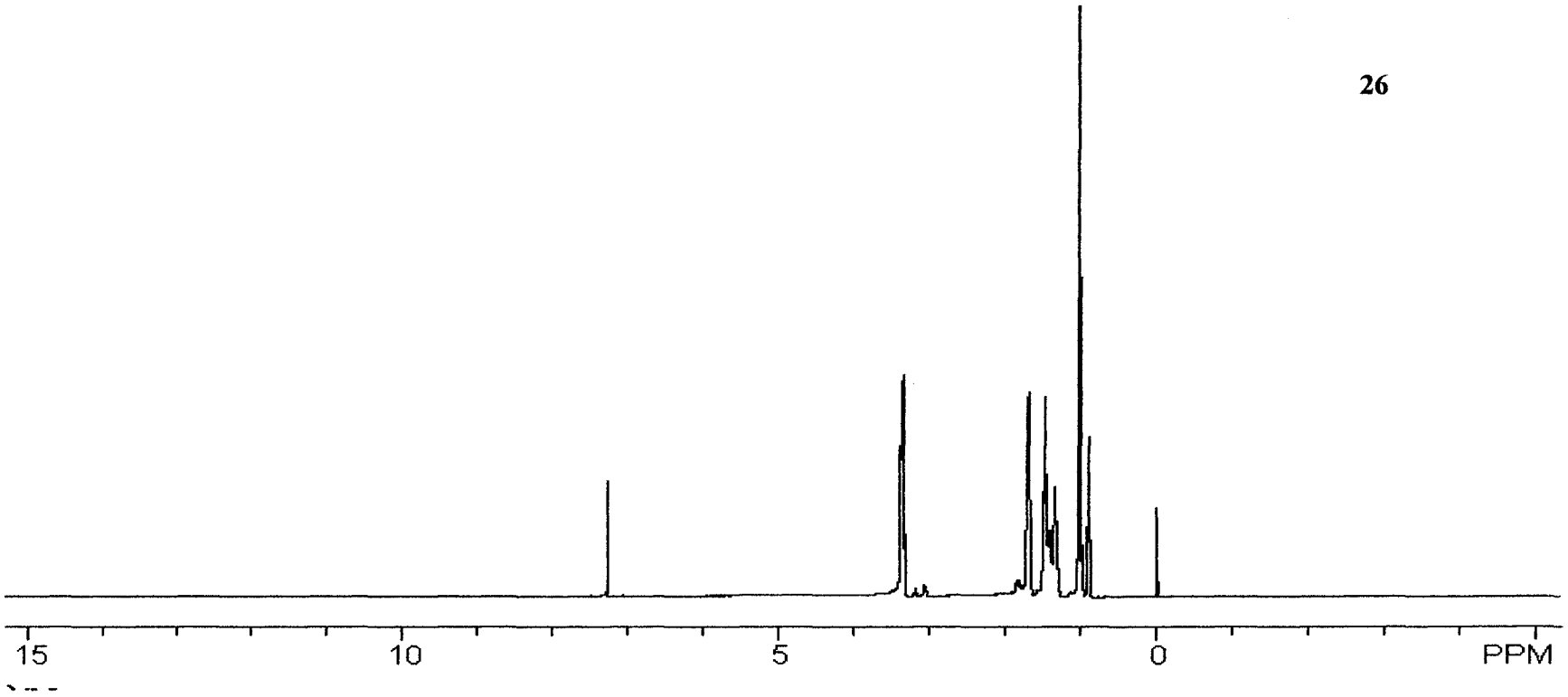

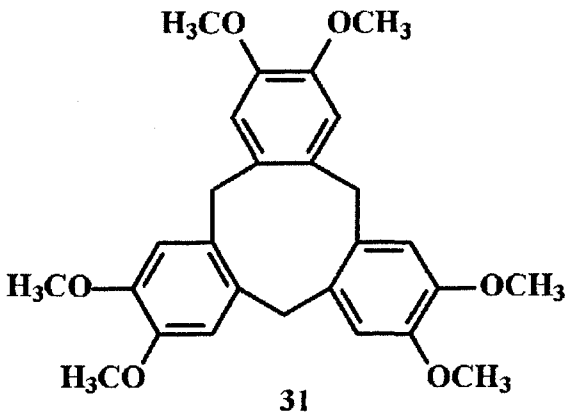

31

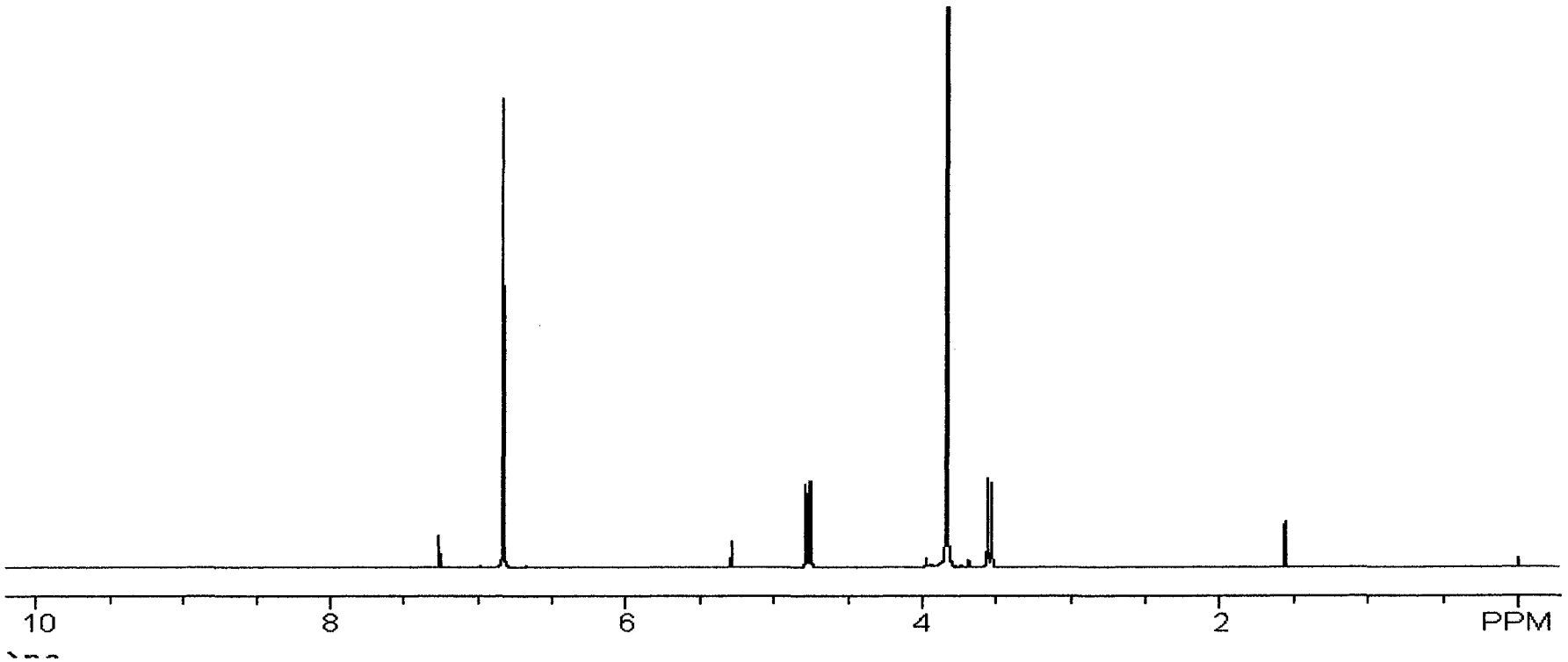

Appendix B

^{1}H NMR of Selected Compounds from Chapter 3

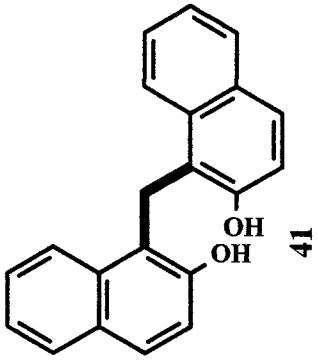

41

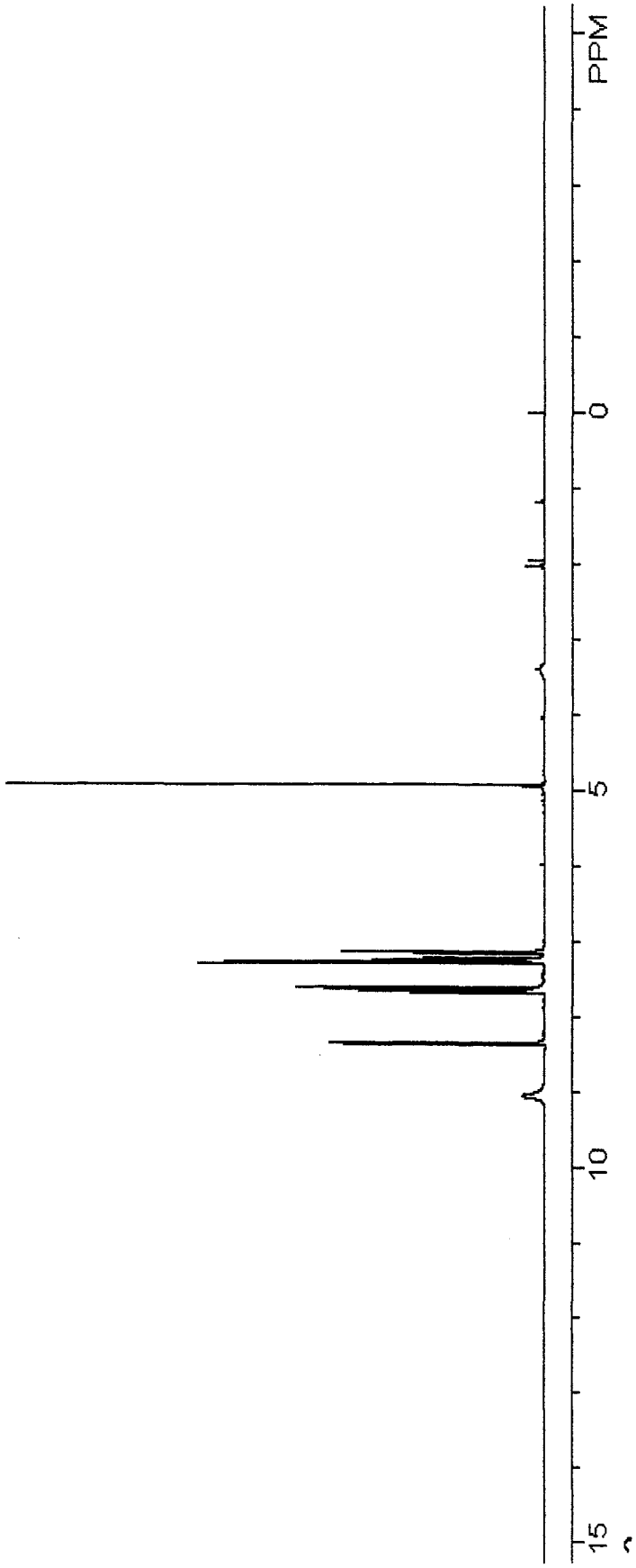

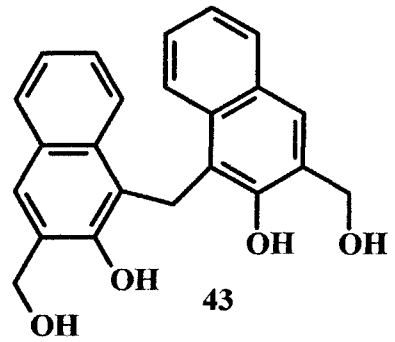

43

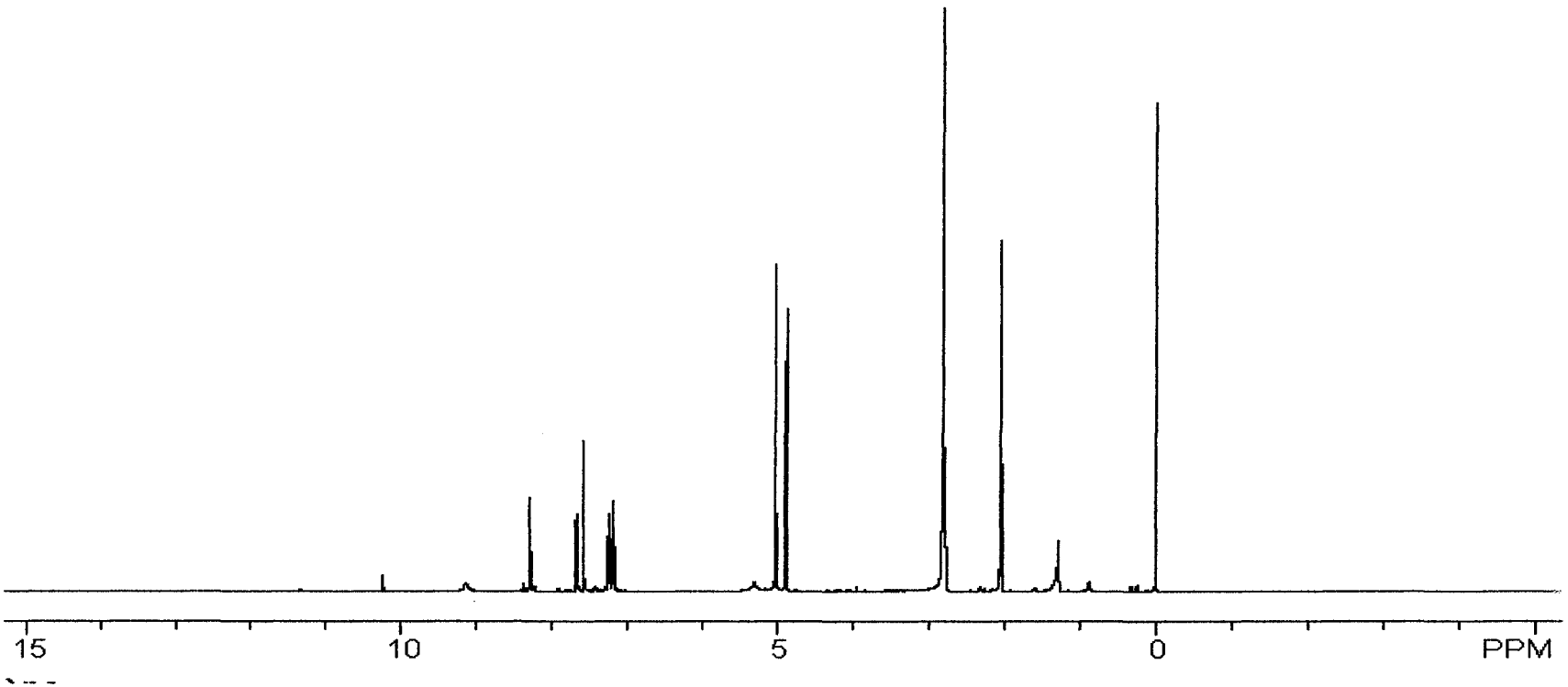

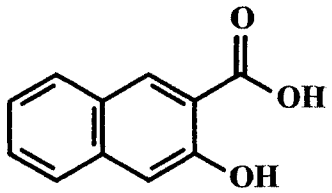

42

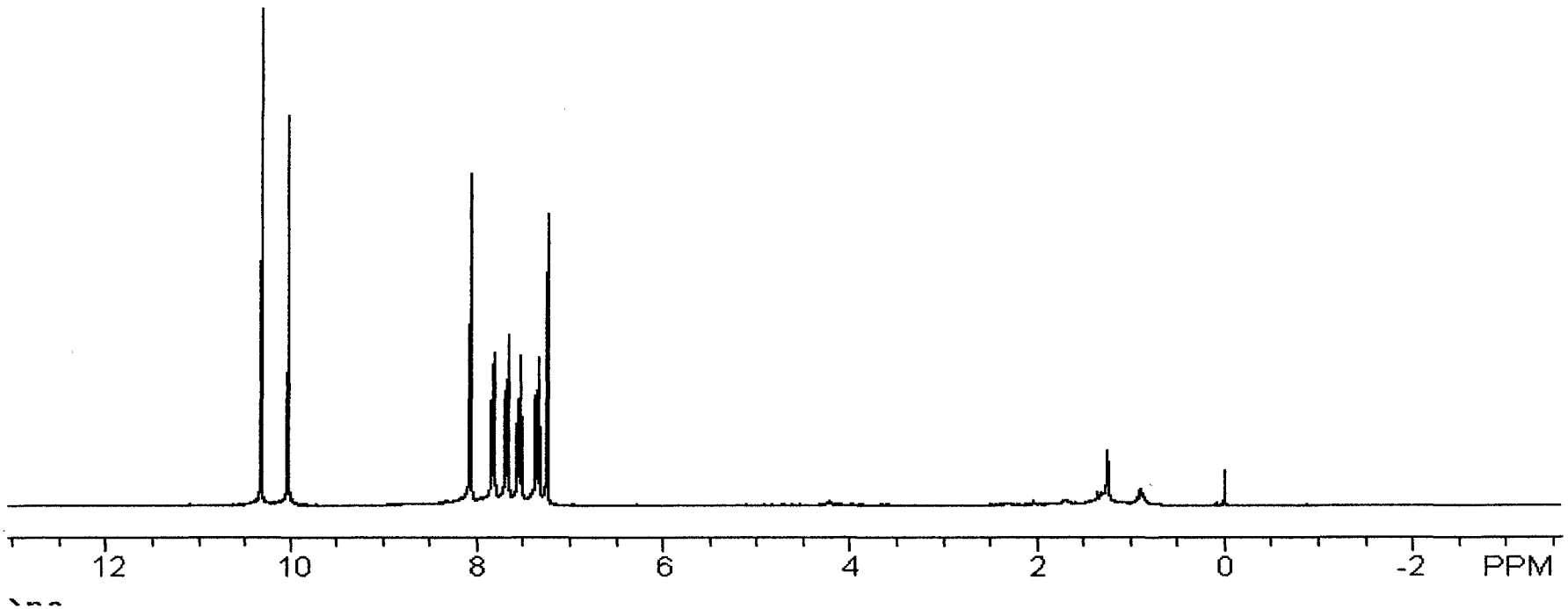

133

Appendix C

Benzene-d_6 Experiment

and

Experimental and Calculated Data for Chapter 4

The data for the experiments in benzene-d_6 were in treated the same manner as those for the experiment in CS_2. The absorbance spectra which were determined in benzene-d_6 were separated into two parts, as shown below. In these spectra, only one isosbestic point is observed, at approximately 602 nm. The presence of this isosbestic point is a possible indication of the formation of a complex.

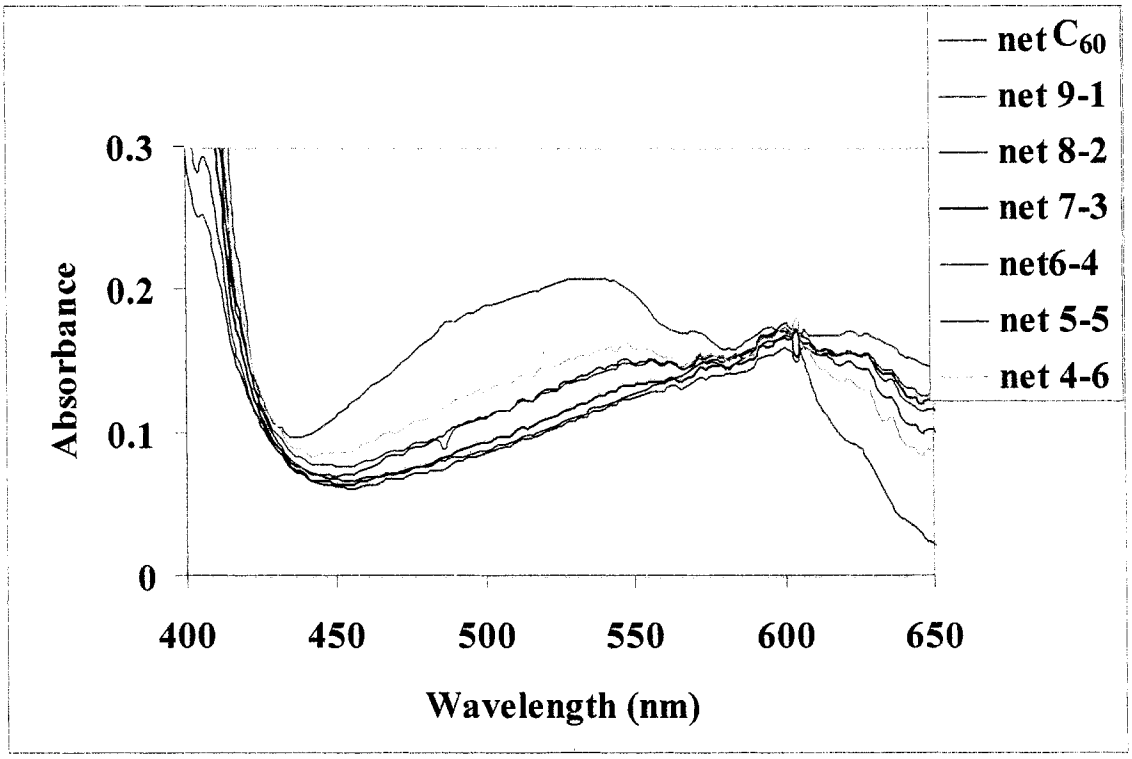

Figure C.1. Absorbance spectra from the continuous variation experiment in benzene-d_6 for the mole ratios of 4:6 to 9:1 of calix[4]azulene to C_{60}. The original solutions were 0.68 mM for calix[4]azulene and 0.69 mM for C_{60}. The correct concentrations for each sample can be found within this appendix. "Net" refers to the calculation in which the absorbance value for the blank (air) is subtracted from the absorbance value of the individual solution being measured.

The low solubility in benzene-d_6 of **11** makes the data in this solvent more difficult to interpret than the data from the experiments in CS_2. The data was however

tested in the same manner as the data which were collected from the CS_2 experiments. This data gave evidence that **11** forms a complex with higher order binding, however due to the solubility restriction, no experiments where performed to obtain a binding constant in benzene-d_6.

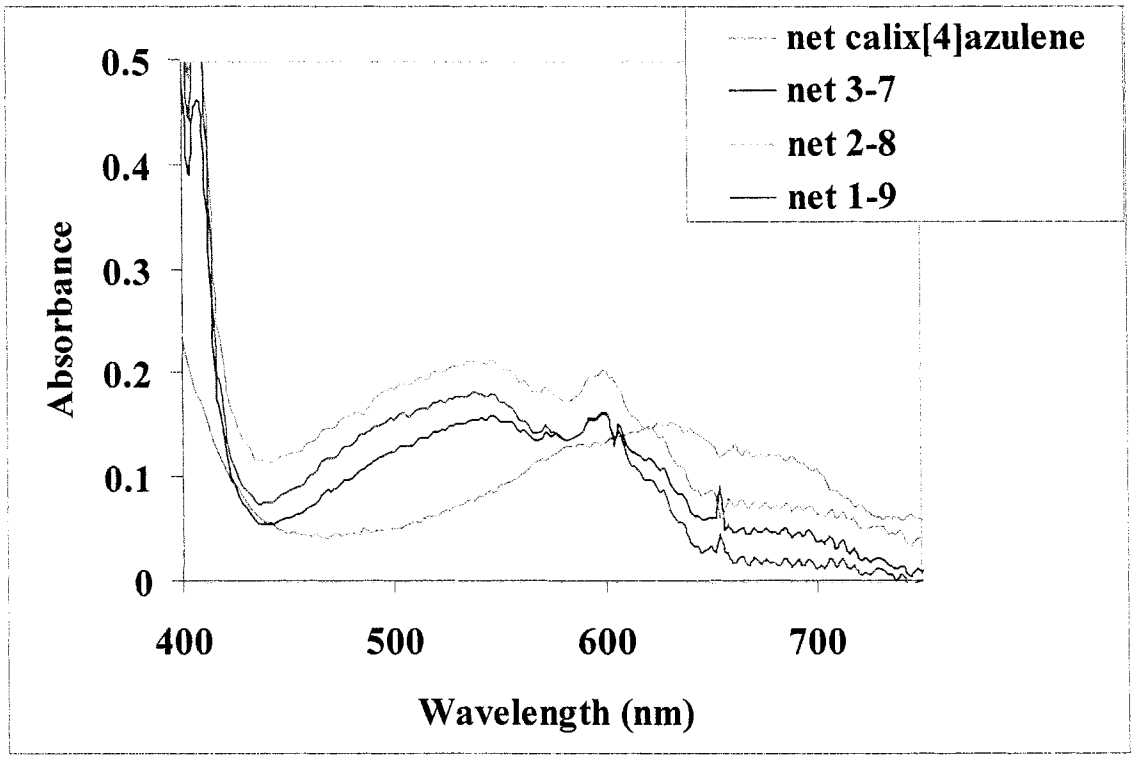

Figure C.2. The absorbance spectra from the continuous variation experiment in benzene-d_6 for the mole ratios of 1:9 to 3:7 of calix[4]azulene to C_{60}. The original solutions were 0.68 mM for calix[4]azulene and 0.69 mM for C_{60}. The correct concentrations for each sample can be found within this appendix. "Net" refers to the calculation in which the absorbance value for the blank (air) is subtracted from the absorbance value of the individual solution being measured.

Below are shown the Job plots for the uv-vis and ^{1}H NMR titration data. The Job plots show complex structures which make it hard to identify the nature of any adducts formed in these experiment. The Job plots, however, support the suggestion that **11** and C_{60} form complexes with higher order binding, as discussed in Chapter 4 of this thesis.

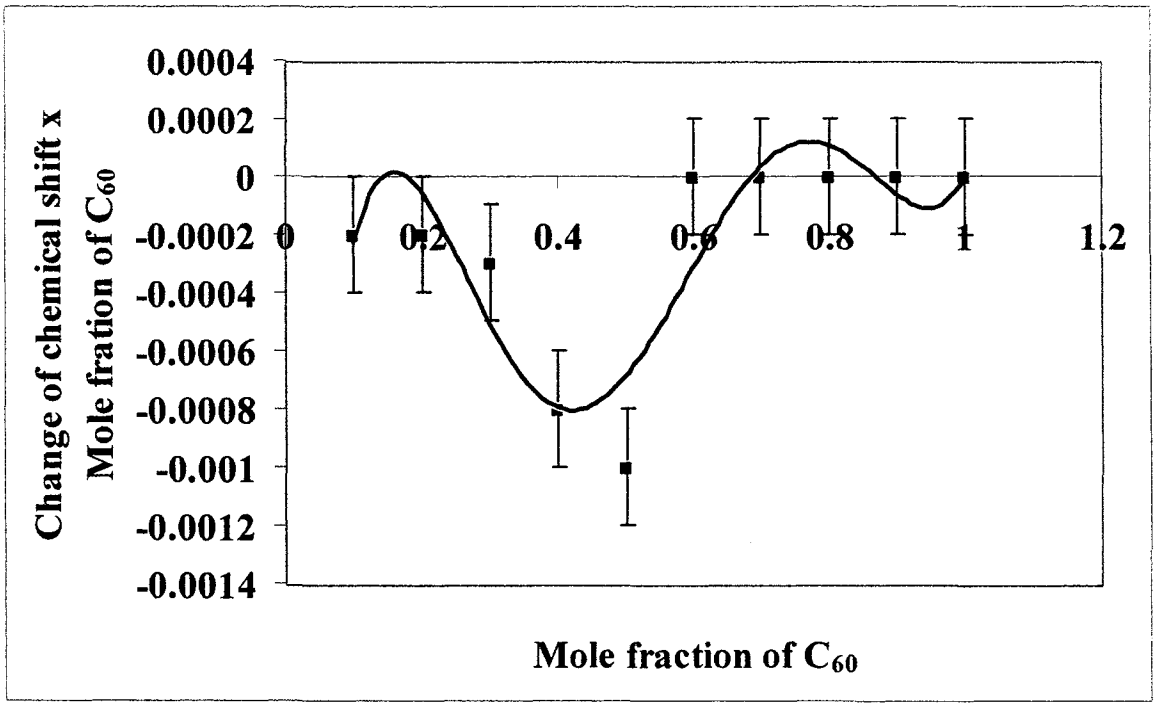

Figure C.3. Job plot of the chemical shift change for the methylene signal of calix[4]azulene in benzene-d_6, as the mole fraction of C_{60} increases.

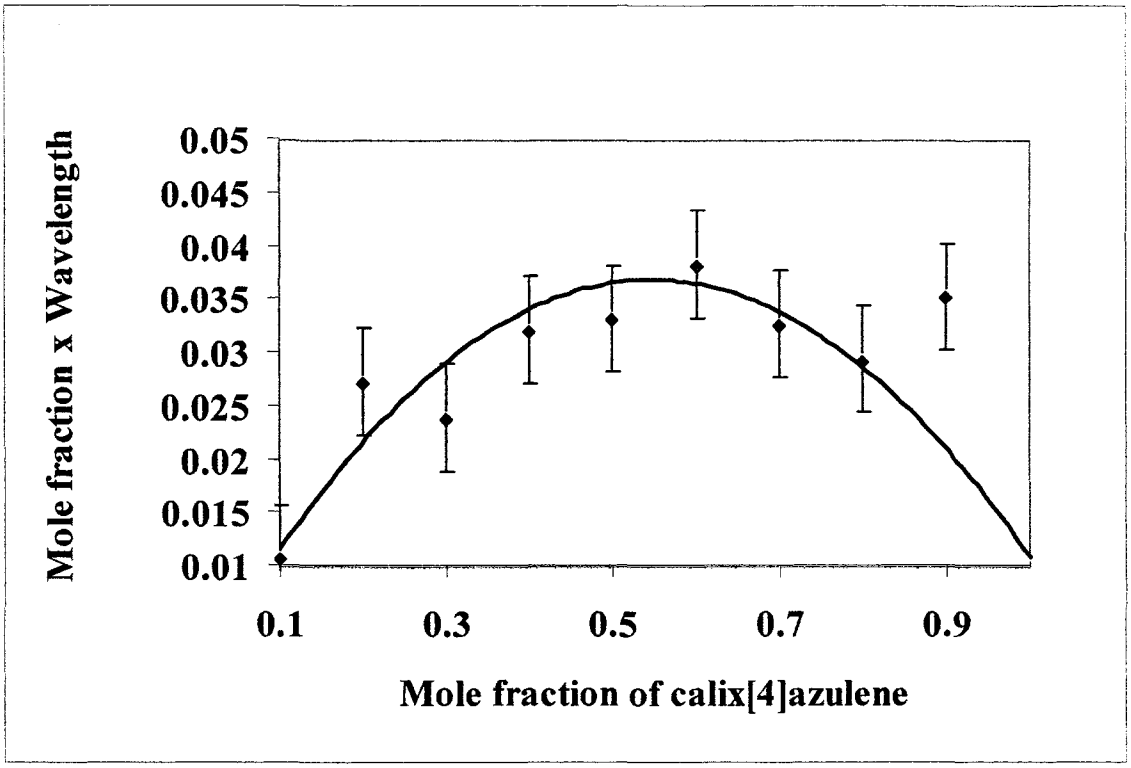

Figure C.4. Job plot of calix[4]azulene vs C_{60} at wavelength 530 nm in benzene-d_6.

Table C.1: The concentrations in CS_2 of C_{60} and 11 used for the in the Job plot.

Mole Ratio of C_{60}:**11**	Concentration of C_{60} (mM)	Concentration of **11** (mM)
9:1	**0.103**	**0.916**
8:2	**0.206**	**0.803**
7:3	**0.300**	**0.700**
6:4	**0.403**	**0.587**
5:5	**0.488**	**0.494**
4:6	**0.563**	**0.412**
3:7	**0.657**	**0.309**
2:8	**0.760**	**0.196**
1:9	**0.854**	**0.093**

Table C.2: The concentrations in benzene-d_6 of C_{60} and 11 used for the Job plot.

Mole Ratio of C_{60}:**11**	Concentration of C_{60} (mM)	Concentration of **11** (mM)
9:1	**0.069**	**0.612**
8:2	**0.138**	**0.544**
7:3	**0.207**	**0.476**
6:4	**0.276**	**0.408**
5:5	**0.345**	**0.340**
4:6	**0.414**	**0.272**
3:7	**0.483**	**0.204**
2:8	**0.552**	**0.136**
1:9	**0.621**	**0.068**

Table C.3: The calculated values used for the ^{1}H NMR Job plot in CS_2.

Mole Fraction of C_{60}	Chemical Shift Changes (ppm)	Mole Fraction of C_{60} x Chemical Shift Changes
1	**0**	**0**
0.9	**0.001 ± 0.0005**	**0.0009 ± 0.0005**
0.8	**0.002 ± 0.0005**	**0.0016 ± 0.0005**
0.7	**0.003 ± 0.0005**	**0.0021 ± 0.0005**
0.6	**0.002 ± 0.0005**	**0.0012 ± 0.0005**
0.5	**0.001 ± 0.0005**	**0.0005 ± 0.0005**
0.4	**0.001 ± 0.0005**	**0.0004 ± 0.0005**
0.3	**0.002 ± 0.0005**	**0.0006 ± 0.0005**
0.2	**0.002 ± 0.0005**	**0.0004 ± 0.0005**
0.1	**0.000 ± 0.0005**	**0.0000 ± 0.0005**
0	**0**	**0**

Table C.4: The calculated values used for the ^{1}H NMR Job plot in benzene-d_6.

Mole Fraction of C_{60}	Chemical Shift Changes (ppm)	Mole Fraction of C_{60} x Chemical Shift Changes
1	**0**	**0**
0.9	**0.000 ± 0.0005**	**0.000 ± 0.0005**
0.8	**0.000 ± 0.0005**	**0.000 ± 0.0005**
0.7	**0.000 ± 0.0005**	**0.000 ± 0.0005**
0.6	**0.000 ± 0.0005**	**0.000 ± 0.0005**
0.5	**-0.002 ± 0.0005**	**-0.001 ± 0.0005**
0.4	**-0.002 ± 0.0005**	**-0.0008 ± 0.0005**
0.3	**-0.001 ± 0.0005**	**-0.0003 ± 0.0005**
0.2	**-0.001 ± 0.0005**	**-0.0002 ± 0.0005**
0.1	**-0.002 ± 0.0005**	**-0.0002 ± 0.0005**
0	**0**	**0**

Table C.5: Calculated values used for the uv-vis Job plot in CS_2.

Mole Fraction of **11**	Change in Absorbance	Mole Fraction x Change in Absorbance
1	**0**	**0**
0.9	**0.048706**	**0.43835**
0.8	**0.081451**	**0.065161**
0.7	**0.114883**	**0.080418**
0.6	**0.136688**	**0.082013**
0.5	**0.158432**	**0.079216**
0.4	**0.191879**	**0.076752**
0.3	**0.205429**	**0.061629**
0.2	**0.263382**	**0.052676**
0.1	**0.253586**	**0.025359**
0	**0.295242**	**0**

Table C.6: Calculated values used for the uv-vis Job plot in benzene-d_6.

Mole Fraction of **11**	Change in Absorbance	Mole Fraction x Change in Absorbance
1	**0**	**0**
0.9	**0.039093**	**0.035184**
0.8	**0.036682**	**0.029346**
0.7	**0.046631**	**0.032642**
0.6	**0.063751**	**0.038251**
0.5	**0.066192**	**0.033096**
0.4	**0.080185**	**0.032074**
0.3	**0.079315**	**0.023795**
0.2	**0.136017**	**0.027203**
0.1	**0.106494**	**0.010699**
0	**0.135406**	**0**

Table C.7: Concentration of samples used for the titration of 11 into a solution of C_{60} in CS_2 (Figure 4.13b).

Addition of **11** aliquot in ml	Concentration of C_{60} in Sample (mM)	Concentration of **11** in sample (mM)	Concentration of C_{60} in reference (mM)
0.2	**0.944**	**0.067**	**0.944**
0.3	**0.914**	**0.097**	**0.914**
0.4	**0.886**	**0.126**	**0.886**
0.5	**0.859**	**0.152**	**0.859**
0.6	**0.833**	**0.177**	**0.833**
0.7	**0.809**	**0.201**	**0.809**
0.8	**0.787**	**0.223**	**0.787**
0.9	**0.766**	**0.244**	**0.766**
1.0	**0.746**	**0.264**	**0.746**
1.1	**0.727**	**0.282**	**0.727**

Table C.8: Concentration of samples used for the titration of C_{60} into a solution of 11.

Addition of C_{60} aliquot in ml	Concentration of **11** in Sample (mM)	Concentration of C_{60} in sample (mM)	Concentration of **11** in Reference (mM)
0	**1.065**	**0**	**1.065**
0.1	**1.027**	**0.0365**	**1.027**
0.2	**0.992**	**0.069**	**0.992**
0.3	**0.959**	**0.090**	**0.959**
0.5	**0.899**	**0.156**	**0.899**
0.6	**0.871**	**0.181**	**0.871**
0.7	**0.846**	**0.205**	**0.846**
0.8	**0.822**	**0.228**	**0.822**
0.9	**0.799**	**0.249**	**0.799**
1.0	**0.777**	**0.270**	**0.777**

Table C.9: Calculated values used for the Benesi-Hildebrand plot for the titration of C_{60} into a solution of 11.

Concentration of C_{60} (mM)	Concentration of **11** (mM)	Absorbance	1/[**11**] (M^{-1})	[C_{60}]/Abs
0	**1.065**	**0.01782**	**0**	**0.059764**
0.0365	**1.027**	**0.02292**	**28066.24**	**0.044808**
0.069	**0.992**	**0.0391**	**14532.77**	**0.025361**
0.090	**0.959**	**0.04587**	**10023.05**	**0.020896**
0.156	**0.899**	**0.063**	**6414.368**	**0.014263**
0.181	**0.871**	**0.06442**	**5512.679**	**0.013527**
0.205	**0.846**	**0.07651**	**4868.549**	**0.011053**
0.228	**0.822**	**0.07803**	**4385.965**	**0.010529**
0.249	**0.799**	**0.07385**	**4009.623**	**0.010814**
0.270	**0.777**	**0.2717**	**3709.199**	**0.00286**

Table C.10: Calculated values used for the Benesi-Hildebrand plot for the titration of 11 into a solution of C_{60} in CS_2.

Concentration of **11** (mM)	Concentration of C_{60} (mM)	Absorbance	1/[C_{60}] (M^{-1})	[**11**]/Abs (M/nm)
0.067	**0.944**	**0.0877**	**1059**	**0.000647**
0.097	**0.914**	**0.121**	**1094**	**0.000709**
0.126	**0.886**	**0.194**	**1128**	**0.000599**
0.152	**0.859**	**0.259**	**1164**	**0.000553**
0.177	**0.833**	**0.271**	**1200**	**0.000617**
0.201	**0.809**	**0.328**	**1236**	**0.000584**
0.223	**0.787**	**0.381**	**1270**	**0.000561**
0.244	**0.766**	**0.420**	**1305**	**0.000560**
0.264	**0.746**	**0.452**	**1340**	**0.000564**
0.282	**0.727**	**0.475**	**1375**	**0.000674**

Table C.11: Calculated and experimental absorbances for the titration of 11 into a solution of C_{60} in CS_2.

Concentration of **11** (mM)	Change in Absorbance Experimental at 480 nm	Change in Absorbance Calculated from Eq. 4.4
0.067	**0.0877**	**0.0610**
0.097	**0.121**	**0.0815**
0.126	**0.194**	**0.0983**
0.152	**0.259**	**0.111**
0.177	**0.271**	**0.121**
0.201	**0.328**	**0.179**
0.223	**0.381**	**0.135**
0.244	**0.420**	**0.140**
0.264	**0.452**	**0.144**
0.282	**0.475**	**0.147**

Appendix D

^{1}H NMR of Compounds 44 and 45

and

Experimental and Calculated data from Chapter 5

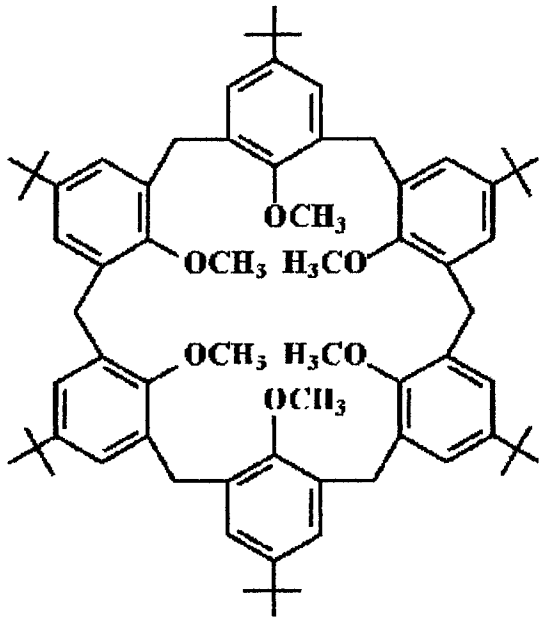

44

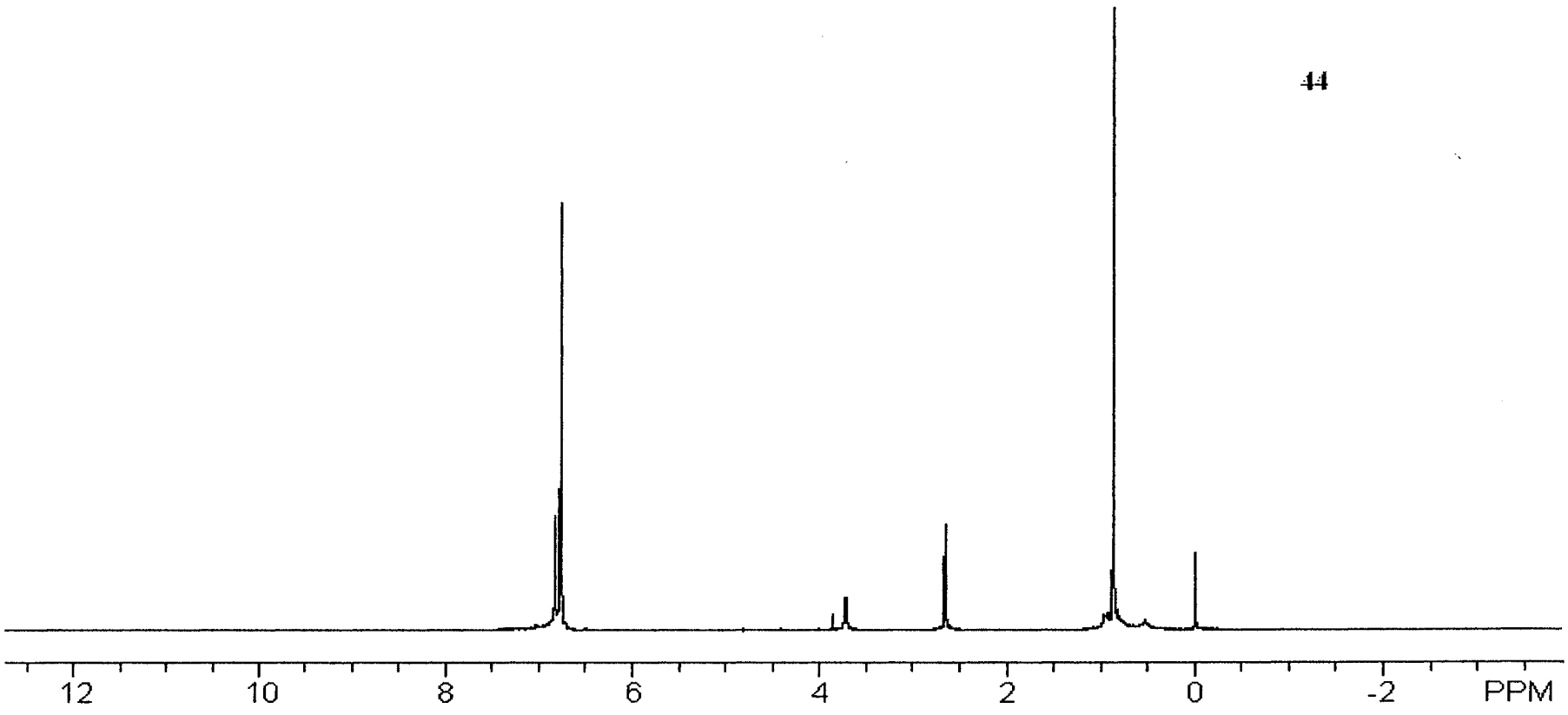

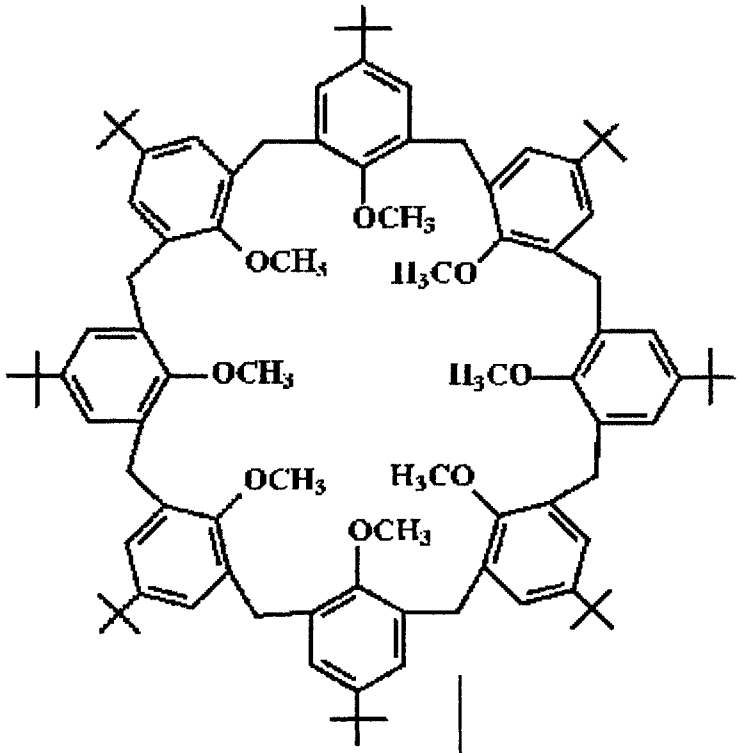

45

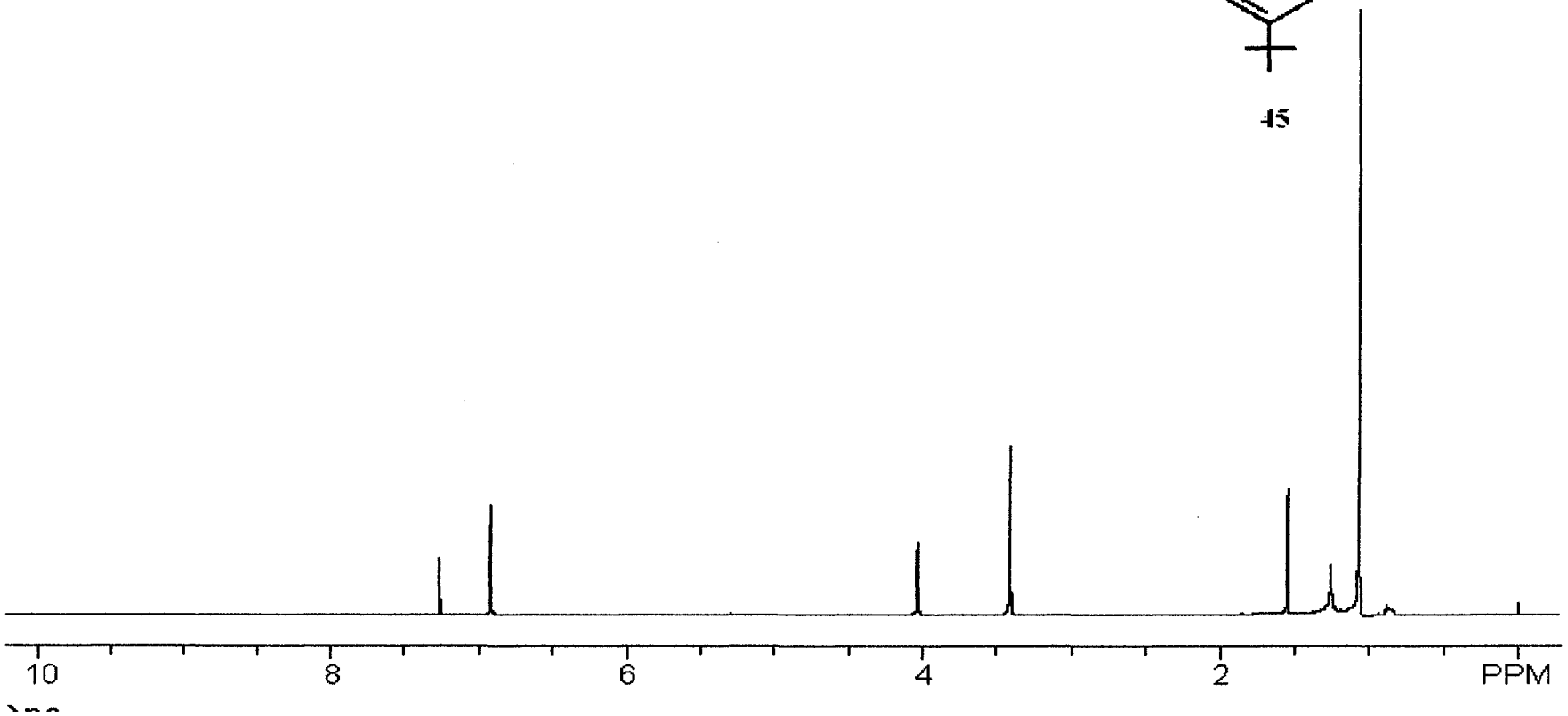

Table D.1: Concentrations in CS_2 of C_{60} and 44 used for the Job plot.

Mole Ratio of C_{60}:**44**	Concentration of C_{60} (mM)	Concentration of **44** (mM)
9:1	**0.128**	**1.20**
8:2	**0.255**	**1.01**
7:3	**0.355**	**0.854**
6:4	**0.465**	**0.686**
5:5	**0.583**	**0.504**
4:6	**0.638**	**0.420**
3:7	**0.712**	**0.308**
2:8	**0.783**	**0.196**
1:9	**0.847**	**0.096**

Table D.2: Concentrations in CS_2 of C_{60} and 45 used for the Job plot.

Mole Ratio of C_{60}:**45**	Concentration of C_{60} (mM)	Concentration of **45** (mM)
9:1	**0.100**	**0.858**
8:2	**0.200**	**0.763**
7:3	**0.300**	**0.667**
6:4	**0.400**	**0.572**
5:5	**0.500**	**0.477**
4:6	**0.600**	**0.381**
3:7	**0.700**	**0.290**
2:8	**0.800**	**0.191**
1:9	**0.900**	**0.095**

Table D.3: Calculated values used for the uv-vis Job plot for 44 in CS_2.

Mole Fraction of **44**	Change in Absorbance	Mole Fraction x Change in Absorbance
1	**0**	**0**
0.9	**0.081665**	**0.03499**
0.8	**0.141327**	**0.113062**
0.7	**0.182282**	**0.127597**
0.6	**0.209229**	**0.125537**
0.5	**0.255463**	**0.127732**
0.4	**0.322098**	**0.128839**
0.3	**0.375259**	**0.112578**
0.2	**0.391922**	**0.078384**
0.1	**0.440414**	**0.044040**
0	**0.553925**	**0**

Table D.4: Calculated values used for the uv-vis Job plot for 45 inCS_2.

Mole Fraction of **45**	Change in Absorbance	Mole Fraction x Change in Absorbance
1	**0**	**0**
0.9	**0.140838**	**0.126754**
0.8	**0.191787**	**0.153430**
0.7	**0.254333**	**0.178033**
0.6	**0.318191**	**0.190915**
0.5	**0.0320358**	**0.160178**
0.4	**0.378158**	**0.151263**
0.3	**0.411484**	**0.123445**
0.2	**0.492080**	**0.098416**
0.1	**0.501312**	**0.050131**
0	**0.616272**	**0**